Project

WENDELSTEIN W VII

IPP 2/204 June 1972

MAX-PLANCK-INSTITUT FÜR PLASMAPHYSIK

GARCHING BEI MÜNCHEN

MAX-PLANCK-INSTITUT FÜR PLASMAPHYSIK

GARCHING BEI MÜNCHEN

Project

WENDELSTEIN W VII

IPP 2/204 June 1972

Die nachstehende Arbeit wurde im Rahmen des Vertrages zwischen dem Max-Planck-Institut für Plasmaphysik und der Europäischen Atomgemeinschaft über die Zusammenarbeit auf dem Gebiete der Plasmaphysik durchgeführt.

Preface

The final decision to build the Stellarator Wendelstein W VII, which has been taken at the end of 1971, was based on a detailed proposal of the project and on many discussions and internal as well as external meetings of specific advisory groups. During the decision preparing processes the original concept of this project was subject to various modifications, such as at first to use the large aperture vessel and not to start with superconducting main field coils but with a conventional coil system suited for steady state operation.

This report covers the main parts of the W VII-proposal which, in form of several Appendixes to the "Application of Preferential support", had been written for the use of the EURATOM boards concerned. By giving also information on the prototype of the superconducting main field coils and the earlier versions of the design of the helical windings it reflects in some way the history of the project thus far. The report is split into two major parts, the first of which is mainly concerned with the scientific aims while the second deals with the technical concept. With respect to the technical parameters quoted there we are referring to the introduction on page 31.

We are thanking all colleagues and groups who helped to this paper, in particular R. Pöhlchen (technical division), who contributed with Figs. 21 - 25. The further design and the construction of W VII will be a joint undertaking of the Exp. Div. 2 and the Techn. Division of our Institute.

APPENDIX 1 to

Project Wendelstein W VII

Application for EURATOM preferential support

SCIENTIFIC AND TECHNOLOGICAL AIMS

The present situation in the physics of low-ß toroidal confinement is characterized on the one hand by the increased understanding of the Stellarator experimental results and on the other hand by the achievements of Tokamaks with respect to the plasma parameters obtained and to the promising and stimulating empirical scaling laws. This is the basis for the scientific and technological aims of the proposed Wendelstein W VII-Stellarator, which can roughly be listed as follows:

1) Extending the experimental investigation of plasma confinement in Stellarators well into the long-mean free path regime with particular emphasis on studying and controlling the theoretically predicted effects of localized particles.

2) Studying the influence of various boundary conditions - such as amount of recycling, presence and shape of limiter or separatrix, application of HF-ohmic heating etc. - on heat and particle losses and on gross plasma confinement.

3) Obtaining similar plasma conditions as in large Tokamaks, thus allowing for the desired comparison between Stellarators and Tokamaks of comparable dimensions (aperture, aspect ratio, magnetic field etc.).

4) Investigating heating schemes beyond the initial ohmic heating, which allow for both, further heating of the ions and maintaining their temperature during steady state operation.

5) Applying particle refuelling methods in order to maintain the particle density constant for steady state operation.

Reprint: May 1972

6) Determining experimentally the limitation on the value of β with respect to MHD-equilibrium and stability.

7) Providing a flexible facility, able to produce a steady state toroidal field of high magnetic energy, the configuration of which can be essentially controlled from outside.

8) Developing and testing a large superconducting coil assembly representing the first step towards the magnetic field technology required for fusion reactors.

The above aims, though often interlinked with each other, will be explained below following the same order.

1. Plasma Confinement

Based on the bulk of the experimental results obtained in the last few years, there is a growing belief that particle and energy transport across the confining magnetic field is fairly well described by the neoclassical and pseudoclassical models. Within the framework of the first of these models the plasma parameters influencing diffusion can be divided in three major regimes: (I) the collision dominated, (II) the indermediate, and (III) the long-mean-free path regime. It is only in the latter where differences between the diffusion in axissymmetric and nonaxissymmetric configurations are expected from theory. In addition to the asymmetries inherent in any practically produced toroidal main field (ripple) which are present in both Stellarators and Tokamaks, the helical windings of a Stellarator produce an additional modulation, ε_H, of the field strength along the magnetic lines of force. For the W VII, ε_h is typically 20 % of ε_t, the modulation of B caused by the rotational motion of the lines of force in the main toroidal field. The diffusion coefficient, D, is plotted qualitatively (in Fig. 1) showing, in the long mean

+) According to the reasons given later, this item is to be developed along a separate line in order to have such technology available when required by the experimental results.

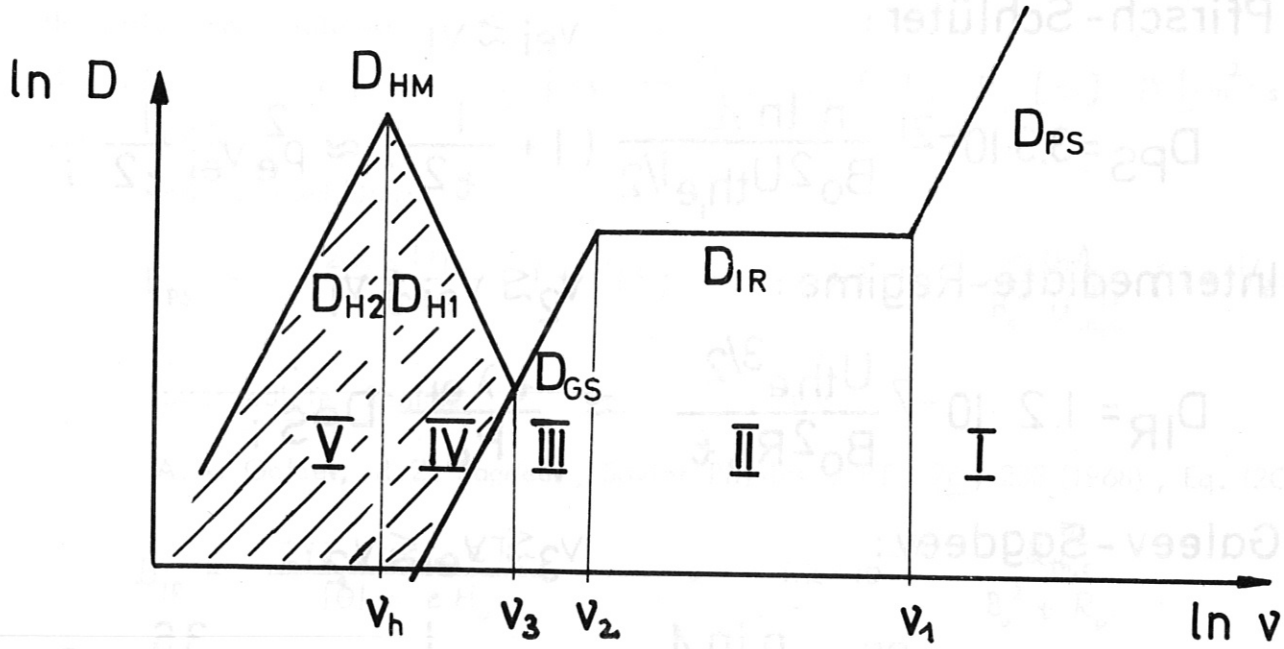

Fig. I

free path regime, the cases with (D_H) and without (D_{GS}) helical mirrors. In Tables I - III the relevant formulae are given together with plots of the corresponding plasma parameters for W VII. These show, for instance, that the influence of the localized particles would play a role whenever $U_{th}^2/n \gtrsim 10^{-7}$ $V^2 cm^{3+)}$. It follows from this criterium that, depending on the value of the working temperature, localized particle diffusion might not become too severe even in a fusion reactor. Evidence for the presence of this effect is expected in W VII with plasma produced by neutral injection methods with not too high beam intensities. An example is shown under item 4) of this paper. However, even in case the localized particles

---

+) $kT = eU_{th}$,

TABLE I

Diffusion Coefficients:

I Pfirsch-Schlüter: $\nu_{ei} \gtrsim \nu_1$

$$D_{PS} = 3.3 \cdot 10^{-21} \frac{n \ln \Lambda}{B_0^2 U_{th,e}^{1/2}} \left(1 + \frac{1}{t^2}\right) \approx \rho_e^2 \nu_{ei} \frac{1}{t^2} ;$$

II Intermediate-Regime: $\nu_2 \lesssim \nu_{ei} \lesssim \nu_1$

$$D_{IR} = 1.2 \cdot 10^{-7} \frac{U_{th,e}^{3/2}}{B_0^2 R_0 t} \approx \frac{t \lambda_{ei}}{R_0} D_{PS} ;$$

III Galeev-Sagdeev: $\nu_3 \lesssim \nu_{ei} \lesssim \nu_2$

$$D_{GS} = 1.71 \cdot 10^{-20} \frac{n \ln \Lambda}{B_0^2 U_{th,e}^{1/2}} \frac{1}{t^2 \varepsilon_t^{3/2}} \approx \frac{3.6}{\varepsilon_t^{3/2}} D_{PS} ;$$

IV Helical Mirrors: $\nu_h \lesssim \nu_{ei} \lesssim \nu_3$

$$D_{HI} \approx \frac{\nu_h}{\nu_{ei}} D_{HM} = 4.65 \cdot 10^5 \frac{\varepsilon_h^{3/2}}{R_0^2} \frac{U_{th,e}^{7/2}}{\ln \Lambda \, n \, B_0^2} \approx$$

$$\frac{1}{2} \varepsilon_h^{3/2} \left(\frac{\lambda_{ei} t}{R_0}\right)^2 D_{PS} ;$$

V Helical Mirrors: $\nu_{ei} \lesssim \nu_h$

$$D_{H2} \approx \frac{\nu_{ei}}{\nu_h} D_{HM} = 2.1 \cdot 10^{-6} \frac{\varepsilon_t^3 R_0^2}{\varepsilon_h^{3/2}} \frac{n \ln \Lambda}{U_{th,e}^{3/2}} \approx$$

$$\frac{1}{2} \frac{\varepsilon_t^3}{\varepsilon_h^{3/2}} \left(\frac{R_0 t}{\rho_e}\right)^2 D_{PS} ;$$

where $D_{HM} = 1/2 \, \varepsilon_t^{3/2} \nu_{ei} \lambda_{ei} \rho_e$;

Bohm: $D_B = \frac{U_{th,e}}{16 B_0}$ for all ν_{ei}

T a b l e Ia

Comparison of the different numerical constants for the Diffusion coefficients as used in the various computations:

Dimensions: $n\ [cm^{-3}]$, $B_o\ [Vs/cm^2]$, $U_{th}\ [V]$, $R_o\ [cm]$, $D\ [cm^2/s]$

1.) Table I :

Pfirsch - Schlüter:

$$D_{PS} = \frac{2 n k T \eta_\perp}{B^2}\left(1 + 1/t^2\right) \longrightarrow 3.3 \cdot 10^{-21} \frac{n \ln\Lambda}{B_o^2 U_{th,e}^{1/2}}\left(1 + 1/t^2\right)$$

Intermediate Regime:

A.A. Galeev, R.Z. Sagdeev, Soviet Physics JEPT, 26, 233 (1968), Eq. (20);

$$D_{IR} = \frac{2\sqrt{\pi}\,\varepsilon^2 r_{ce}\, c T_e}{|\Theta|\, r\, e H_o} \longrightarrow 1.2 \cdot 10^{-7} \frac{U_{th,e}^{3/2}}{B_o^2\, t\, R_o}$$

Galeev - Sagdeev :
Eq. (42) of the above paper:

$$D_{GS} = 3.6 \frac{\nu_e r_{ce}^2}{\varepsilon^{3/2}} \frac{4\pi^2}{l^2} \longrightarrow 1.71 \cdot 10^{-20} \frac{n \ln\Lambda}{B_o^2 U_{th,e}^{1/2}} \frac{1}{t^2 \varepsilon_t^{3/2}}$$

2.) Numerical Computations on Ohmic Heating by Dr. Girard:

$$D_{PS} = 5.7 \cdot 10^{-4} \frac{n_e\left(1 + 1/t^2\right)}{T_e^{1/2} B^2\,[Gauß]} \xrightarrow{\ln\Lambda = 15} 3.8 \cdot 10^{-21} \frac{n \ln\Lambda}{B_o^2 U_{th,e}^{1/2}}\left(1 + 1/t^2\right)$$

$$D_{IR} = 2.4 \cdot 10^{7} \frac{T_e^{3/2}}{t\, B^2\,[Gauß]} \xrightarrow{R_o = 50\ cm} 1.2 \cdot 10^{-7} \frac{U_{th,e}^{3/2}}{B_o^2\, t\, R_o}$$

$$D_{GS} = 3.6 \frac{\nu_e r_{Le}^2}{\varepsilon^{3/2}} \left(\frac{2\pi}{\tau}\right)^2 \longrightarrow 1.71 \cdot 10^{-20} \frac{n \ln\Lambda}{B_o^2 U_{th,e}^{1/2}} \frac{1}{t^2 \varepsilon_t^{3/2}}$$

3.) Numerical computations on Neutral Injection:

$$D_{PS} = \rho_e^2 \nu_{ei} \frac{1}{t^2} \longrightarrow 4.75 \cdot 10^{-21} \frac{n \ln\Lambda}{B_o^2 U_{th,e}^{1/2}} \frac{1}{t^2}$$

$$D_{IR} = \frac{\rho_e}{R_o} \omega_{ce} \frac{\rho_e^2}{t} \longrightarrow 6.7 \cdot 10^{-8} \frac{U_{th,e}^{3/2}}{B_o^2 t R_o}$$

$$D_{GS} = 4.9 \rho_e^2 \nu_{ei} \frac{1}{t^2 \varepsilon_t^{3/2}} \longrightarrow 2.33 \cdot 10^{-20} \frac{n \ln\Lambda}{B_o^2 U_{th,e}^{1/2}} \frac{1}{t^2 \varepsilon_t^{3/2}}$$

TABLE II

Definitions and Abbreviations:

$\nu_{ei} = 4.2 \cdot 10^{-6}\, n \ln\Lambda / U_{th\,e}^{3/2}\ [s^{-1}]$ – electron-ion coll. frequency;

$$\nu_1 = \frac{t\ \lambda_{ei}}{R_o}\ \nu_{ei}\ [s^{-1}];$$

$$\nu_2 = \varepsilon_t^{3/2}\ \nu_1\ [s^{-1}];$$

$$\nu_3 = 2.68\ \frac{1}{\alpha^{3/4}\,\varepsilon^{3/2}\,t}\ \frac{R_o}{\lambda_{ei}}\ \nu_{ei}\ [s^{-1}];$$

$$\nu_h = \alpha^{3/2}\ \frac{\lambda_{ei}\,\rho_e}{R_o^2}\ \nu_{ei}\ [s^{-1}];$$

$\lambda_{ei} = 1.4 \cdot 10^{13}\ U_{th,e}^2 / n \ln\Lambda$ [cm] – mean free path;

$\rho_e = 3.36 \cdot 10^{-8}\ U_{th,e}^{1/2} / B_o$ [cm] – El. Larmor radius;

$\varepsilon_t = r_{PL} / R_o$; $\alpha = \varepsilon_h / \varepsilon_t \approx 0.2$ for W VII;

n = density $[cm^{-3}]$; $U_{th} \hat{=}$ temperature [V] $(kT \rightarrow eU_{th})$;

B_o = main magnetic field $[Vs/cm^2]$; R_o = large radius of the vessel [cm]; r_{PL} = plasma radius [cm] D = diffusion coefficient $[cm^2\,s]$;

Influence of Helical Mirrors:

$$\frac{D_{HI}}{D_{GS}} = 2.7 \cdot 10^{25}\ \frac{\alpha^{3/2}\,\varepsilon_h^3\,t^2}{R_o^2\ \ln^2\Lambda}\ \frac{U_{th\,e}^4}{n^2};$$

Example for W VII:

$\alpha = 0.2$; $\varepsilon_t = 0.15$; $t = 0.1$; $R_o = 215$ cm; $\ln\Lambda = 15$; $n = 10^{13}$;

$\frac{D_{HI}}{D_{GS}} \gtrsim 1$; for $U_{th,e} \gtrsim 2$ keV;

Tabelle III

$n = 10^{13}$; $R_o = 215$ cm ; $r_{PL} = 30$ cm ; $B_o = 3.5 \cdot 10^{-4}$ Vs / cm^2 ; $\ln \Lambda = 15$;

U_{th}, e V	10			10^2			10^3			10^4		
diffusion regime	collision dominated (PS)			intermediate regime (IR)			long mean free path (GS)			GS		
t	0.1	0.23	0.5	0.1	0.23	0.5	0.1	0.23	0.5	0.1	0.23	0.5
D [cm^2/s]	130	25	6.4	46	20	9.1	1300	240	57	400	76	16
τ_p [s]	1.2	6.2	24	3.4	7.8	17	0.12	0.65	3.1	0.39	2.1	9.7
D_B / D	14	72	280	390	900	$2 \cdot 10^3$	140	750	$3.5 \cdot 10^3$	$4.5 \cdot 10^3$	$2.4 \cdot 10^4$	$1.1 \cdot 10^5$
D_B [cm^2/s]	$1.8 \cdot 10^3$			$1.8 \cdot 10^4$			$1.8 \cdot 10^5$			$1.8 \cdot 10^6$		
β	$6.7 \cdot 10^{-6}$			$6.7 \cdot 10^{-5}$			$6.7 \cdot 10^{-4}$			$6.7 \cdot 10^{-3}$		
E_{PL} [Ws]	120			$1.2 \cdot 10^3$			$1.2 \cdot 10^4$			$1.2 \cdot 10^5$		
V_D / V_S (t = 0,5)	19, 3			6.1			1.93			0.61		

$$\tau_p = \left(\frac{r_{PL}}{2.4}\right)^2 \frac{1}{D} \quad ; \quad \beta = 8.05 \cdot 10^{-27} \, U_{th} \, n / B_o^2 \quad ; \quad E_{PL} = 4\pi^2 r_{PL}^2 \, R_o \, n \, e \, U_{th} \quad ;$$

$$V_D / V_S = 1.22 \cdot 10^{15} \, t / n \, U_{th}^{1/2}$$ (for a plasma current at half the Kruskal Limit : t = 0.5)

The effect of particles localised in the helical mirrors (Table I) has not been taken into account here.

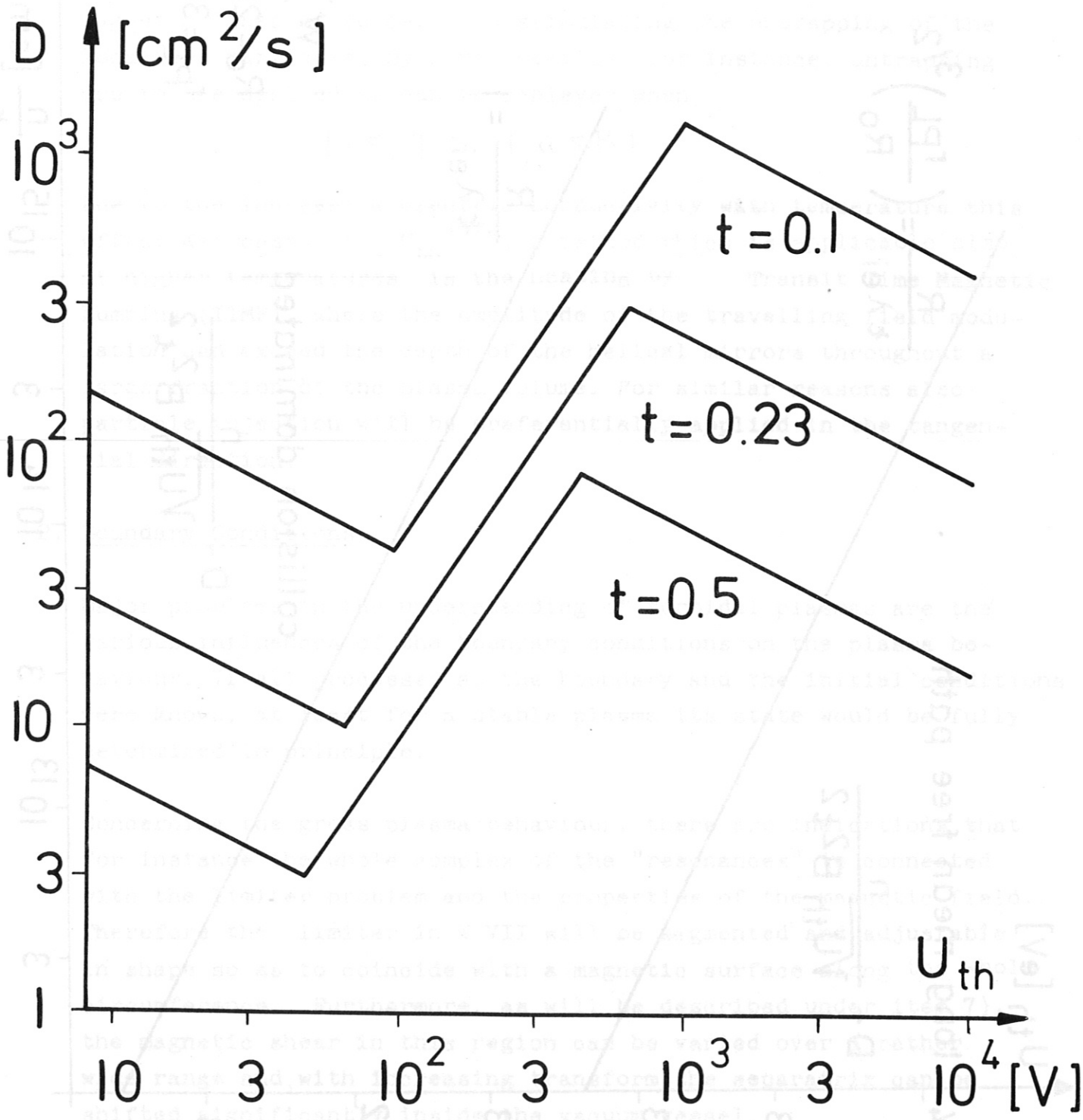
$n = 10^{13}$ [cm^{-3}]
$r_{PL} = 30$ [cm]
D [cm^2/s]
10^3
3
10^2
3
10
3
1
t = 0.1
t = 0.23
t = 0.5
U_{th}
10
3
10^2
3
10^3
3
10^4 [V]

Fig. 1a

Fig. 2

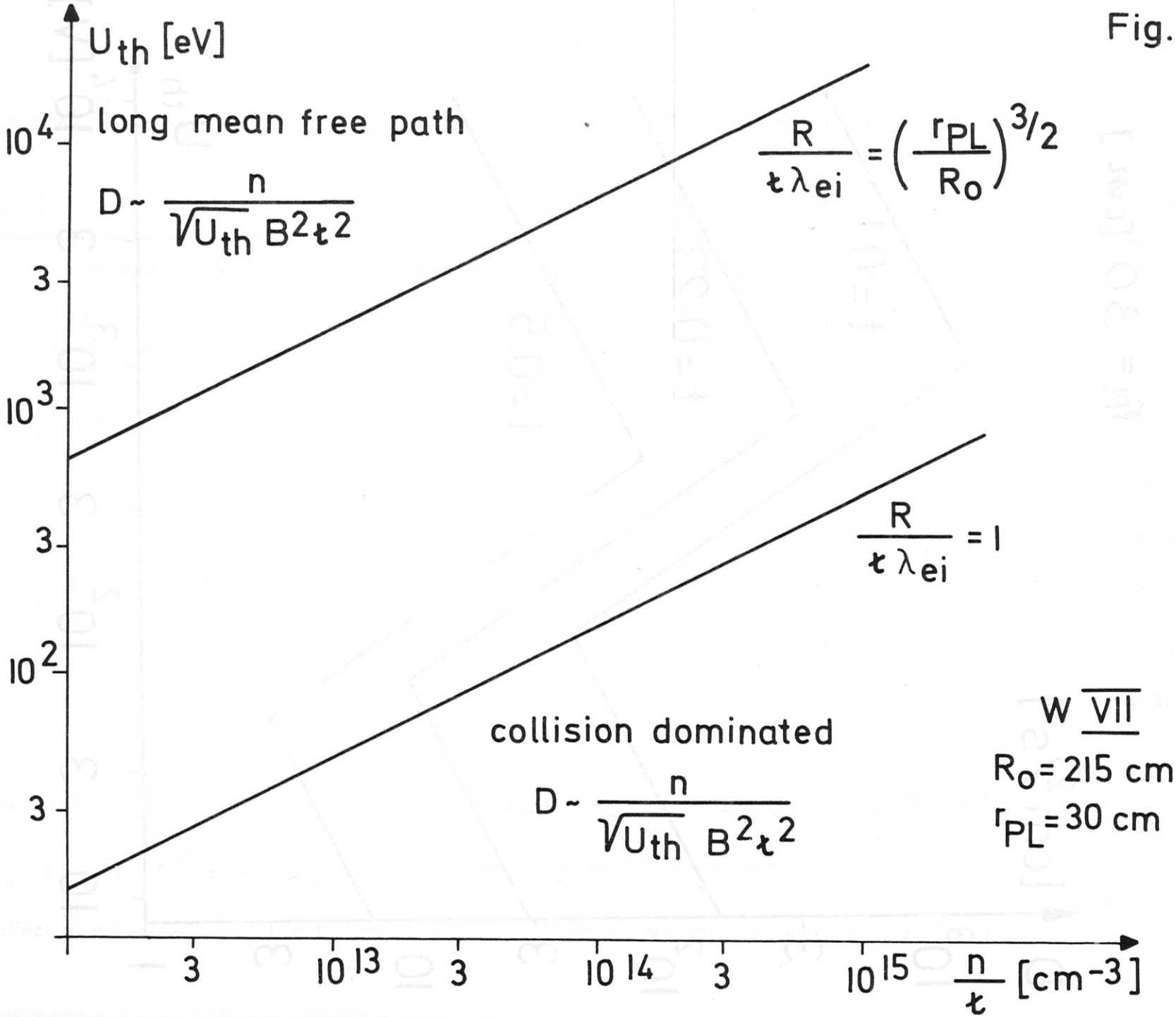
U_{th} [eV]
long mean free path
$D \sim \frac{n}{\sqrt{U_{th}}\, B^2 t^2}$
$\frac{R}{t\lambda_{ei}} = \left(\frac{r_{PL}}{R_0}\right)^{3/2}$
$\frac{R}{t\lambda_{ei}} = 1$
collision dominated
$D \sim \frac{n}{\sqrt{U_{th}}\, B^2 t^2}$
W VII
R_0 = 215 cm
r_{PL} = 30 cm
10^4
3
10^3
3
10^2
3
3
10^{13}
3
10^{14}
3
10^{15}
$\frac{n}{t}$ [cm^{-3}]

should pay a role for the containment of high temperature plasmas in Stellarators, methods are envisaged to control their influence. The basic idea is to favour the input of energy parallel to the magnetic lines of force, thus stimulating the untrapping of the localized particles. By ohmic heating, for instance, untrapping due to the applied $E_{\parallel}$ can be achieved when

$$|eE_{\parallel}| > |\mu \nabla B|$$

Due to the increasing electric conductivity with temperature this effect decreases with $U_{th}^{-5/2}$. A method which is applicable also at higher temperatures is the heating by Transit Time Magnetic Pumping (TTMP), where the amplitude of the travelling field modulation can exceed the depth of the helical mirrors throughout a large fraction of the plasma volume. For similar reasons also particle injection will be preferentially applied in the tangential direction.

2. Boundary Conditions

Major problems in the understanding of toroidal plasmas are the various influences of the boundary conditions on the plasma behaviour. If all processes at the boundary and the initial conditions were known, at least for a stable plasma its state would be fully determined in principle.

Concerning the gross plasma behaviour, there are indications that for instance the whole complex of the "resonances" is connected with the limiter problem and the properties of the magnetic field. Therefore the limiter in W VII will be segmented and adjustable in shape so as to coincide with a magnetic surface along the whole circumference. Furthermore, as will be described under item 7), the magnetic shear in this region can be varied over a rather wide range and, with increasing transform, the separatrix can be shifted significantly inside the vacuum vessel.

At least of equal interest, however, are the microscopic processes governing effects like recycling and heat transfer to the wall. Since heat conduction perpendicular to B by the ions can exceed energy losses via particle diffusion by a large factor, the plasma temperature at the boundary is of great importance; it is determined by the interaction processes between the plasma at the boundary and the surrounding neutral gas. Such processes are believed to be responsible for the continuous changes of the current distribution in presently existing Tokamaks, indicating no stationary state in such discharges might have been achieved yet. Considerations of the flux balance for a stationary surface layer on the wall lead to the conclusion that many particle life times may be required in order to constitute even quasi-stationary conditions. Operation of W VII in a steady or quasi-steady state should allow these problems to be more easily and independently investigated.

In order to support such experiments from the theoretical side, a numerical code is under development where the effects of the various individual processes can be isolated. For a given power input, recycling and heat transfer between plasma and wall determine not only the state of the plasma, but also, in case of neutral particle injection, whether a large flux of particles with a relatively low individual energy is required or a lower flux at high energy.

3. Comparison with Tokamaks

As in the smaller Stellarator Wendelstein W II b, ohmic heating is the standard method for producing a plasma with a density of $\sim 10^{13} cm^{-3}$ and, in the case of W VII, a temperature of several hundred electron volts. This plasma will then be subject to further studies.

The provision of vertical fields, of sufficiently high and long lasting loop voltages and of a stainless steel vessel wall, together with the plasma aperture of typically 60 - 70 cms, provide conditions which are close to the requirements for Tokamak operation during the ohmic heating phase. From the Princeton ST experiments it is concluded that the importance of the conventional Tokamak copper shell for plasma stability might have been overrated, and that, owing to the different regimes of operation, there is no clearcut evidence of a contradiction between the Model C and the ST results. In addition, a comparison between the URAGAN Stellarator and the T-3 Tokamak indicate agreement of the confinement properties when the Tokamak sealing is applied to Stellarator results. These facts may indicate that in the Stellarator W VII a mode of operation can be achieved which is closely related to that in Tokamaks of comparable dimensions. In Figures 3 - 5 graphs are shown for both a 20 cm and a 60 cm aperture ohmically-heated plasma. The results plotted there are from calculations by GIRARD[+)] (Fontenay-aux-Roses) using his ohmic heating code. For comparison, Fig. 6 shows estimates of the maximum value of T_i based on the empirical scaling given by ARTSIMOVICH et al. Similar results are obtained by simplified estimates using the neoclassical model and the heat transfer from electrons to ions. Also in this context it has to be stated that more information on the processes determining the boundary conditions is required in order to refine the models applied thus far.

The W VII machine is designed for producing and studying such plasmas within the whole range from typical and traditional Stellarator operation towards Tokamak operation. As indicated already by the first results of W II b, the independent control

---

+) We would like to thank Dr.J. Girard for applying his code to the parameters of W VII.

Fig. 3

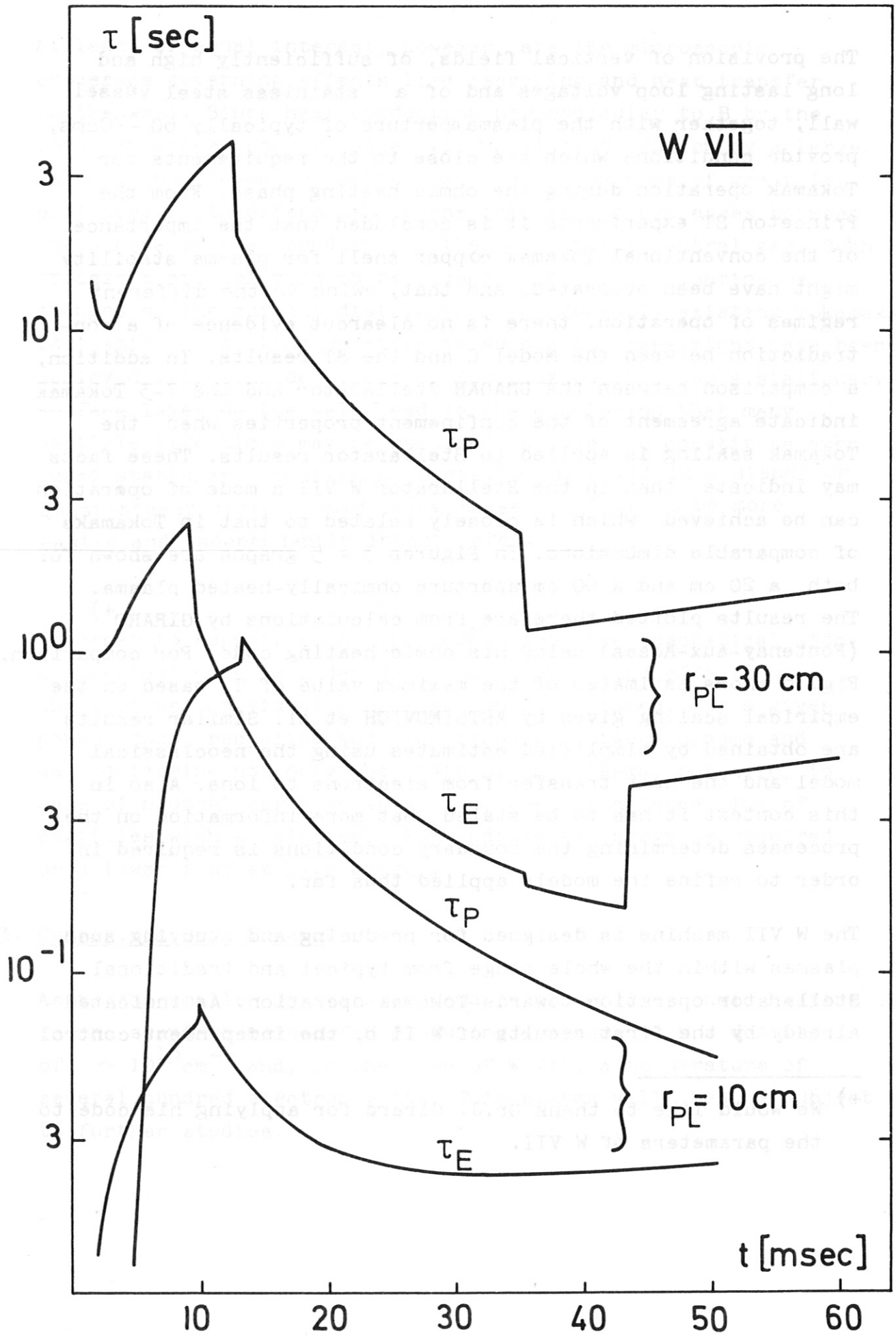
τ [sec]
W VII
3
10¹
3
10⁰
3
10⁻¹
3
τP
τE
τP
τE
r_PL = 30 cm
r_PL = 10 cm
t [msec]
10
20
30
40
50
60

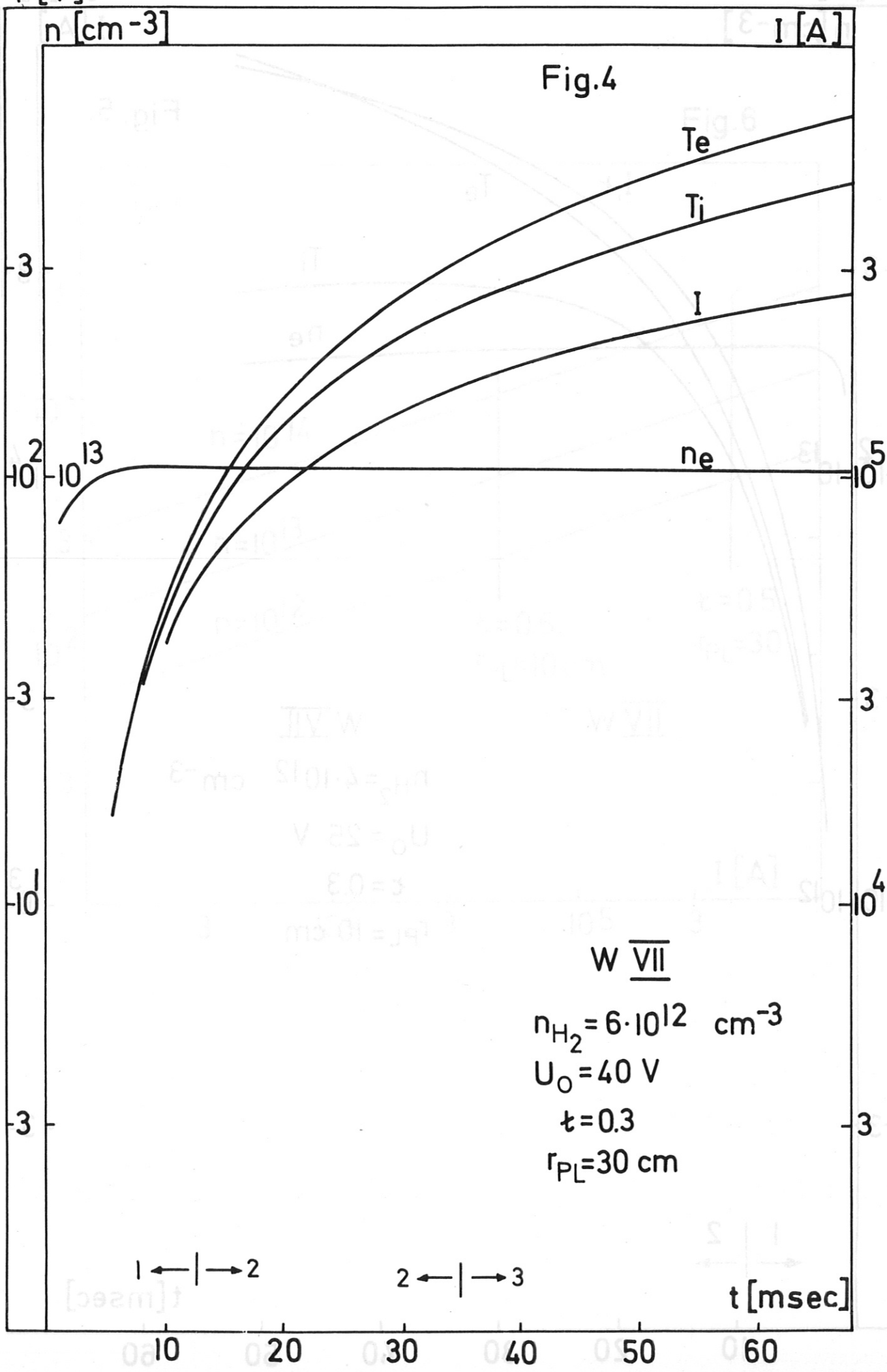
T [V]
n [cm⁻³]
I [A]
Fig.4
Te
Ti
I
ne
10²
10¹³
10⁵
10¹
10⁴
3
W VII
n_H2 = 6·10¹² cm⁻³
U_O = 40 V
t = 0.3
r_PL = 30 cm
1 ← | → 2
2 ← | → 3
t [msec]
10
20
30
40
50
60

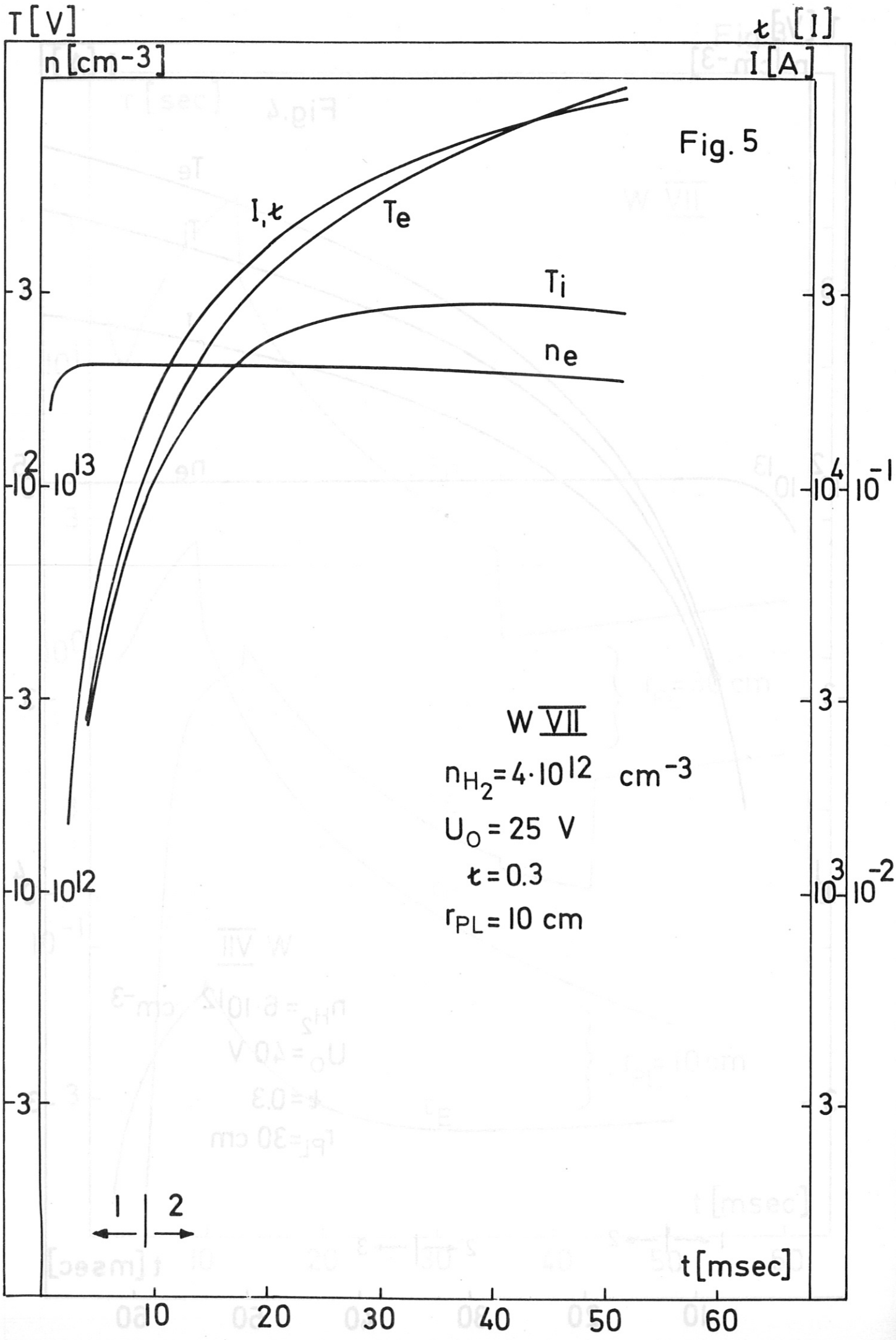
T[V]
t [I]
n[cm-3]
I[A]
Fig. 5
I, t
Te
Ti
ne
3
2
10
10^13
3
10
10^12
3
3
10^4
10^-1
3
10^3
10^-2
3
W VII
n_H2 = 4·10^12 cm^-3
U_0 = 25 V
t = 0.3
r_PL = 10 cm
1
2
t[msec]
10
20
30
40
50
60

Fig.6

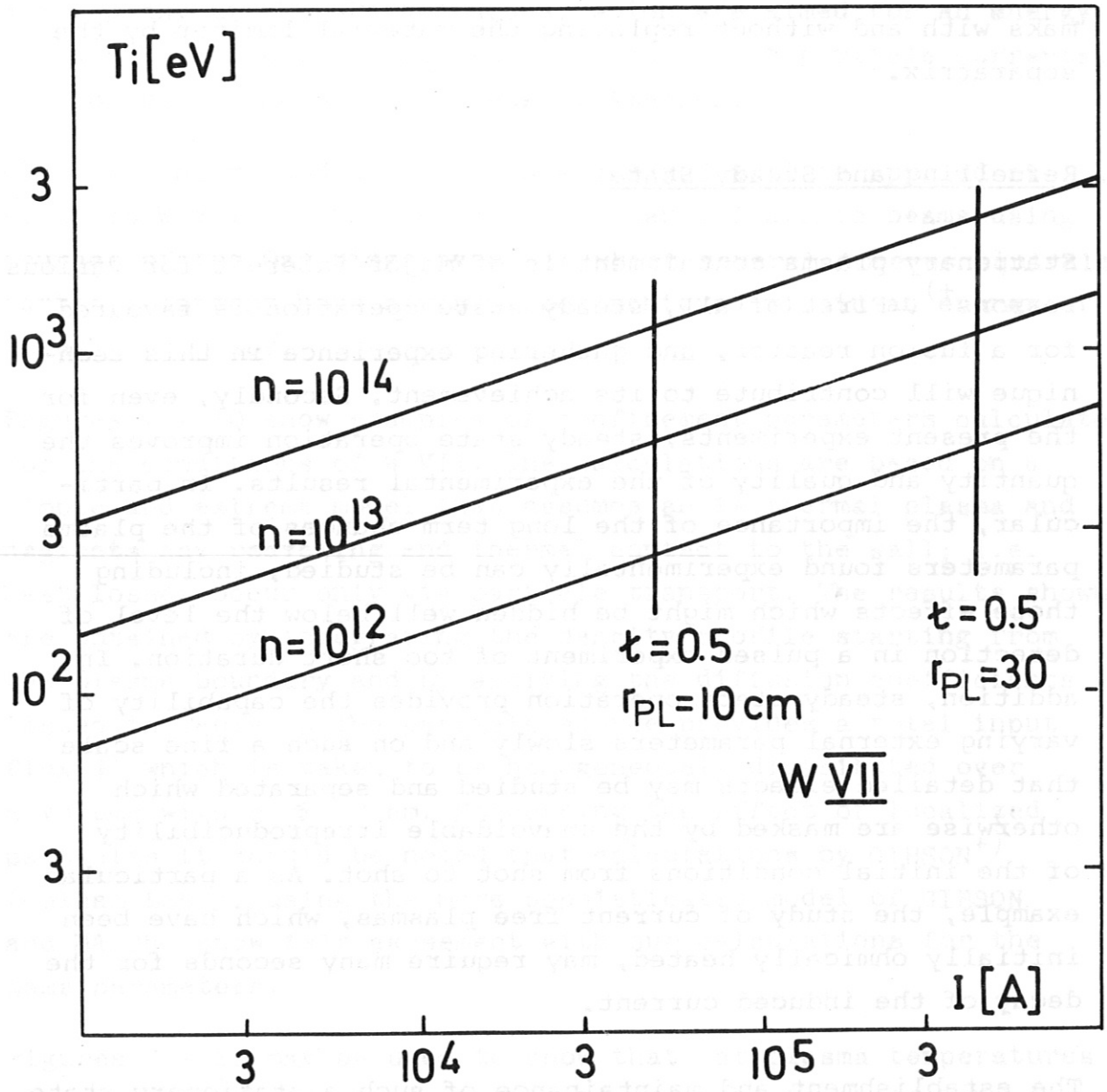
Ti[eV]
3
10^3
3
10^2
3
n=10^14
n=10^13
n=10^12
t=0.5
r_PL=10 cm
t=0.5
r_PL=30
W VII
I [A]
3
10^4
3
10^5
3

of rotational transform and plasma current will present a useful access to the physics of such discharges, and it will allow for a fair comparison between Stellarators and Tokamaks with and without replacing the material limiter by the separatrix.

4. Refuelling and Steady State

Stationary plasma containment is of major interest for various reasons[+)]. First of all, steady state operation is favoured for a fusion reactor, and gathering experience in this technique will contribute to its achievement. Secondly, even for the present experiments, steady state operation improves the quantity and quality of the experimental results. In particular, the importance of the long term changes of the plasma parameters found experimentally can be studied, including those effects which might be hidden well below the level of detection in a pulsed experiment of too short duration. In addition, steady state operation provides the capability of varying external parameters slowly and on such a fine scale that detailed effects may be studied and separated which otherwise are masked by the unavoidable irreproducibility of the initial conditions from shot to shot. As a particular example, the study of current free plasmas, which have been initially ohmically heated, may require many seconds for the decay of the induced current.

The establishment and maintainance of such a stationary state requires provision for replacement of the inherent particle and heat losses. Whereas for the balance of heat losses a whole spectrum of methods is generally proposed, the discussion on fuelling and refuelling is concentrated on neutral particle injection. The condition for the reinjected particles to carry at least an energy equal to the thermal energy of the plasma particles is not imposed primarily by heating purposes but, in contrast, to avoid additional heat losses occurring from charge exchange which is the dominant process at the temperatures of interest.

+) see also Appendix 2

There are promising prospects, that this condition can be met with postaccelerated beams of clusters, like these under development at the GFK Karlsruhe, which are aimed for an energy per atom up to several keV and for equivalent particle currents, Γ , of up to the order of tens of Amperes.

However, the method which it is envisaged will be applied at first to W VII is the injection of neutral atomic beams using sources of the Oak-Ridge type, in which several Amperes equivalent particle current have already been achieved within an energy of about 5 - 30 keV.

Figures 7 - 10 show examples of confinement parameters calculated for the conditions of W VII. The calculations are based on a simple and extreme model that assumes an isothermal plasma and neglects any recycling and thermal contact to the wall; i.e. heat losses occur only via particle transport. The results shown are obtained by integrating the density profile starting from the plasma boundary and by applying the diffusion coefficients listed in Table Ia.The particle source provides a total input flux Γ which is taken to be homogeneously distributed over a volume with $r \leq 10$ cm. Concerning the effect of localized particles it should be noted that calculations by GIBSON[+)] (Culham Lab.), using the more sophisticated model of GIBSON and MASON, show fair agreement with our calculations for the same parameters.

Figures 7 - 10 may be used to show that at plasma temperatures of about 1 keV and above the localized particles - if behaving as considered - might play an essential role unless the input flux is made sufficiently high. It should be stressed, however, that in case of substantial recycling two effects might occur counteracting the above mentioned "localized particle losses":

[+)] We gratefully acknowlidge the calculations of Dr. A. Gibson and the work done by Mrs. Colvin.

Fig.7

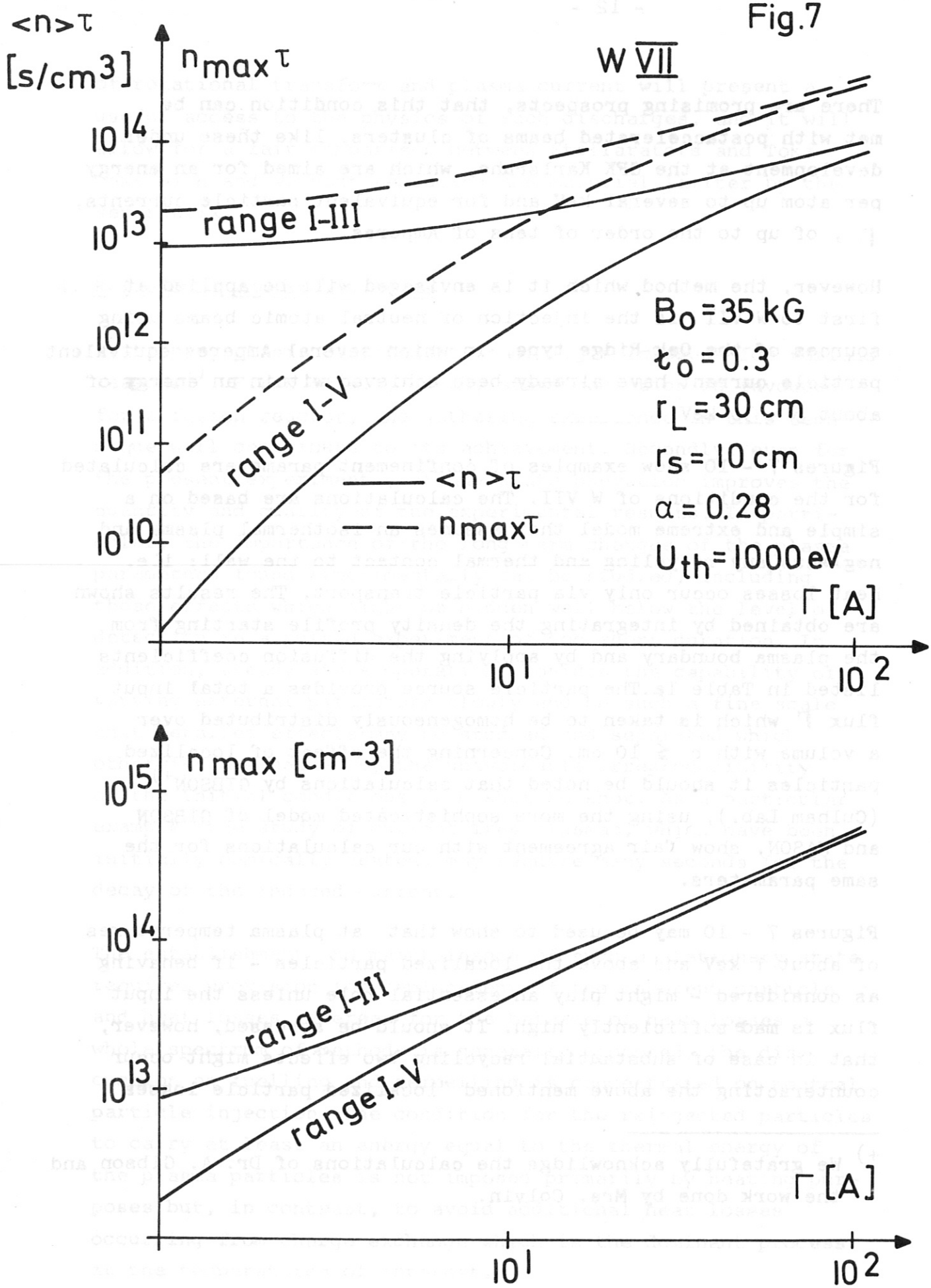
<n>τ
[s/cm3]
nmaxτ
W VII
10^14
10^13
10^12
10^11
10^10
range I-III
range I-V
<n>τ
nmaxτ
B0 = 35 kG
t0 = 0.3
rL = 30 cm
rs = 10 cm
α = 0.28
Uth = 1000 eV
Γ [A]
10^1
10^2
nmax [cm-3]
10^15
10^14
10^13
range I-III
range I-V
Γ [A]
10^1
10^2

Fig. 8

W VII

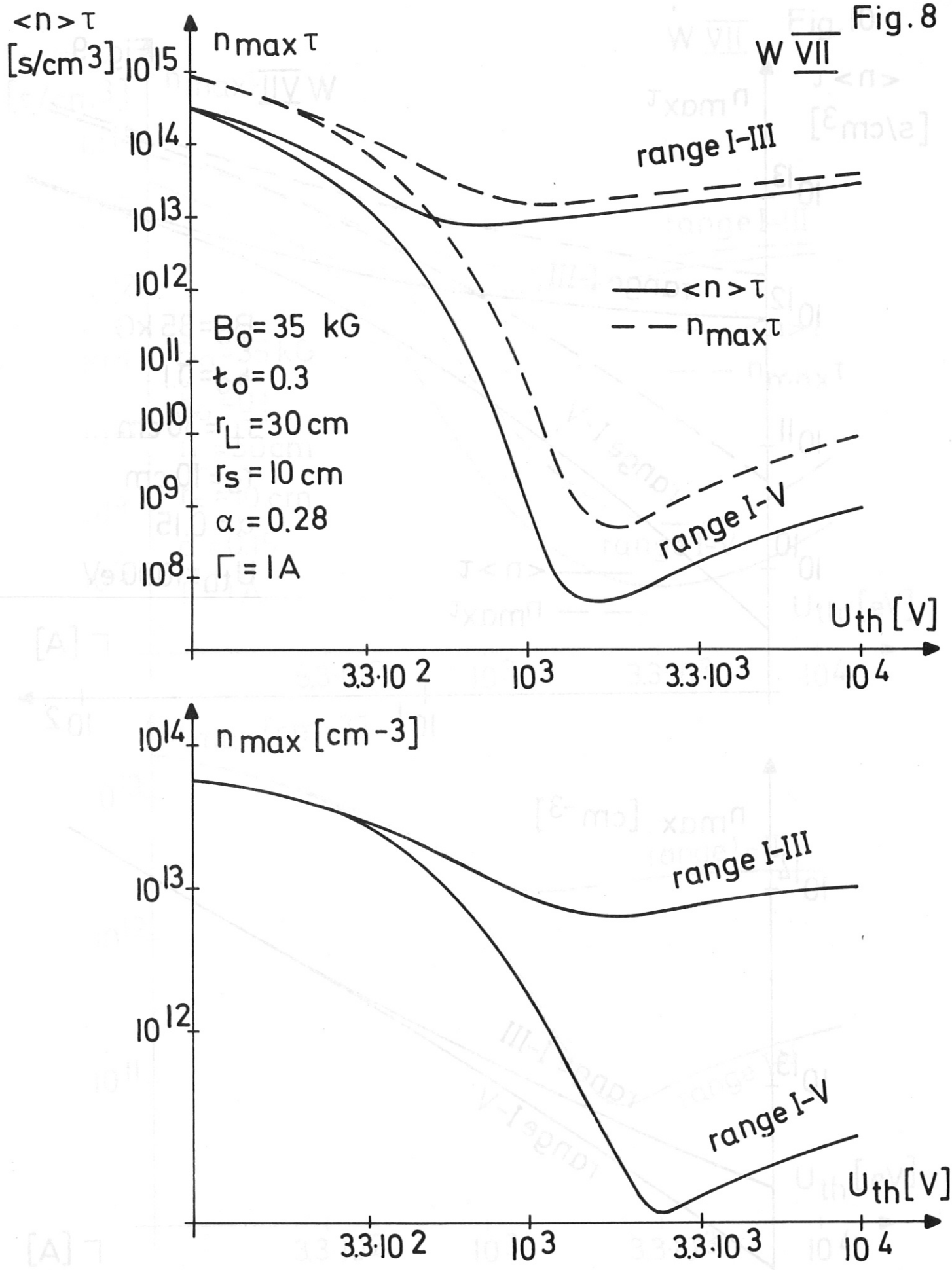

$$\langle n \rangle = \frac{\int n\,dV}{\int dV}\ ;\quad V = \text{volume}\ ;\quad \alpha = \frac{\varepsilon_H}{\varepsilon_t}\ ;\quad \left.\begin{matrix} r_L = \text{limiter} \\ r_s = \text{source} \end{matrix}\right\} \text{radius}$$

Fig. 9

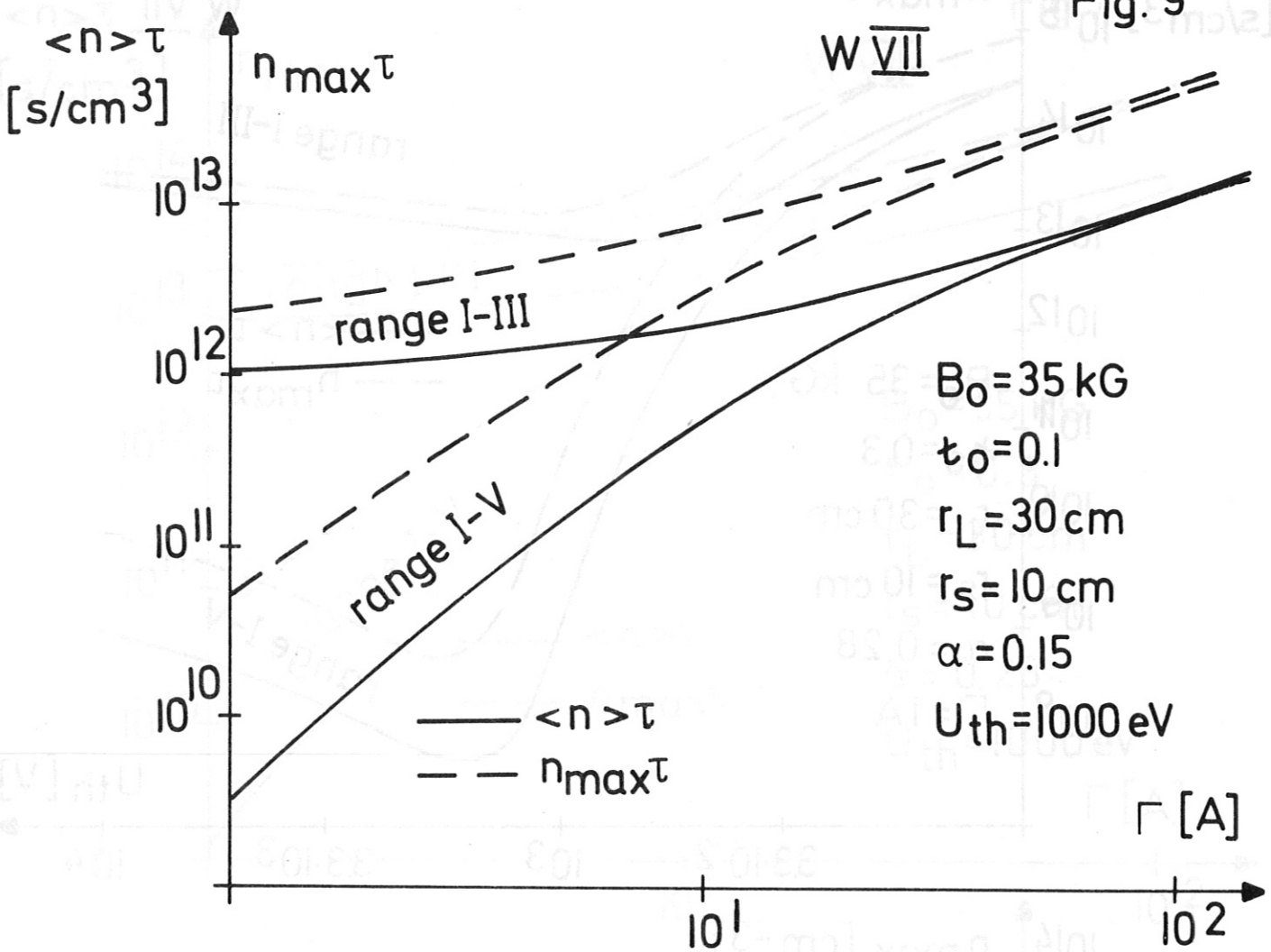
<n>τ [s/cm3]
nmaxτ
W VII
10^13
10^12
10^11
10^10
range I-III
range I-V
Bo=35 kG
to=0.1
rL=30 cm
rs=10 cm
α=0.15
Uth=1000 eV
<n>τ
nmaxτ
Γ [A]
10^1
10^2

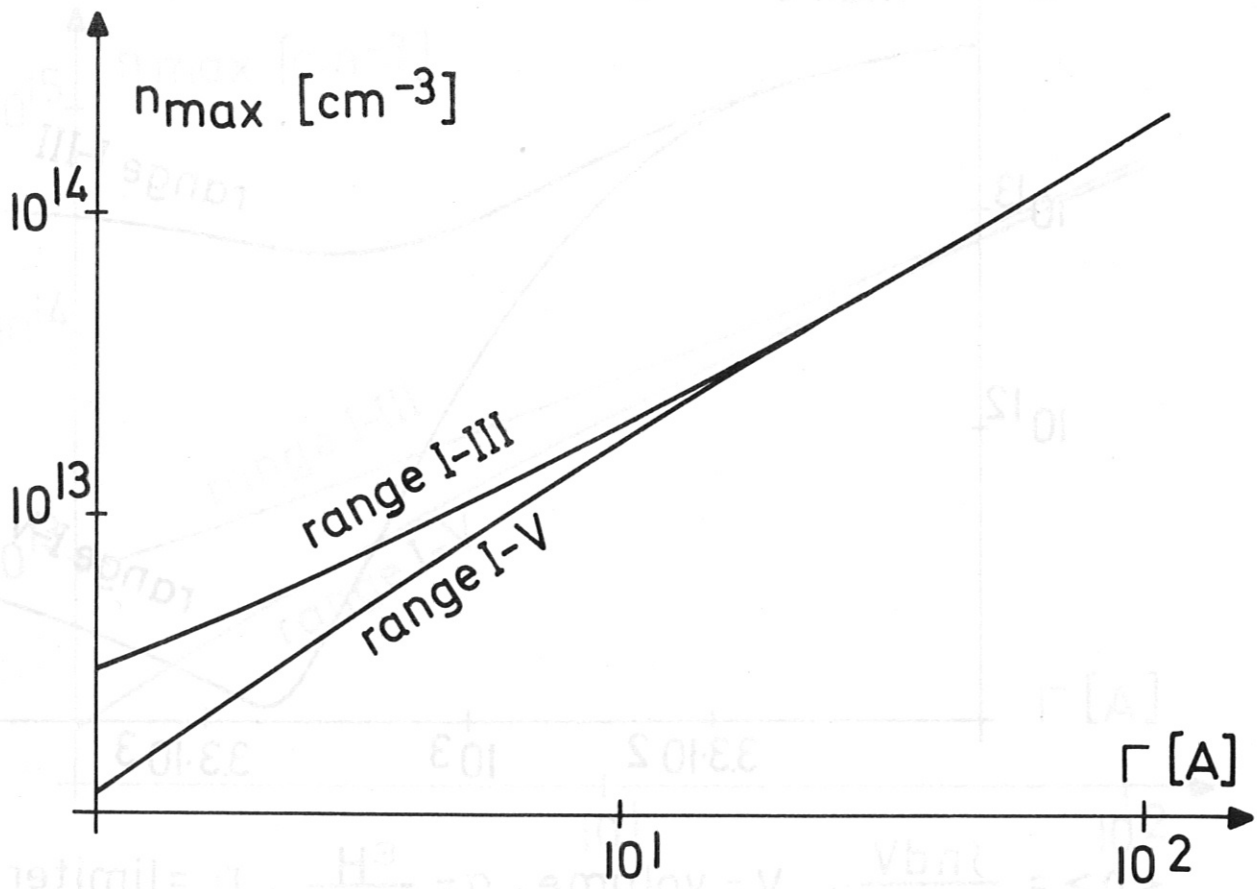
nmax [cm-3]
10^14
10^13
range I-III
range I-V
Γ [A]
10^1
10^2

W VII Fig.10

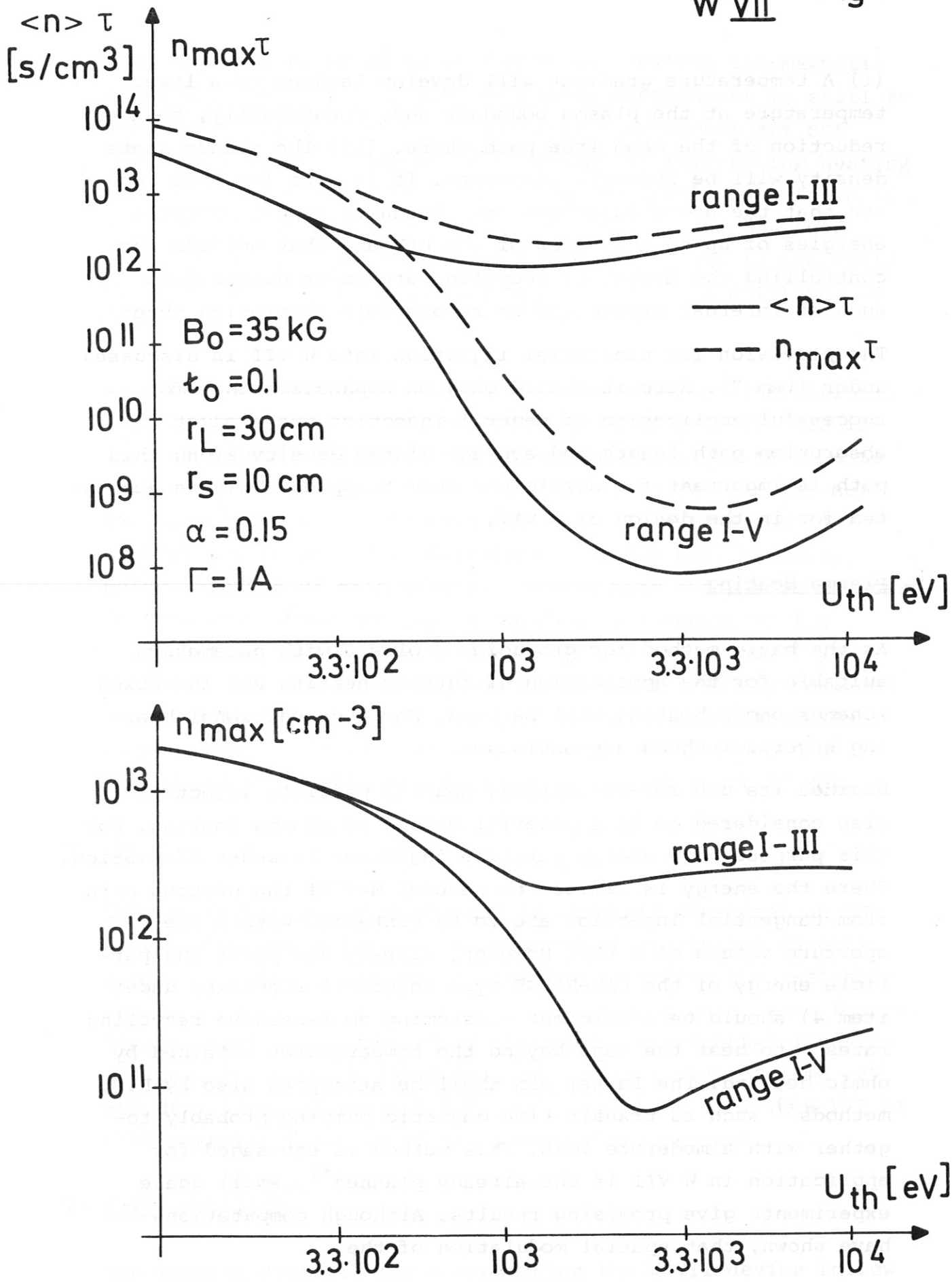

$\langle n \rangle = \frac{\int n dV}{\int dV}$; V=volume ; $\alpha = \frac{\varepsilon_H}{\varepsilon_t}$ r_L=limiter, r_s=source } radius

(i) A temperature gradient will develop leading to a lower temperature at the plasma boundary and, consequently, to a reduction of the mean free path there. (ii) The steady state density will be strongly increased. It is also for this reason that the above injectors are chosen to supply particle energies of up to the order of loo keV and that methods for controlling the amount of recycling are under discussion, such as internal cryo-pumps or recoverable absorption sheets.

The provision for tangential injection into W VII is discussed under item 7). Here it should only be emphasized that for successful application of neutral injection the product of absorption path length and average plasma density along this path is important for sufficient beam trapping. This is accounted for in the design of W VII.

5. Plasma Heating

As the basic method for producing a plasma with parameters suitable for the application of further heating and injection schemes ohmic heating will be used. For the additional heating several methods are envisaged.

Besides its use for refuelling, neutral particle injection is also considered to be a powerful method of plasma heating. For this purpose high energy particle injection is under discussion. There the energy is limited to several MeV if the protons born from tangential injection are to be contained within the aperture volume of W VII. However, already the power and particle energy of the OAK-RIDGE type injectors specified under item 4) should be sufficient - assuming no excessive recycling rates - to heat the ions beyond the temperatures obtained by ohmic heating. The latter aim shall be attempted also by R.F. methods[+)] such as transit time magnetic pumping probably together with a moderate ICRH. This method is envisaged for application in W VII if the already planned[+)] small scale experiments give promising results. Although computations have shown, that spatial modulation of the

---

[+)] A cooperation is being started within various EURATOM associated laboratories.

main magnetic field up to 10 % does not destroy the magnetic surfaces, the effect of TTMP on plasma containment is still an open question. If energy and particle containment are not severely affected, TTMP would represent an interesting heating method in which the energy input goes primerily into ion motion parallel to the magnetic field. Estimates of the RF-power required for heating factors of the order of one to ten yield about 20 MW with corresponding magnetic field modulations of about 1 %.

As a further heating method, quite distinct from conventional ohmic heating, A.C. ohmic heating is considered. If this is applied together with neutral injection one might be able to maintain a plasma free of D.C. currents, to replace the net particle and part of the heat losses by injection and to control the temperature distribution by the A.C. heating, which, because of skin effect, occurs near the plasma boundary. In this case ohmic heating is applied to a region of low conductivity and the energy losses of the electrons, from ionizing of the recycling neutrals, can be readily replaced. By adjusting the operating frequency, the thickness of the current sheath can be matched to the penetration depth of the recycling neutrals. This would happen at about 10 kHz.

6. The value of ß

The economy of a fusion reactor is strongly dependent on the plasma pressure which can be balanced by reasonable magnetic field strengths. According to present estimates the desirable values of ß are several percent. Limits on ß calculated theoretically require corresponding intensive experimental investigations. As shown in table III, for temperatures of some keV and densities of several 10^{13} cm^{-3} the value of ß in W VII at full magnetic field is of the order of one percent.

7. W VII Facility +)

The leading criteria for dimensioning the W VII device follow

+) See also page 31 and following. The technical figures here are previous to those given there.

from the scientific aims briefly discussed above. They are in particular:

a) For a high temperature plasma, lying in the long mean free path regime, the particle excursions from the magnetic surfaces, i.e. the values of ϱ_i, ϱ_i/t and $\varrho_i/t\sqrt{\epsilon_t}$ should be small compared to the plasma radius for a sufficiently large range of the magnetic field.

b) A sufficient length of the absorption path for neutral injection should be provided.

c) It should be possible to vary essential parameters such as magnetic field, rotational transform, shear, plasma radius and loop voltage over a sufficiently large and meaningful range.

d) The duration of the magnetic field configuration should be sufficiently long to allow for quasi-steady state discharge conditions. Genuine steady state operation should be possible when required by the experimental results.

e) Aperture, aspect ratio and main magnetic field should be similar to those of future large Tokamaks.

f) The device should be flexible enough to allow changes of both the magnetic field geometry and the mode of operation.

g) Space should be provided for a powerful ohmic heating air core transformer.

h) The ripple of the main field should be kept below the modulation arising from the current in the helical windings.

Compromises, governed also by cost, flexibility and reliability arguments, had to be made to arrive at the following machine parameters:

The main magnetic field is produced by 4o water-cooled copper coils (described in Appendix 5) giving 4o kG at R = 2oo cm. These coils are energized from a 1.4 GJ flywheel generator allowing for a flat-top pulse duration of about 12 sec once every 7 minutes. As shown in Fig. 11, by this design the ripple at the limiter does not exceed the order of 1 % and it is about 0.01 % on the magnetic axis.

Fig. 11

W VII

$$\varepsilon_r = \frac{1}{2}\,\frac{\Delta B}{B_0}$$

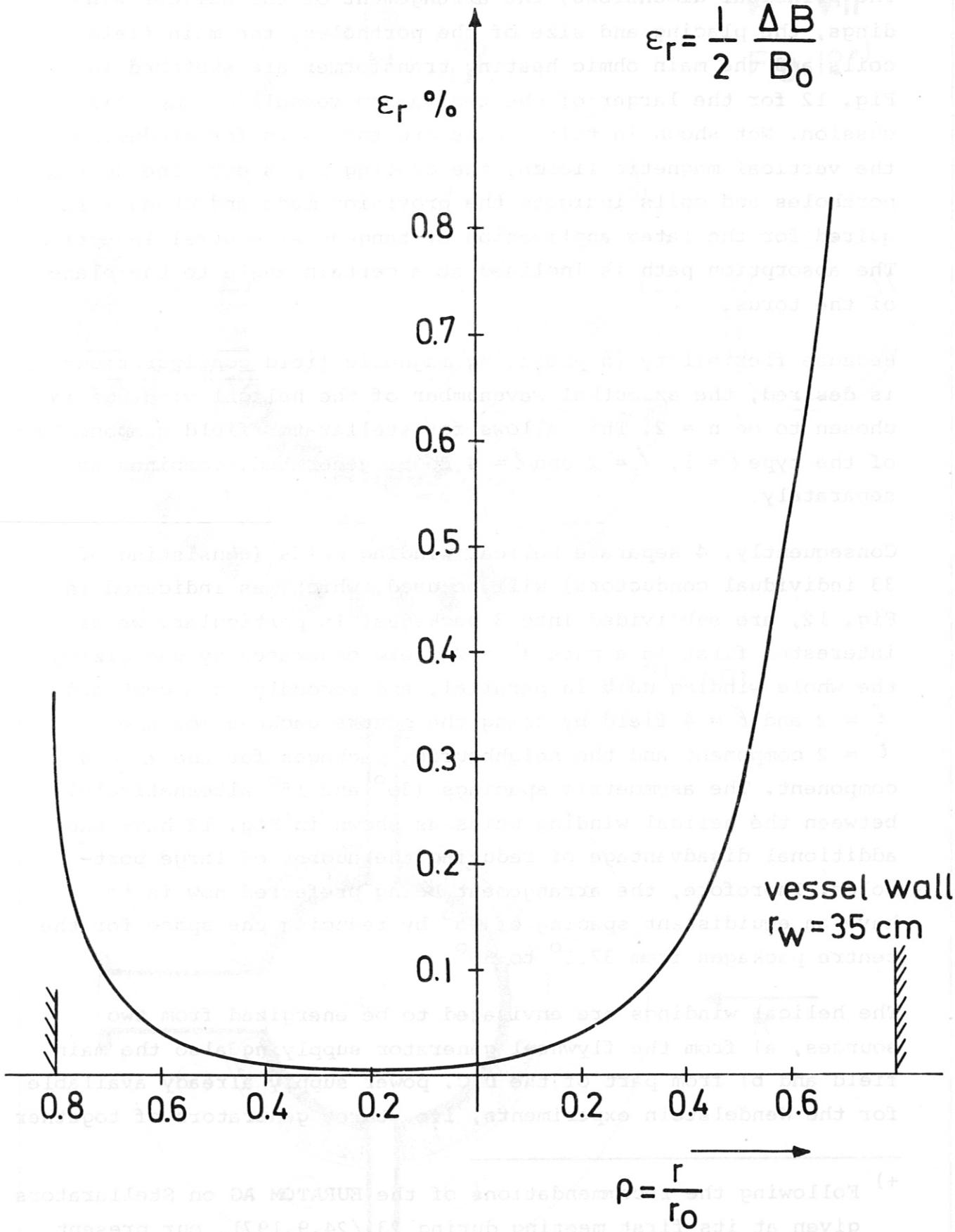

r_0: mean minor radius of hel. winding

The principal dimensions, the arrangement of the helical windings, the placing and size of the portholes, the main field coils and the main ohmic heating transformer are sketched in Fig. 12 for the larger of the two vacuum vessels[+)] under discussion. Not shown in this figure are the coils for producing the vertical magnetic fields, the cooling pipes etc. The dotted portholes and coils indicate the provision made and changes required for the later application of tangential neutral injection. The absorption path is inclined at a certain angle to the plane of the torus.

Because flexibility in producing magnetic field configurations is desired, the azimuthal wavenumber of the helical windings is chosen to be n = 2. This allows for stellarator field components of the type $\ell = 1$, $\ell = 2$ and $\ell = 4$ to be generated, combined or separately.

Consequently, 4 separate helical winding units (consisting of 33 individual conductors) will be used, which, as indicated in Fig. 12, are subdivided into 3 packages. In particular, we are interested first in a pure $\ell = 2$ field generated by energizing the whole winding unit in parallel, and secondly in a combined $\ell = 2$ and $\ell = 4$ field by using the centre package for the $\ell = 2$ component and the neighbouring packages for the $\ell = 4$ component. The asymmetric spacings (30° and 15° alternatively) between the helical winding units as shown in Fig. 12 have the additional disadvantage of reducing the number of large portholes. Therefore, the arrangement being preferred now is to have an equidistant spacing of 30° by reducing the space for the centre packages from 37.5° to 30°.

The helical windings are envisaged to be energized from two sources, a) from the flywheel generator supplying also the main field and b) from part of the D.C. power supply already available for the Wendelstein experiments, i.e. three generators of together

---

+) Following the recommendations of the EURATOM AG on Stellarators given at its first meeting during 23./24.9.1971, our present intention concentrates on the larger vacuum vessel.

W VII

Fig. 12*)

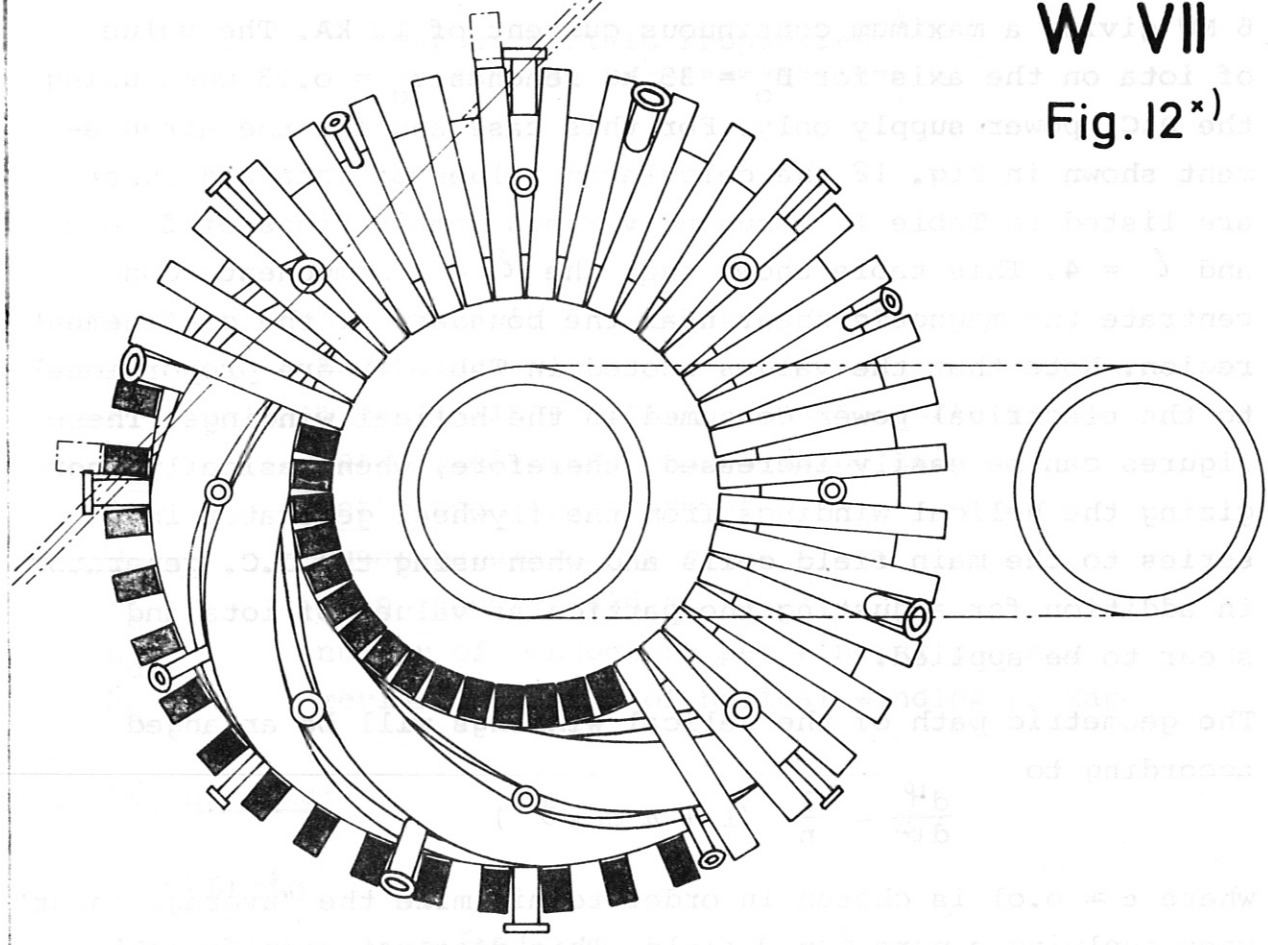

$R_0 = 215$ cm

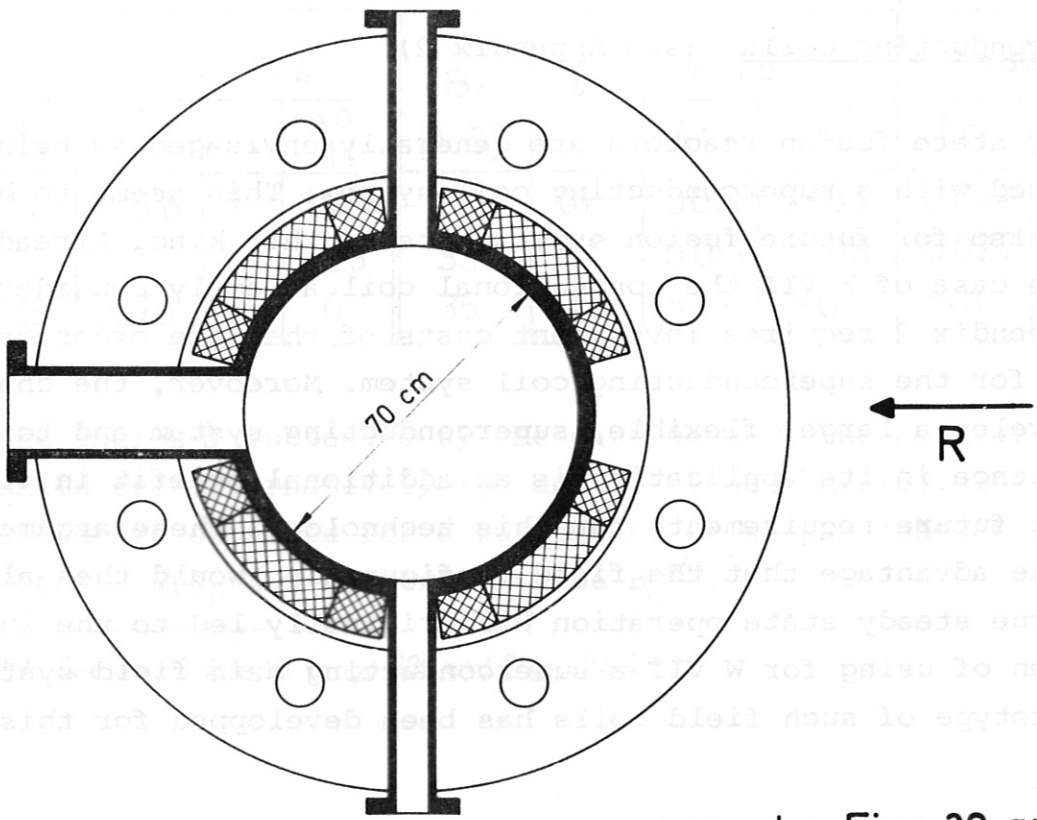

*) see also Figs. 30 and 34

6 MW giving a maximum continuous current of 12 kA. The value of iota on the axis for B_o = 35 kG reaches t_o = o.23 when using the D.C. power supply only. For this case and for the arrangement shown in Fig. 12 the calculated values of iota and shear are listed in Table IV assuming various combinations of ℓ = 2 and ℓ = 4. This table shows that the ℓ = 4 components concentrate the magnetic shear near the boundary of the confinement region. Note that the values quoted in Table IV are proportional to the electrical power consumed in the helical windings. These figures can be easily increased, therefore, when basically energizing the helical windings from the flywheel generator in series to the main field coils and when using the D.C. generator in addition for adjusting the particular values of iota and shear to be applied.

The geometric path of the helical windings will be arranged according to

$$\frac{d\varphi}{d\vartheta} = \frac{1}{n} \quad (1 + \alpha \cos \vartheta)$$

where $\alpha \approx$ o.ol is chosen in order to minimize the "average shear" when applying a pure ℓ = 2 field. This does not significantly affect the average magnetic well depth.

8. Superconducting Coils (see Appendix 2)

Steady state fusion reactors are generally envisaged as being equipped with a superconducting coil system. This seems to hold true also for future fusion experiments of this kind. Already in the case of W VII the conventional coil assembly considered in Appendix 2 requires investment costs of the same order as those for the superconducting coil system. Moreover, the chance to develop a large, flexible, superconducting system and to gain experience in its application is an additional benefit in view of the future requirements for this technology. These arguments and the advantage that the field configuration would then allow for true steady state operation had originally led to the intention of using for W VII a superconducting main field system. A prototype of such field coils has been developped for this

TABLE IV

Magnetic Field Properties[+)]

Symbols:

l	multiplicity of helical windings
R_o	major radius
r	average minor radius of magn. surface
t_o	rotational transform at magn. axis
t_r	rotational transform at r
Θ_r	shear parameter at r
B_o	main magnet. field at R_o
n_c	number of conductors per winding package
ϑ_H	meridional angle of helical winding package

Definitions:

$$\Delta t_r = t_r - t_o$$

$$\Theta_r = \frac{r2}{R_o} \frac{dt_r}{dr} \cdot 100\ [\%]$$

l = 2		l = 4		B_o	t_o	r = 25		r = 30	
n_c	ϑ_H^o	n_c	ϑ_H^o	[kG]		Δt_r	Θ_r	Δt_r	Θ_r
19	38.8	7	14.3	30.3	0.1	0.021	0985	0.044	2.46
21	43	6	12.3	33.5	0.1	0.013	0606	0.027	1.48
33	67.5	0	0	35	0.23	≈0.	≈0.	≈.0	≈0.

The angles ϑ subtended by the gaps between the helical winding units are alternatively 15^o and 30^o (see Fig. 12). The values shown are obtained for a current of 12 KA per conductor. t_o, Θ_r and Δt_r are proportional to B_o^{-2}.

+) See also Table VI (page 33) and Figs. 26-29.

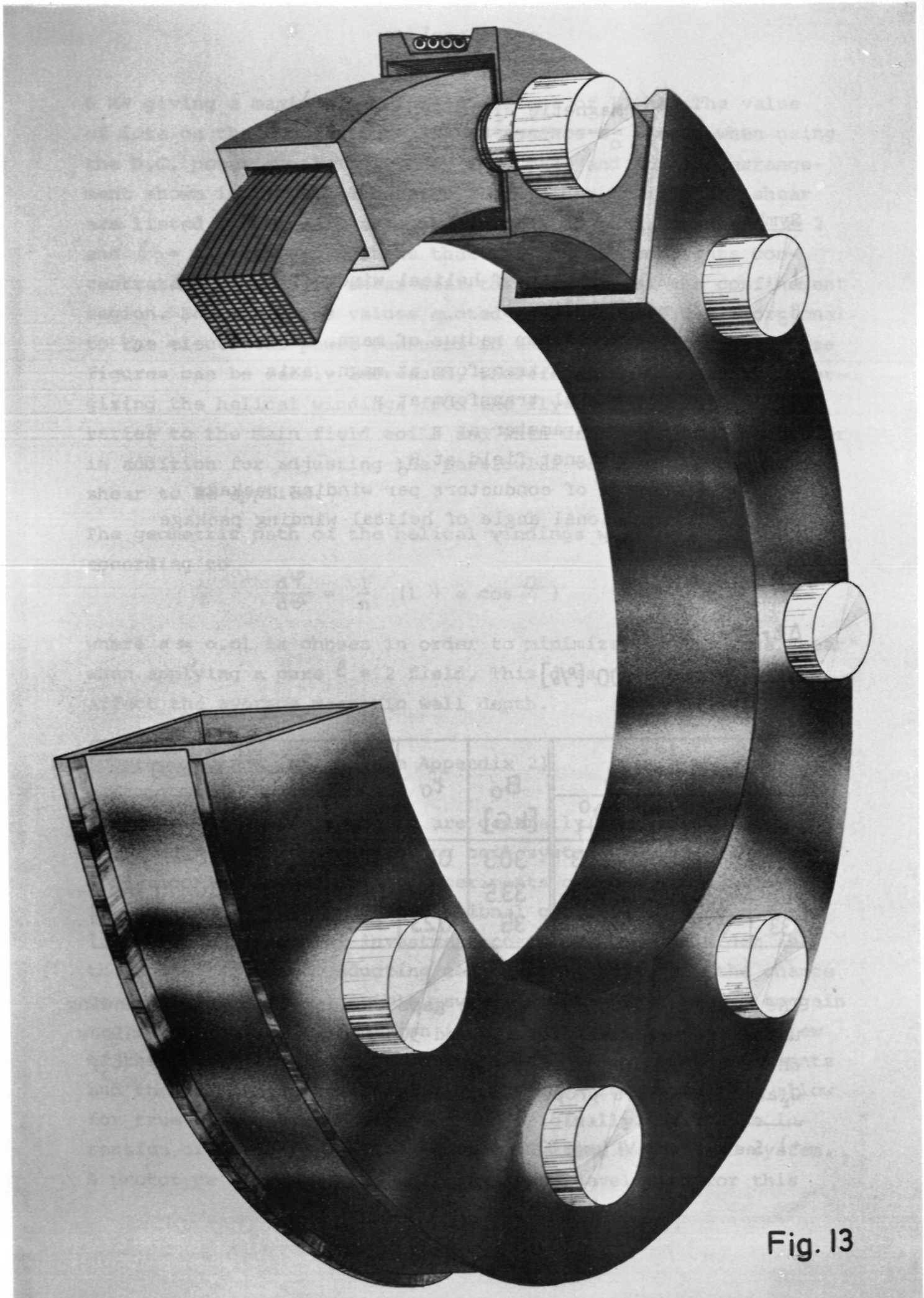

Fig. 13

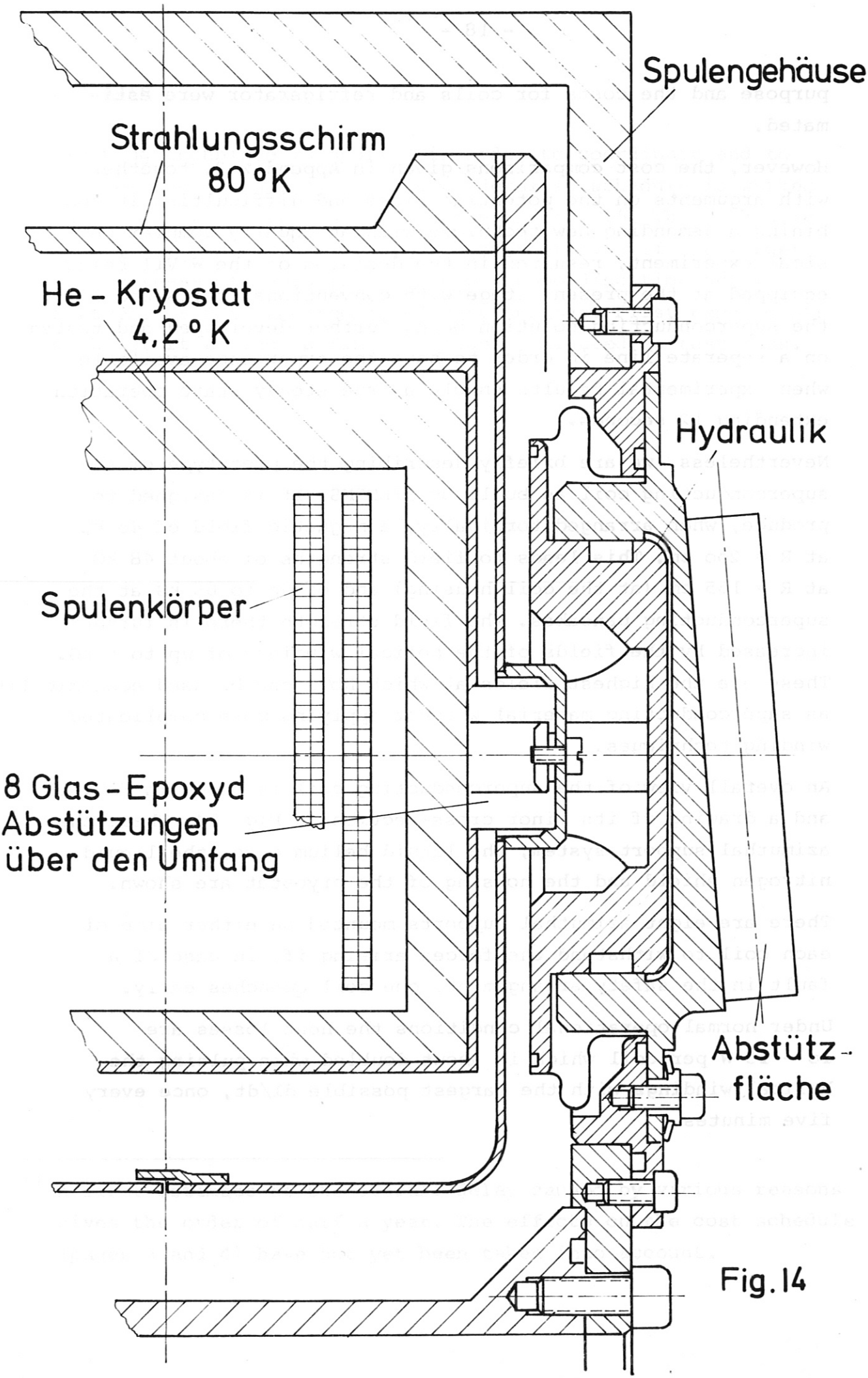
Spulengehäuse
Strahlungsschirm
80 °K
He - Kryostat
4,2 °K
Hydraulik
Spulenkörper
8 Glas - Epoxyd
Abstützungen
über den Umfang
Abstütz-
fläche

Fig. 14

purpose and the costs for coils and refrigerator were estimated.

However, the cost comparisons given in Appendix 2, together with arguments on the potential risks and difficulties in combining a demanding new technique with an equally complex physical experiment, resulted in the decision of the W VII being equipped at the present stage with conventional coils and of the superconducting solution being further developped and tested on a seperate line in order to have the experience available when experimental results enable a true steady state operation extending 12 seconds.

Nevertheless, we are briefly describing the prototype of the superconducting coil as built by SIEMENS. It is designed to produce, when arranged toroidally, a magnetic field of 4o kG at R = 2oo cm. This leads to field strengths of about 48 kG at R = 165 cm (at the coil housing) and of up to 65 kG at the superconducting pancakes. The field strength there is further increased by the fields of the helical windings of up to 5 kG. These are the highest fields at which NbTi can be used economically as superconducting material without applying more complicated winding techniques.

An overall view of the superconducting coil is shown in Fig. 13 and a drawing of its minor cross-section in Fig. 14. There the azimuthal support system, the liquid helium case, the liquid nitrogen shield and the housing of the cryostat are shown.

There are eight azimuthal supports mounted on either side of each coil to withstand the forces arising if, in case of a fault in the safety arrangement, one coil quenches early.

Under normal operational conditions the heat losses are 1o - 15 W per coil which is about doubled when pulsing the helical windings with the largest possible dI/dt, once every five minutes.

9. Schedule

Planning technique is applied in order to coordinate and to control the various operations. A detailed schedule is worked out, an extract from which is shown in Fig. 15. This schedule is not yet corrected[+)] for the changes arising if the larger vacuum vessel is used first. The corresponding time delay, however, is not expected to be very serious. First experiments might start already during the phase indicated as test runs.

+) A first estimate of the overall delay caused by various reasons gives the order of half a year. The effects on the cost schedule (pages 3 and 4) have not yet been taken into account.

APPENDIX 2 to

Project Wendelstein W VII

Application for EURATOM preferential support

MAIN FIELD SYSTEM

- Time Scales -

The main contribution to the overall investment costs for the whole W VII project is given by the system for generating and maintaining the main magnetic field. This fact revived the discussions on this problem which had taken place some years ago and had originally lead to the solution of using superconducting magnets.

In order to have a basis for selecting the optimum solution we shall present estimates on the costs of the competitive methods of producing the main magnetic field. It has been pointed out in detail that one of the substantial advantages of a stellarator is its capacity for steady state operation. Therefore the first system to be compared with the superconducting solution is an adequate steady state power station and watercooled, conventional coils operated at normal temperature (item B). The whole situation becomes more complicated if we start to question the necessity of a genuine steady state operation. In this case we have to consider the various time scales relevant to the kinds of experiments to be performed in W VII.

The fastest time scale of interest is represented by the energy and particle confinement times expected from the neoclassical models, and computations on both ohmic heating and neutral injection show that confinement times of the order of one second have to be considered. Therefore, even for the fastest responding plasma parameters to become quasi-stationary, a flat top pulse duration of several seconds is required. Closely connected with these characteristic neoclassical times is the time scale required for establishing the related macroscopic plasma motions,

e.g. the plasma rotation due to the radial electric fields necessary to allow for ambipolar diffusion. Calculations (see Madison CN-28/C-12) on the time needed to set up this rotation yield about $(R/r)^{3/2}$ times the neoclassical ion thermal equilibration time.

The next time scale involved is that related to the plasma conductivity and, in turn, to the skin effect. For quasi-stationary conditions any changes in plasma current density, rotational transform etc. must be applied slowly compared to these time scales. For a typical hydrogen plasma of $U_{th,e} = 1$ kV, $\ln\Lambda = 14$, and absence of impurities the value of η is 2.3×10^{-6} Ω cm. Therefore, using the skin relation

$$\delta \approx 5 \times 10^{3} \sqrt{\frac{\eta}{\nu}}$$

it follows that for $\delta = r_p = 30$ cm the value of $\nu = 0.064$ sec^{-1}. Taking the characteristic time for an e-folding penetration to be about $1/4\nu$, one obtains $\tau \approx 4$ sec. By comparison, the decay time of the plasma current, $I\varphi$, is ($L \approx 6 \times 10^{-6}$ H, $R \approx 10^{-6}$ Ω) about 6 seconds (the plasma heating from this process, depending on $I\varphi$ and τ_E, may be sufficient to maintain a low resistivity). This time scale is particularly important for studying heating of and injection into "current-free" plasmas initially generated by an ohmic heating pulse.

The time scales discussed up to now are the results of relatively simple considerations. More complicated is an estimate on how long it takes for the processes at the wall to establish a stationary equilibrium with the discharge. The total number of ions in a W VII plasma with a mean density of 10^{13} cm^{-3} is about 4×10^{19}. By comparison[+], the number of atoms deposited in a monomolecular layer at the inner vessel wall is about 15×10^{19} when using a coverage of 5×10^{14} atoms/cm^2. So it would take roughly four particle confinement times for replacing this monomolecular layer once. It is more relevant, however, to ask

---

[+] We thank Dr. Vernickel for supplying us with these figures and for helpful discussions.

for the saturation time of the wall loading with particles of the energy eU_i. Here the estimate is that the saturation coverage is approximately lo^{16} particles/cm^2, i.e. it takes about loo particle confinement times for reaching this state. Considerations on the sputtering of an oxygen layer deposited on the vessel wall yield time constants of the same order of magnitude. Thus one finds that for the wall processes to achieve a stationary state a considerably longer time is required than for all the other processes considered above. In this connection it should be stressed again that a steady state plasma is determined by its boundary conditions. Therefore, a continuous change of these conditions is synonymous with a continuous variation of the basic plasma parameters and of the impurity content with all its implications on the energy balance.

Compared with the time scales for wall equilibrium a flat-top pulse of about 12 sec duration, which is the basis of the later cost estimates, is too short. However, it is considered satisfactory with respect to the inherent plasma time scales discussed above. From this point of view it is believed to be of no disatvantage to start the W VII experiment with a 12 sec flat-top pulsed magnetic field system and to turn later to a true d.c. operation when experimental results enable plasmas of interest to be maintained far beyond these 12 seconds.

The last point to be considered here is the size of the conventional coils that can be tolerated. For minimizing the required power, rather large coils with the corresponding low resistance would be preferable. However, already for the superconducting coils, vital experimental and technical conditions such as sufficient space for observation and pumping portholes, ohmic heating transformer, vertical field coils, water and current supplies for helical windings etc., and the tangential access for various diagnostics and for neutral injection without modifying more than one main coil in each case, restricted the overall dimensions of these coils to a minor cross-section of 2o x 3o cm^2. This was done in spite of the various intrinsic technical requirements such as: minimization of heat losses,

support of the forces even in case of a system fault, sufficient space for the superconducting material, sufficient cooling channels, liquid nitrogen shield, shielding of HF-fields, etc., which had to be met. It is not possible, therefore, to use coils of a much larger size than that of the superconducting solution without severely restricting the rest of the experimental program. The size of these coils is a technical boundary condition determing the required power for a conventional coil arrangement.

The coils considered are mounted in a steel casing of 2 cm wall thickness in order to control the forces arising during normal operation and in particular in case of a system failure. With respect to the cross section of this casing, and under the assumption that another part of the cross section is occupied by insulating material (lo %) and by water cooling channels (lo %), an overall filling factor of 55 % is assumed. We shall attempt to increase this quantity in order to gain in pulse duration or maximum field strength.

For these coils the total main field energy stored in W VII is 88 MJ at full field strength and the ohmic power dissipated is P_o = 95 MW. It is one benefit of the conventional solution, that some more power is then available for energizing the helical windings, thus allowing for both, the desired higher values of iota and shear, and the preferable equidistant spacing of $3o^o$ between the helical winding units (see Fig. 12 and Table IV). Serving those purposes, another 15 MW have to be added to the 95 MW for the main field. This gives a total consumed electrical power of llo MW.

APPENDIX 5 to

Project Wendelstein W VII

Application for EURATOM preferential support

TECHNICAL CONCEPT

Introduction

In the following we shall present information on the technical concept of W VII, but it is understood that up to now final decisions are taken only on those components of the device which determine its essential properties and are time consuming in their manufaction. The other technical details will be fixed at the latest possible time. This procedure guarantees that the apparatus at the time it goes into operation does not deviate too much from what will be desired then.

For a pulse operation of 10 - 20 seconds duration and a field strength of 40 kG the magnetic field system requires a power of about 100 MW and an energy of 1 - 2 GJ. On the other hand, it turned out that the largest fly-wheel which can be made in one piece has a weight of 240 tons and leads to a useful energy of 1.45 GJ. Therefore additional energy is relatively cheap up to this limit; any larger amount of stored energy requires two fly-wheels at least which might excite dangerous oscillations if both are coupled to the generator. Influenced by these reasons the laboratory has ordered the generator with the specifications given in table VII.

Based on the limitations set by this generator and by the power supplies already existing and used for the present Wendelstein experiments the optimization of the parameters of the W VII experiment was reexamined. Guided by the scientific aims

Reprinted: May 1972

TABLE VI

W VII Parameters

DIMENSIONS

major radius		R_o =	200 cm	
minor radii				
coil	r_e = 100 cm			r_i = 55 cm
bandages	r_e = 53.5 cm			r_i = 50.5 cm
helical windings	r_e = 50 cm			r_i = 41 cm
vessel	r_e = 40.5 cm			r_i = 36.0 cm
limiter		r_L ≳	34 cm	
plasma		r_{PL} ≈	20 - 34 cm	
width of main field coil		d =	18.5 cm	
minimum spacing of main field coils		δ =	2.5 cm	
width of helical winding unit at R_o (ϑ = meridional angle)		ϑ =	60°	

MAIN MAGNETIC FIELD

field strength at R_o (maximum attainable 45 kG)	B_o =	40	kG
ripple at r_L	$\frac{1}{2}\frac{\Delta B}{B}$ ≲	$5 \cdot 10^{-3}$	
ripple at magn. axis	$\frac{1}{2}\frac{\Delta B}{B}$ ≈	$5 \cdot 10^{-4}$	
electric power dissipated	P_M =	72	MW
magnetic field energy	E_M =	135	MJ
inductance	L =	170	mH
resistance (at end of pulse)	R =	45	mΩ
resistance (at begin of pulse)	R =	40	mΩ
pulse duration (flat top; for 35 kG: τ = 14 sec)	τ ≈	10	sec
repetition rate	once every	7	min
number of coils	n_c =	40	
turns per coil (double pancake)	n_d =	2 x 12.5	
current per turn (max. value 45 kA)	I_o =	40	kA

TABLE VI (continued - 2 -)

HELICAL MAGNETIC FIELD

multipolarity		max. rot. transform at R_o with B_o
$l = 2$	negligible shear	$\iota_o = 0.5$
$l = 2$ $l = 4$	shear at r_L: $\Theta \approx 2\,\%$	$\iota_o = 0.15$

number of conductors per winding unit	n_H	=	24
current per conductor	I_H	=	40 kA
electric power dissipated	P_H	=	28 MW
resistance	R_H	=	14.5 mΩ
number of field periods	m	=	5

PORTHOLES

number of horizontal portholes	n_{PH}	=	10
bore of horizontal portholes	b_h	$\approx$	20 cm
bore of tangential portholes	b	$\approx$	15 cm
number of vertical portholes	n_{PV}	=	15
pumping speed through separate portholes (without internal getter techniques)		$\approx$	6×10^4 l/s

as outlined earlier, the major points to be weighted and balanced were: main magnetic field strength, rotational transform and shape of magnetic surfaces, space for the OH-transformer, plasma aperture, and access for observation, pumping and injection. This resulted in the machine parameters shown in table VI. More detailed reasons for this particular choice are given in the following by shortly discussing and describing the essential individual components.

1) Power Supplies

a) Main generator

The essential parameters of the generator are listed in table VII, a circuit diagram is shown in Fig. 16 and a schematic view in Fig. 17. The generator is designed such that it can deliver the full power of 155 MW for 15 sec if the load is ohmic. For stand-by conditions the static oscillator supplying the motor allows to run the generator at a speed of 1.350 rev/min so that the friction losses are reduced. The generator is equipped with two independent three phase windings which allow operation in series (6.6 kV, 22.5 kA) or in parallel (3.3 kV, 45 kA). Their output is fed into a silicon six phase rectifier, and voltage and current mentioned are available at the output of this rectifier.

Output dc voltage and current are controlled by two feed back circuits acting on the excitation of the generator, one for the voltage and one for the current. This allows for a fast excitation of the stellarator magnetic field by applying a large voltage. As soon as the current has reached the desired value the second circuit takes over and keeps the current constant within an accuracy of $< 0.5\,\%$ for the rest of the pulse, and then deexcites the generator if the energy is used (see Fig. 18 a, b). This would be the normal way of operation but other programs can be fed into the feed back circuits.

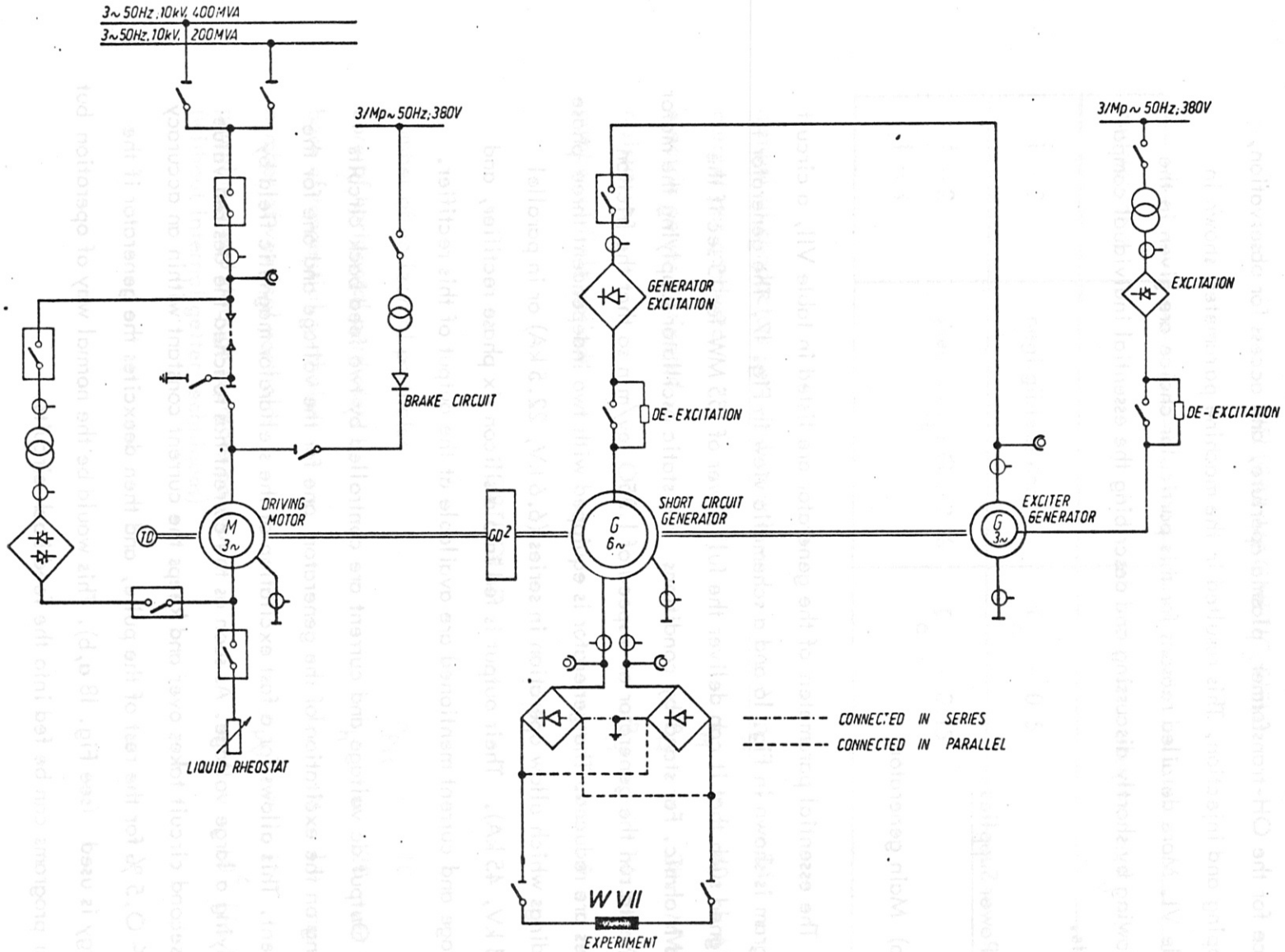

Circuit diagram of the main generator

W VII Fig. 16

				Datum	1.2.72	Max-Planck-Institut für Plasmaphysik	SIEMENS AKTIENGESELLSCHAFT	Stoßleistungsanlage Garching Übersichtsschaltplan E484/441460
				Bearb.	Muller			
				Gepr.				
Ausg.	Änderung	Datum	Name	Norm.				Bl/Ltr, Blatt

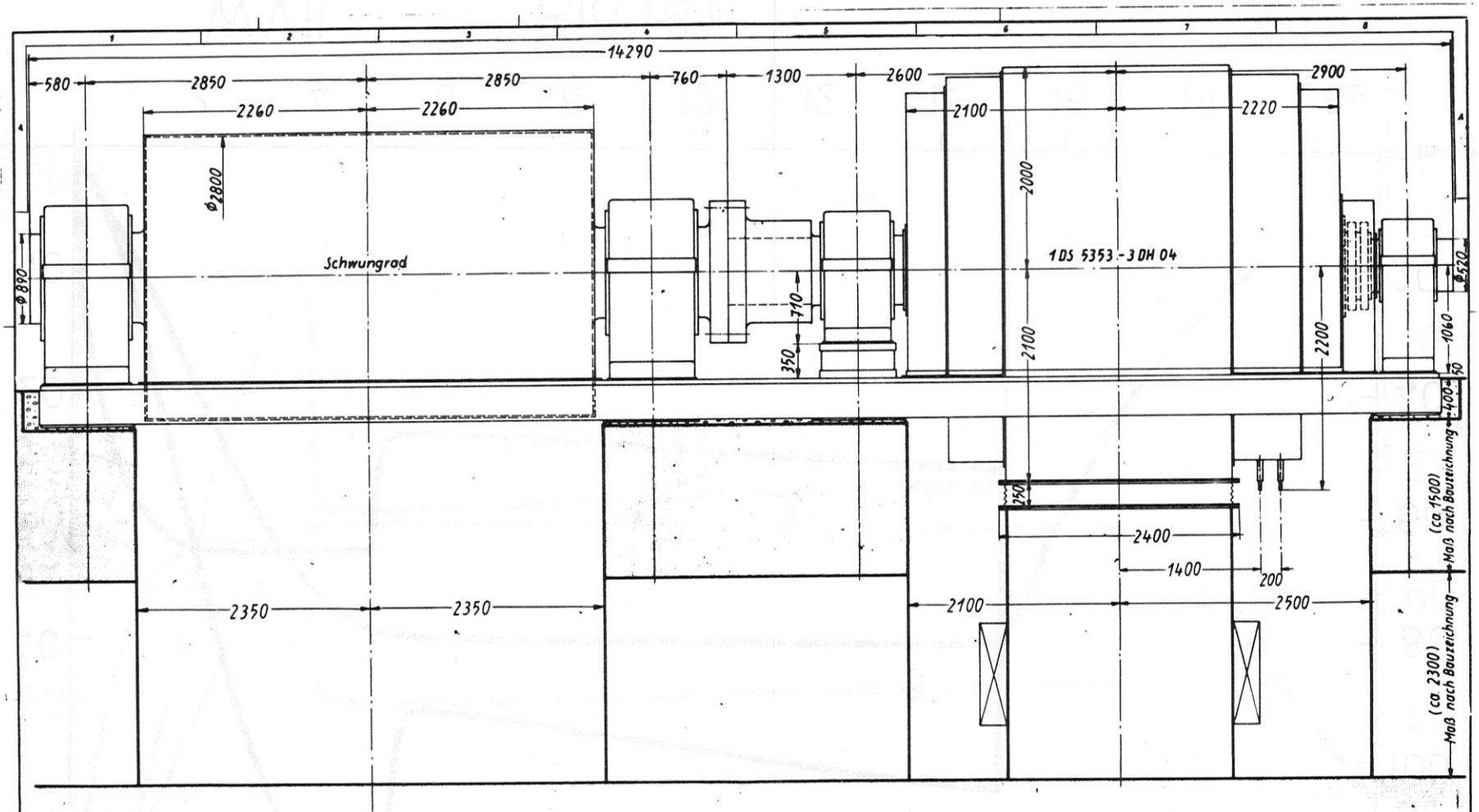

Maße unverbindlich. Ohne Antriebsmotor und Wellengenerator.

Schematic view of the main generator

W VII Fig. 17

Freimaßtoleranzen —	Änderungen			
Tag 221271	Name Jobst		Garching 2	Maßstab 1:25 1:100
			Maßbild (unverbindlich) 1DS 5353 - 3DH 04	
SIEMENS AKTIENGESELLSCHAFT Dynamowerk			2D 1.0110 - 200119	

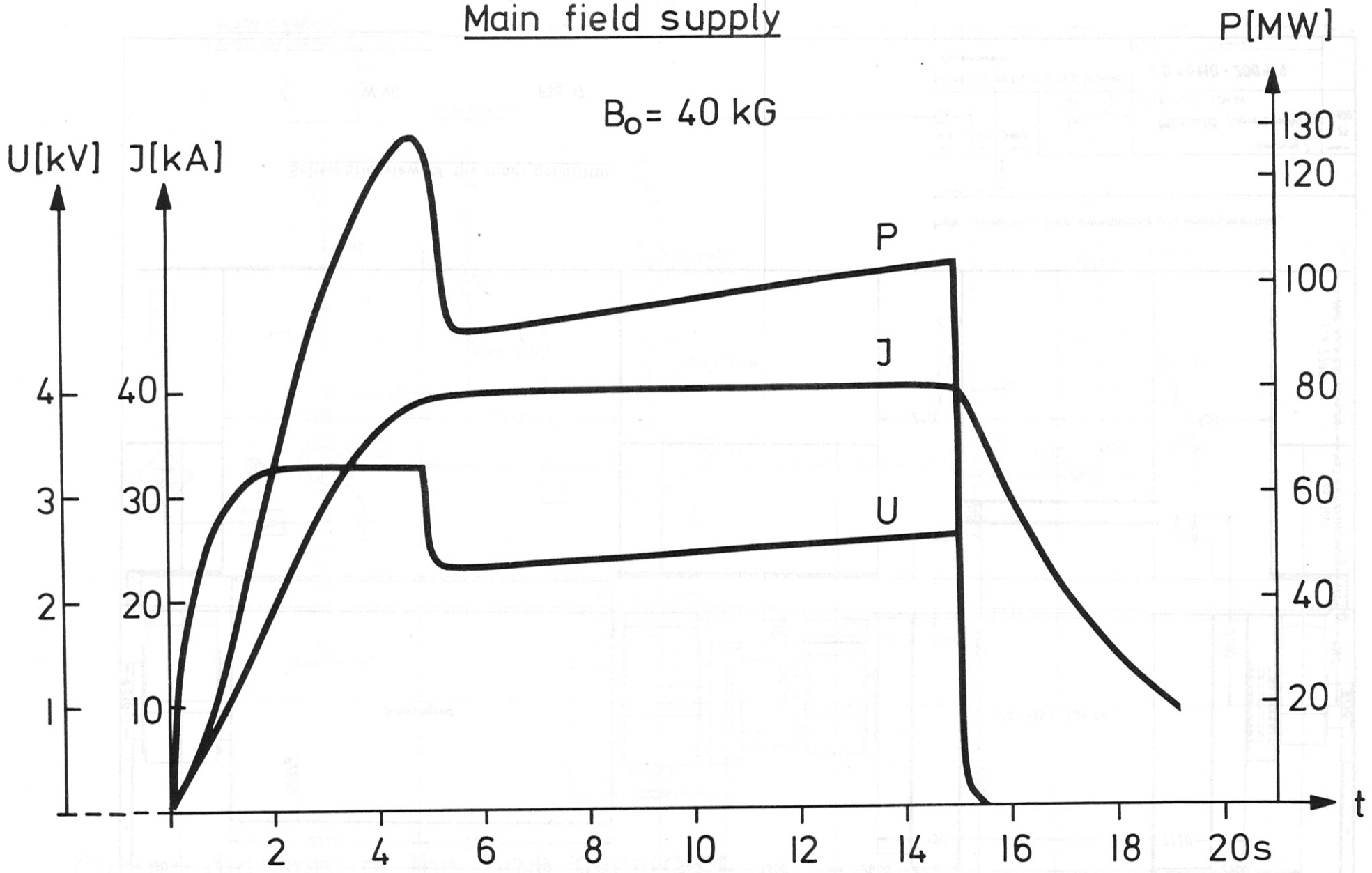
Main field supply
B_o= 40 kG
U[kV]
J[kA]
P[MW]
P
J
U
4
3
2
1
40
30
20
10
130
120
100
80
60
40
20
2
4
6
8
10
12
14
16
18
20s
t

WVII Fig. 18 a

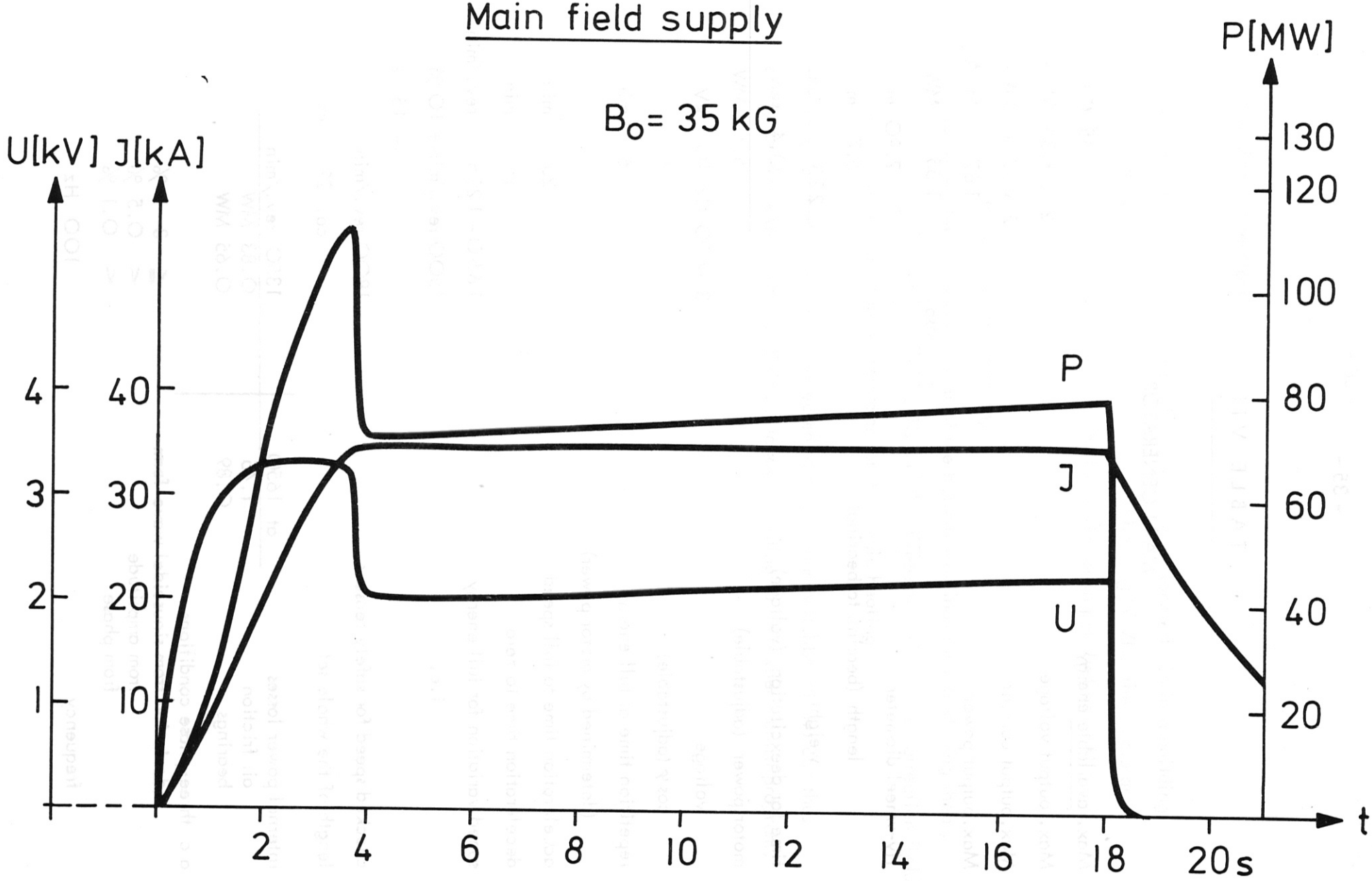
Main field supply
B_o= 35 kG
U[kV] J[kA]
P[MW]
4
3
2
1
40
30
20
10
130
120
100
80
60
40
20
P
J
U
2
4
6
8
10
12
14
16
18
20s
t

WVII Fig. 18 b

TABLE VII

MAIN GENERATOR

Max. available energy		1.45	GJ
Max. output voltage		2 x 3.3	kV =
Max. output current		2 x 22.5	kA =
Max. output power		167	MVA
	resp.	155	MW
fly-wheel diameter		2.90	m
length (bearing to bearing)		5.7	m
weight		223	tons
time for deexcitation (voltage)		0.4	sec
motor power (adjustable)		5.7	MW
voltage		3 ~ 50 Hz 10	kV
cos φ (adjustable)		1	
repetition time at full energy (determined by motor power)		6	min
acceleration time to full speed		25	min
deceleration time to zero		15	min
speed variation for full energy		1650 - 1275	rev./min
i.e.		1500 rev./min	+ 10 %
			- 15 %
checked speed for safety reasons		1800 rev./min	
length of the whole set		ca. 22	m

internal power losses	at 1650	1350 rev./min
air friction	1.45	0.83 MW
bearings	0.89	0.65 MW

a c three-phase conditions		
deviation from sinusoidal wave form		≦ 3 %
from amplitude		< 0.5 %
from phase		< 0.1 %
frequency		100 Hz

b) Auxiliary generators

A number of additional but smaller generators is located within a building directly attached to L 7, the experimental hall housing W VII. Their data are listed in table VIII. They can be switched in series or in parallel and will be used for

varying the rotational transform,
exciting the $\ell = 4$ component of the helical windings for introducing shear,
energizing the vertical field coils and the different coils for the correction fields,
supplying the air core transformer for the ohmic heating.

All the generator outputs are connected to a cross-bar switchboard and can thus easily be connected to the individual loads according to the experimental program.

TABLE VIII

Maximum ratings of the auxiliary generators

	d.c. operation			pulsed operation		
	power MW	voltage V	current A	available energy MJ	power MW	current kA
Hertha I	1.6	900	2000	5	10	12
Hertha II	1.6	900	2000	5	10	12
Hertha III	1.6	900	2000	2.5	10	12
Clara I	0.3	280	1350	3	1	3.8
Clara II	0.4	150	3300			6.0
Berta I	1.0	250	3200	6	2	6.0
Berta II		250	3200			6.0
Central power station of the institute	2	10 kV~		15	50	

2) Main magnetic field

The main magnetic field is excited by 40 coils being equally spaced around the azimuth. The number of 40 was chosen to obtain a sufficiently small ripple of the field, Fig. 19, to allow for a satisfactory large number of partholes and for a sufficiently large tangential access for neutral injection and diagnostics. For the latter purpose, however, some of the coils have to be modified. Optimum use of the helical symmetry can be made if the number of coils is a multiple of $4 \cdot m$, m being the number of $\ell = 2$ field periods around the torus. $m = 5$ in our case would lead to 20, 40 or 60 coils, and 40 seemed to be the optimum number under the above considerations.

The parameters of the coils were optimized according to the following conditions:

1) The coils must be easy and accurate to manufacture and easy to adjust in place.

2) The minimum distance between two neighboured coils must not be smaller than 2.5 cm. This distance allows for a space of 60 cm width when all coils are shifted together, so that the bridges of the helical windings and the intermediate piece of the vacuum tube can be removed when mounting or demounting the machine.

3) At the position of the portholes with $\vartheta \lesssim 45^{\circ}$ the distance between the coils should not be restrictive compared to the distance between the helical windings there. In this case no space is wasted if using portholes of circular cross-section.

4) In order to guarantee manual access to the vacuum tube for all the daily mounting and adjustment work the radial thickness of the winding must not exceed 40 cm, or 45 cm including its frame.

5) The forces must be manageable.

6) The bore of the coil should be as large as possible.

7) There should be sufficient space for the OH-transformer.

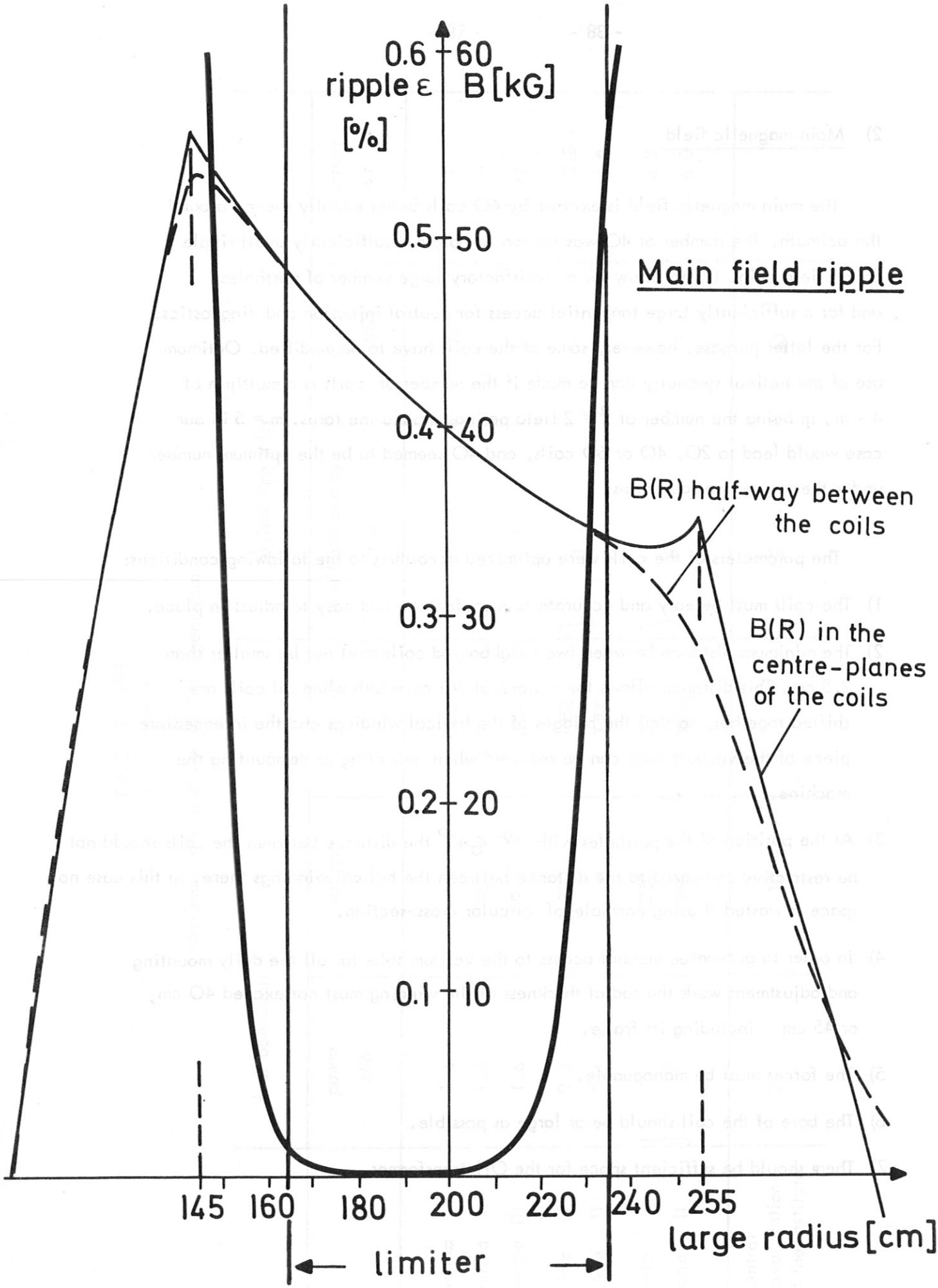
0.6
60
ripple ε
B [kG]
[%]
0.5
50
Main field ripple
0.4
40
B(R) half-way between
the coils
B(R) in the
centre-planes
of the coils
0.3
30
0.2
20
0.1
10
145
160
180
200
220
240
255
large radius [cm]
limiter

Fig. 19

8) The power dissipated must be small enough to allow for a sufficiently long time of operation.

These conditions led to the dimensions of the coil listed in table VI or shown in Fig. 20, i.e. essentially to a bore of 110 cm diameter and a power dissipation of 72 MW at 40 kG main magnetic field.

Since the main generator can deliver either 20 or 40 kA (leaving 10 % for safety) 25 or 50 turns per coil would be possible. Power transfer conditions would favour the 50 turn case but a rather cheap solution was found to transfer the energy with a current of 40 kA over 200 m with only 1 % losses so that this argument is not a very strong one. On the other hand, it is a condition that the coils allow true d.c. operation and this requirement strongly favours the 25 turn case where cooling is much easier. The cooling channels shown in Fig. 19 allow to cool off all the power if two cooling circuits are used in parallel and the water pressure is increased to about 30 atomospheres.

A serious problem is to balance all the forces. In case of symmetric operation only 65 atmospheres expansion forces and 206 tons per coil centripetal forces arise. The first ones can still be balanced by the strength of the copper material which will be used whereas the second ones require a suitable frame which will be described later. More dangerous is an operation deviating from axisymmetry which might arise in case of system failure or be introduced deliberately for doing mirror experiments.As shown in Fig. 21 and 22 the force in this direction could become larger than 1000 tons if only half of the coils are fully excited. Such a situation could occur in case of a short-circuit since the electric midpoint is grounded. To balance these forces the coil is bolted to a strong frame at 4 points around its azimuth, which are chosen such that their center of gravity roughly coincides with the point where the forces arise. Finally, to make the winding more stable against azimuthal forces, the copper bars will get a surface with a triangular structure as indicated on the insert of Fig. 19. Tests will be made to check if these means are sufficient. If this will not be the case, additional wedges will be put between the individual coils.

More detailed informations on internal stresses and magnetic field energy are given in Figs. 23-25.

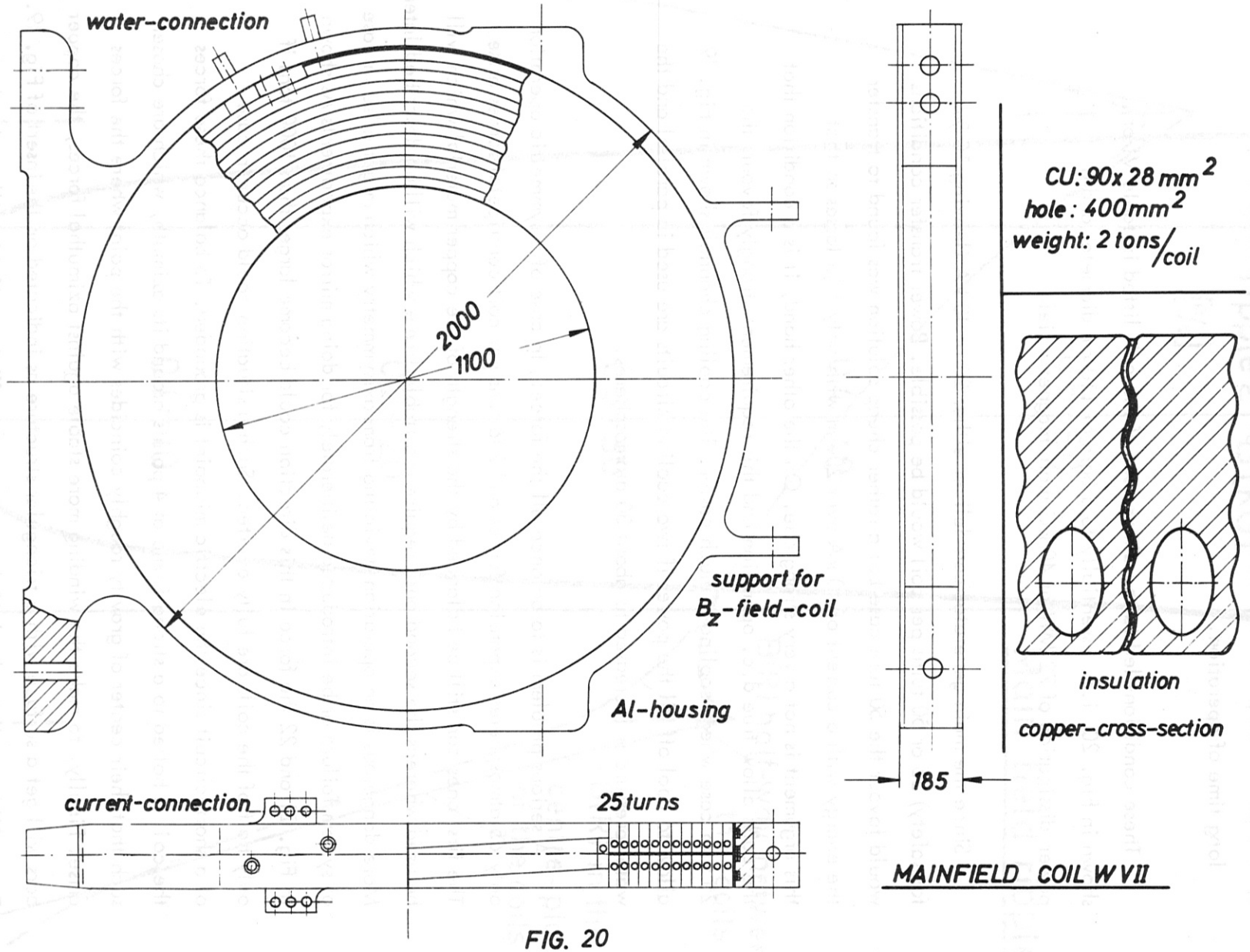
water-connection
2000
1100
support for
B_z-field-coil
Al-housing
current-connection
25 turns
CU: 90x 28 mm^2
hole : 400 mm^2
weight: 2 tons/coil
insulation
copper-cross-section
185
MAINFIELD COIL W VII

FIG. 20

Section of the main field coil system of the W VII
(water cooled coils)

The arrows represent the net forces for each of the coils in case of absence of current in one of the fourty coils. The system of tangential and radial net forces is equivalent, with regard to supporting reactions, to the magnetic body forces in the windings.

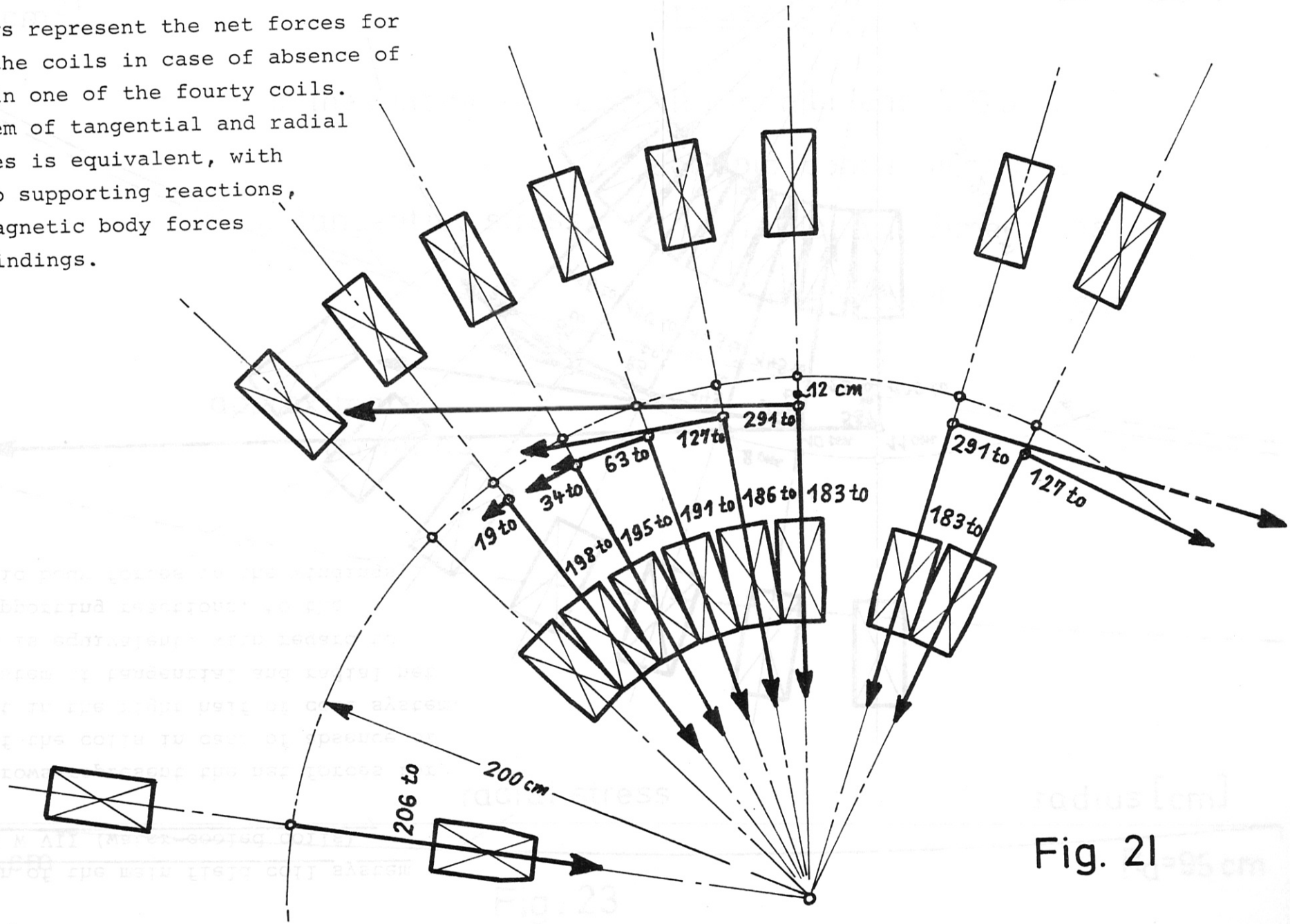

Fig. 21

Section of the main field coil system of the W VII (water-cooled coils).

The arrows represent the net forces for each of the coils in case of absence of current in the right half of coil system. The system of tangential and radial net forces is equivalent, with regard to the supporting reactions, to the magnetic body forces in the windings.

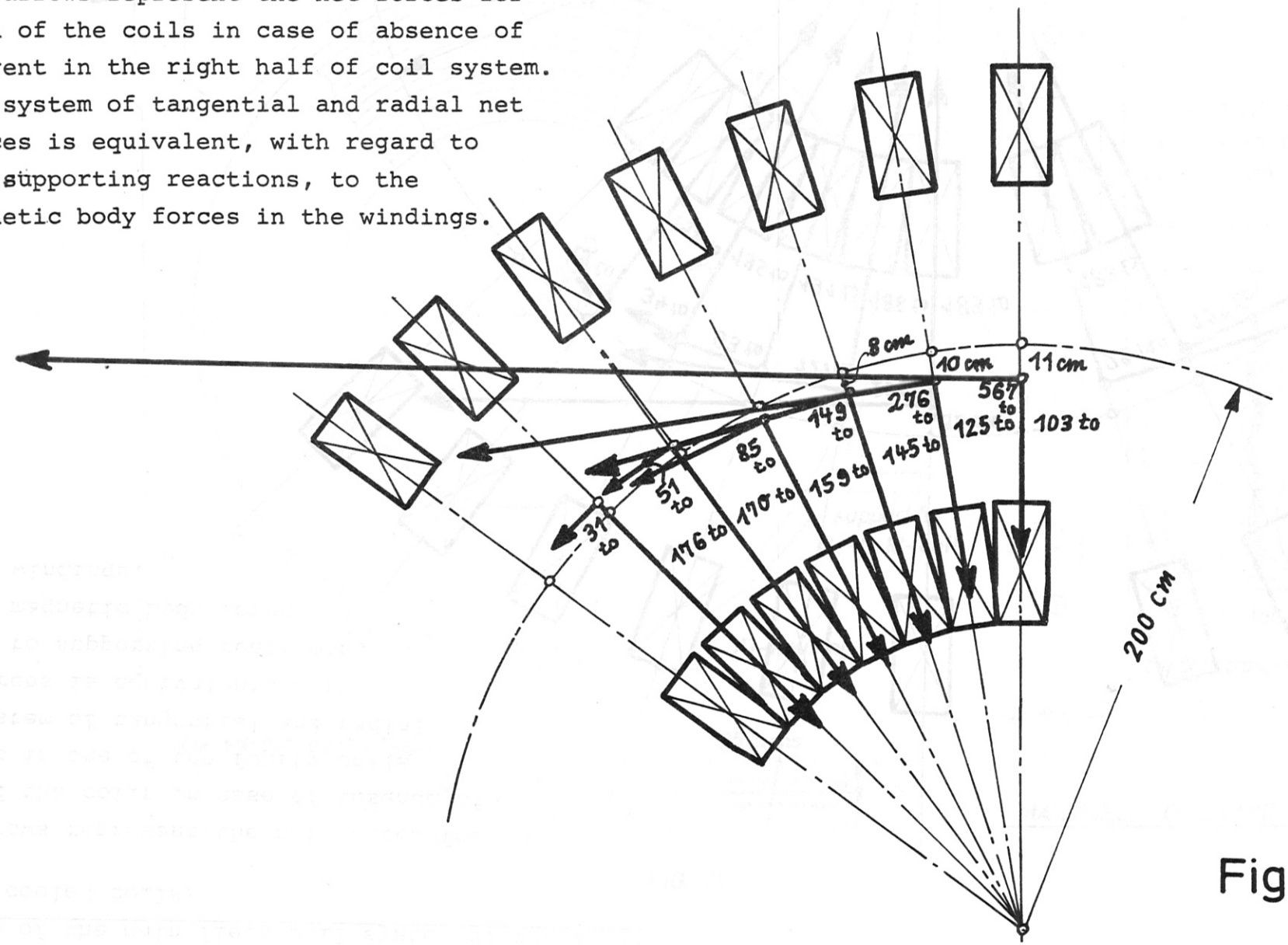

Fig. 22

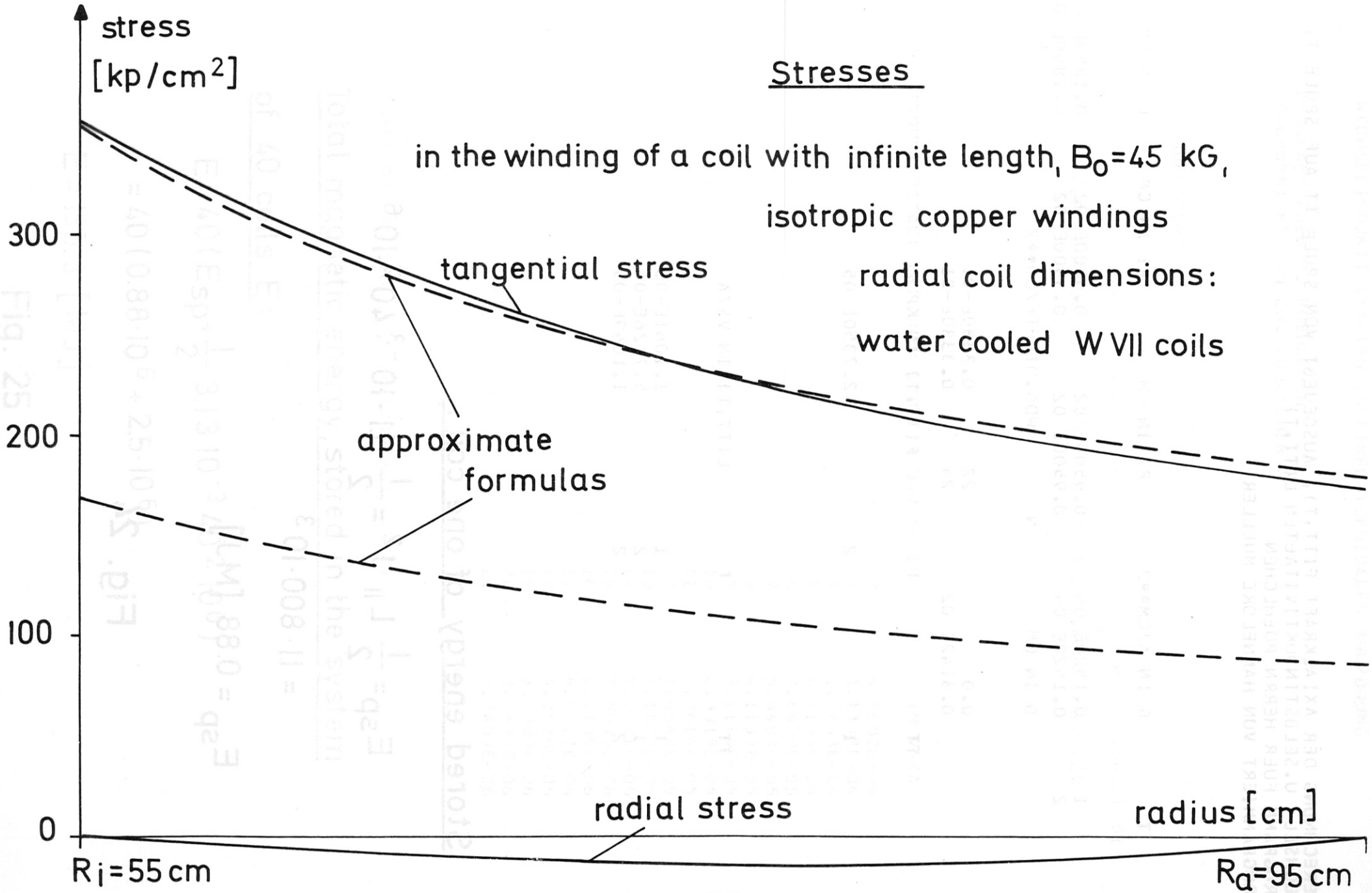
stress
[kp/cm²]
Stresses
in the winding of a coil with infinite length, B₀=45 kG,
isotropic copper windings
radial coil dimensions:
water cooled W VII coils
300
200
100
0
tangential stress
approximate
formulas
radial stress
radius [cm]
Ri=55 cm
Ra=95 cm

Fig. 23

BERECHNUNG DER AXIALKRAFT F(TT,T), AUSGEUEBT VON SPULE TT AUF SPULE T,
WECHSEL- U.SELBSTINDUKTIVITAETEN L(TT,T)
PROGRAMM FUER HERRN POEHLCHEN
PROGRAMMIERT VON HANNELORE MUELLER

T	G IN A/CM**2	RA IN CM	RI IN CM	L IN CM
1	0.1520E 04	0.9500E 02	0.5500E 02	0.1850E 02
2	0.1520E 04	0.9500E 02	0.5500E 02	0.1850E 02

D IN CM	N	WDG.DICHTE/CM**2
0.0	22	0.3380E-01
0.3142E 02	24	0.3380E-01

TT	T	F(TT,T) IN KP
1	2	-2.7350E 05

TT	T	L(TT,T) IN VS/A
1	1	1.1061E-03
1	2	5.7126E-04
2	2	1.1049E-03

Stored energy of one coil :

$$E_{sp} = \frac{1}{2} L_{II} J^2 = \frac{1}{2} 1.1 \cdot 10^{-3} \cdot 40^2 \cdot 10^6$$

$$= 1.1 \cdot 800 \cdot 10^3$$

$$E_{sp} = 0.88 \text{ [MJ]}$$

Fig. 24

WECHSELINDUKTIVITAETEN IN EINER TOROIDALEN ANORDNUNG

PROGRAMM FUER R. POEHLCHEN
PROGRAMMIERT VON CH. LUDESCHER

EINGABEDATEN:

B = 200.00 RA = 95.00 RI = 55.00 W = 2.5000E 01

ANZAHL DER SPULEN: 40 ANZAHL DER STUETZSTELLEN *2 :20

INDUKTIVITAET ZWISCHEN SPULE 1 UND SPULE	IN VS/A
2	6.4602E-04
3	3.1332E-04
4	1.7843E-04
5	1.1198E-04
6	7.6820E-05
7	5.5483E-05
8	4.1139E-05
9	3.1119E-05
10	2.3915E-05
11	1.8614E-05
12	1.4642E-05
13	1.1622E-05
14	9.3021E-06
15	7.5076E-06
16	6.1185E-06
17	5.0517E-06
18	4.2528E-06
19	3.6909E-06
20	3.3538E-06
21	3.2409E-06

SUMME DER 40 SPULEN : 3.1280E-03 (VS/A)

Total magnetic energy, stored in the system of 40 coils E:

$$E = 40\left(E_{sp} + \frac{1}{2}\, 3.13\, 10^{-3}\, 40^{2}\, 10^{6}\right)$$

$$= 40\,(0.88 \cdot 10^{6} + 2.5 \cdot 10^{6})$$

$$E = 135.3\ [MJ]$$

Fig. 25

3) Helical Windings

As is the case with most parameters of W VII, type, geometry and size of the helical windings were chosen by comparing the various scientific aims with the technical requirements and boundary conditions (power supply). The latter showed it being practically impossible to combine in one set of helical windings such an amount of control on the field configuration that one can achieve both, a high value of iota, ι_o, on the axis, and, only when desired, a large value of shear, $\Theta = \frac{d\iota}{dr} \cdot \frac{r^2}{R}$, throughout the whole plasma volume. However, also the chosen principle of an $\ell = 2/\ell = 4$ combination as already described (e.g. page 16) now allows at full main field B_o for values of ι_o up to 0.5 and, when fully energizing the $\ell = 4$ components, for values of Θ up to 2 % concentrated on the outer plasma regions. This shear can be increased by a factor of 4 if B_o is reduced to half of its value, i.e. to 20 kG. Moreover, a specific high shear experiment is under discussion, which could be carried out by using the smaller vacuum vessel for W VII already manufactured (R_o = 200 cm; r_i = 17,5 cm; r_e = 20,5 cm) and supplying it with an adequate set of $\ell = 3$ helical windings.

In the following we are describing the larger vacuum vessel recommended by the first session of the Stellarator AG on W VII and the chosen set of helical windings to be mounted upon it (see also table VI). Owing to the largely increased power supply now available three disadvantages of the original design (e.g. Fig. 12) as described on page 16 can be eliminated. i) The meridional spacing between the individual helical winding units is now an equidistant one of $\langle\vartheta\rangle = 30^\circ$. This does not only symmetrize the relative location of the helical winding units, which is particularly important for the $\ell = 4$ components not affecting ι_o (on the axis!), but it allows also for twice the number of large portholes and for better access with respect to neutral injection. ii) The originally rather moderate values of ι_o and Θ to be achieved are now increased to those already quoted. iii) The original number of field periods, m = 4, mainly chosen in order to push up the values of ι_o and Θ to be achieved, could undergo a detailed reconsideration, the

result of which is now to use m = 5.

There are physical and technical arguments for this choice, concentrating on properties of the field configuration and compatability with W II b on the one hand and the better access for pumping and injection portholes on the other hand. As to the magnetic field configuration, the m-numbers 4, 5 and 6 were considered. Fig. 26 shows the computed value of ι_o (the helical current lines are assumed at a minor radius r_o = 45,8 cm) as a function of the total current flowing in each helical winding unit, its maximum being $I_h \cdot n_h$ = 24 x 40 kA = 960 kA. From this figure it follows, as expected, that using m = 4 would give the highest value of ι_o to be achieved. In order to analyze the meaning of this result, by contrast, Fig. 27 shows the average radius $\overline{r}_{PL}$ of the outermost magnetic surface (with zero vertical field) as a function of ι_o, from which it follows, that m = 4 is most disadvantegous in this respect. Note that the kink in these curves stems from the fact that beyond $\iota_o \approx 0.4$ the limiting surface is solely determined by the separatrix, whereas below this value the limiter - chosen here at r_L = 34,4 cm - is partly responsible for reducing the plasma cross section. Finally, in Fig. 28, the product of the maximum plasma cross section times $(1 + \iota_o^{-2})^{-1}$, a quantity roughly proportional to the expected confinement times, is plotted vs. ι_o. Although from this figure the m = 6 arrangement would be favoured, m = 5 is chosen, since it still allows to obtain $\iota_o = 0.5$ (resonances !) and to have sufficient range in ι_o where the separatrix is well inside the vessel bore. Compared to these considerations, the ratio $\varepsilon_h/\varepsilon_t$ (see page - 6 - and following) is not significantly dependent on the choice of m. In Fig. 29 the value of $\varepsilon_h/\varepsilon_t$ is plotted for the m = 5 arrangement as a function of r and ι_o, indicating that at a given radius $\varepsilon_h/\varepsilon_t$ is approximately proportional to $\sqrt{\iota_o}$. One can see, that for $\iota_o = 0.2$ the value of ε_h at the limiter is typically 5 %, thus the ripple of the main field there is sufficiently below this value.

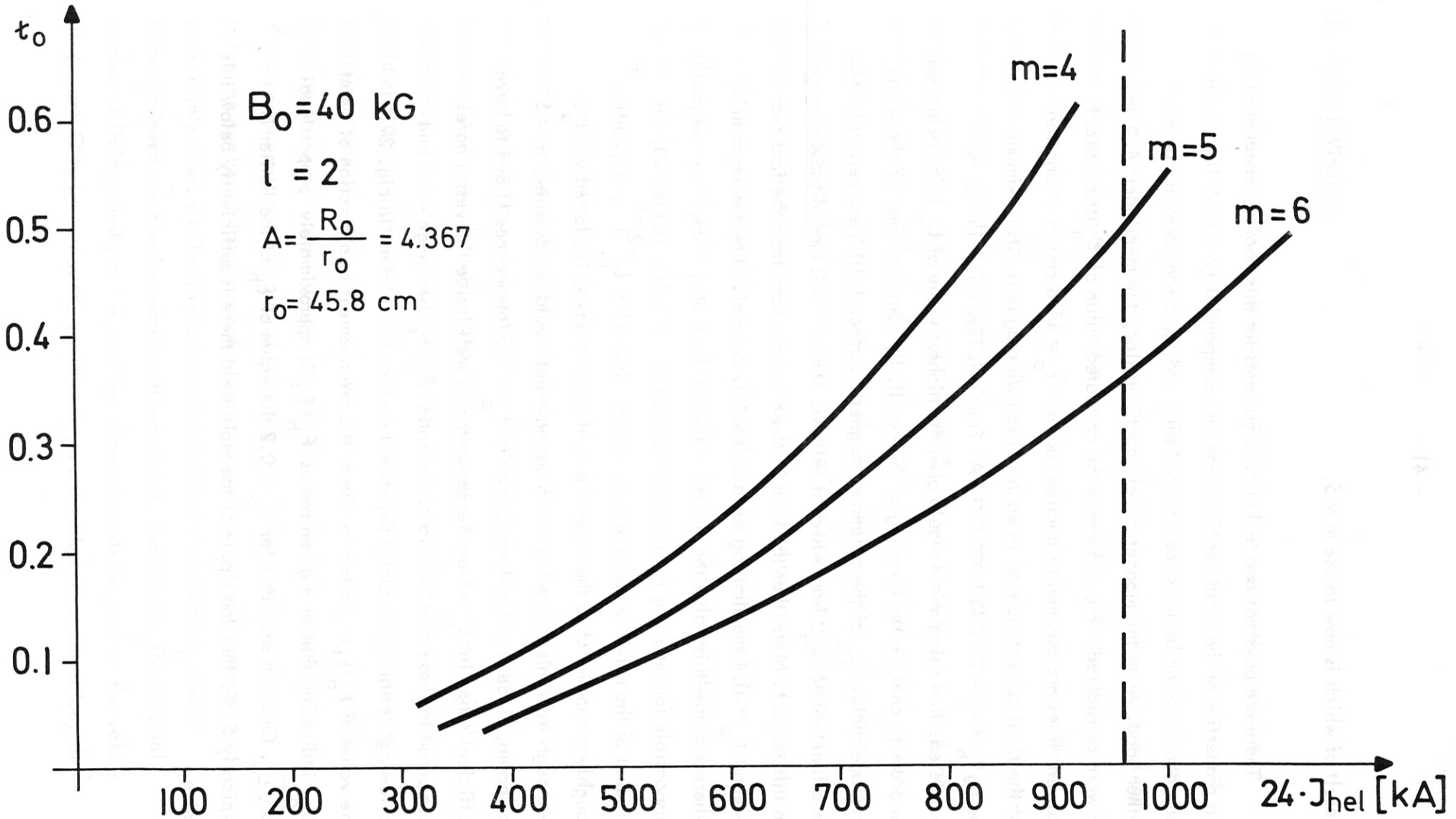
t_o
0.6
0.5
0.4
0.3
0.2
0.1
B_o=40 kG
l = 2
$A = \frac{R_o}{r_o}$ = 4.367
r_o= 45.8 cm
m=4
m=5
m=6
100
200
300
400
500
600
700
800
900
1000
$24 \cdot J_{hel}$ [kA]

W VII Fig. 26

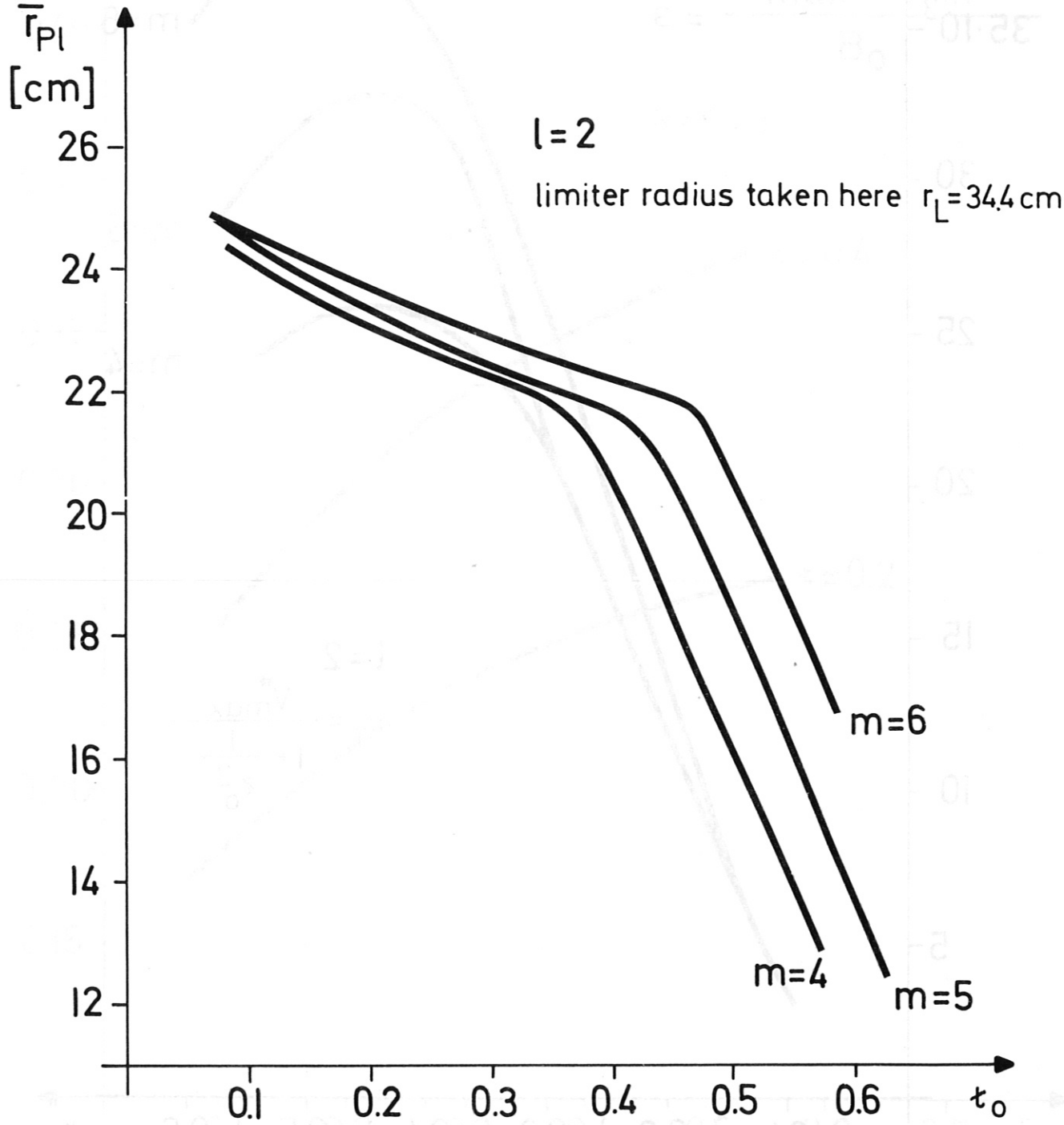

W VII Fig. 27

$\bar{r}_{Pl}$ is the "average radius" of the outermost magnetic surface.

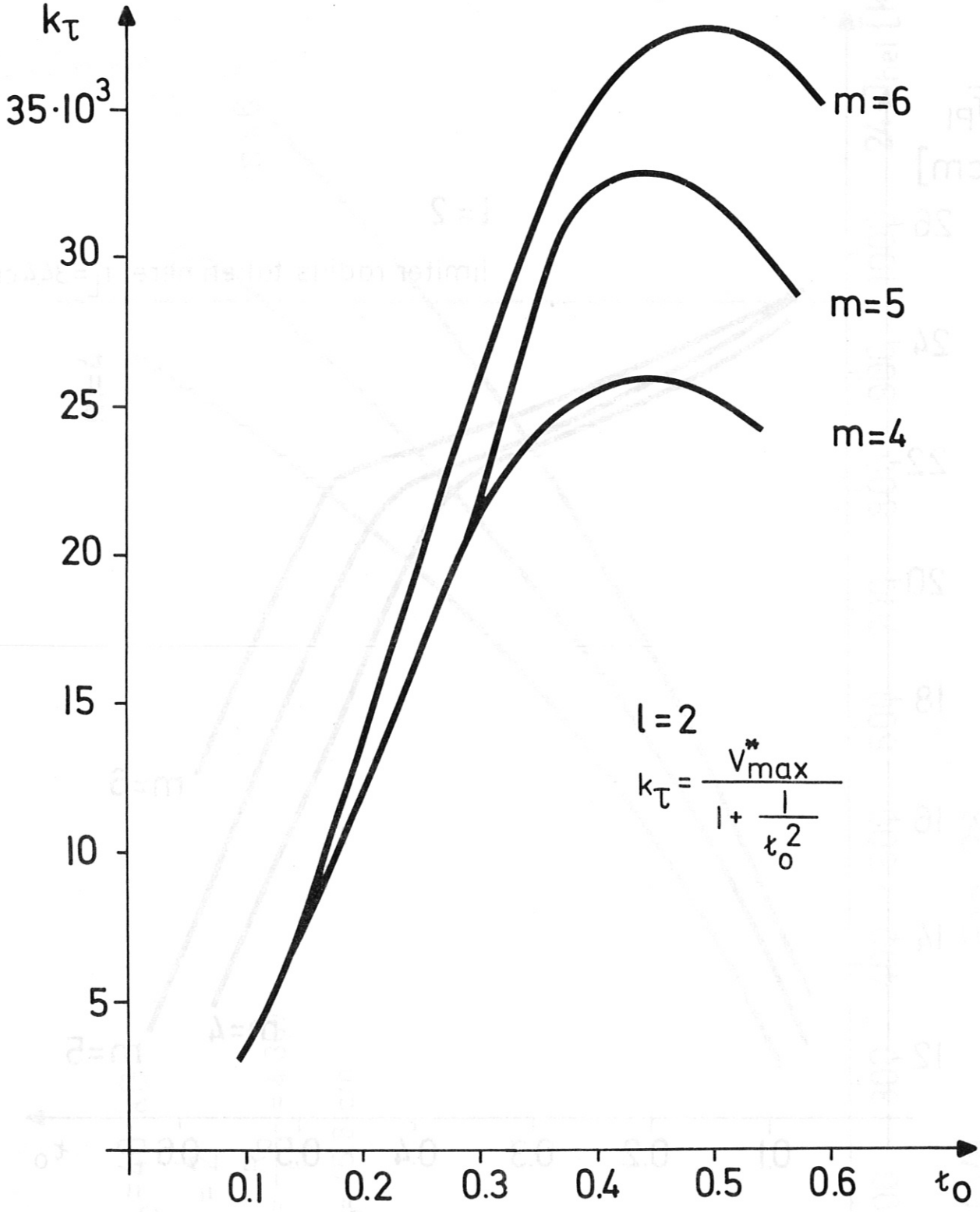

W VII Fig. 28

V^*_{max} is the cross-section of the outermost magnetic surface normalized to πr_o^2 ($r_o = 45.8$ cm minor radius of helical current lines).

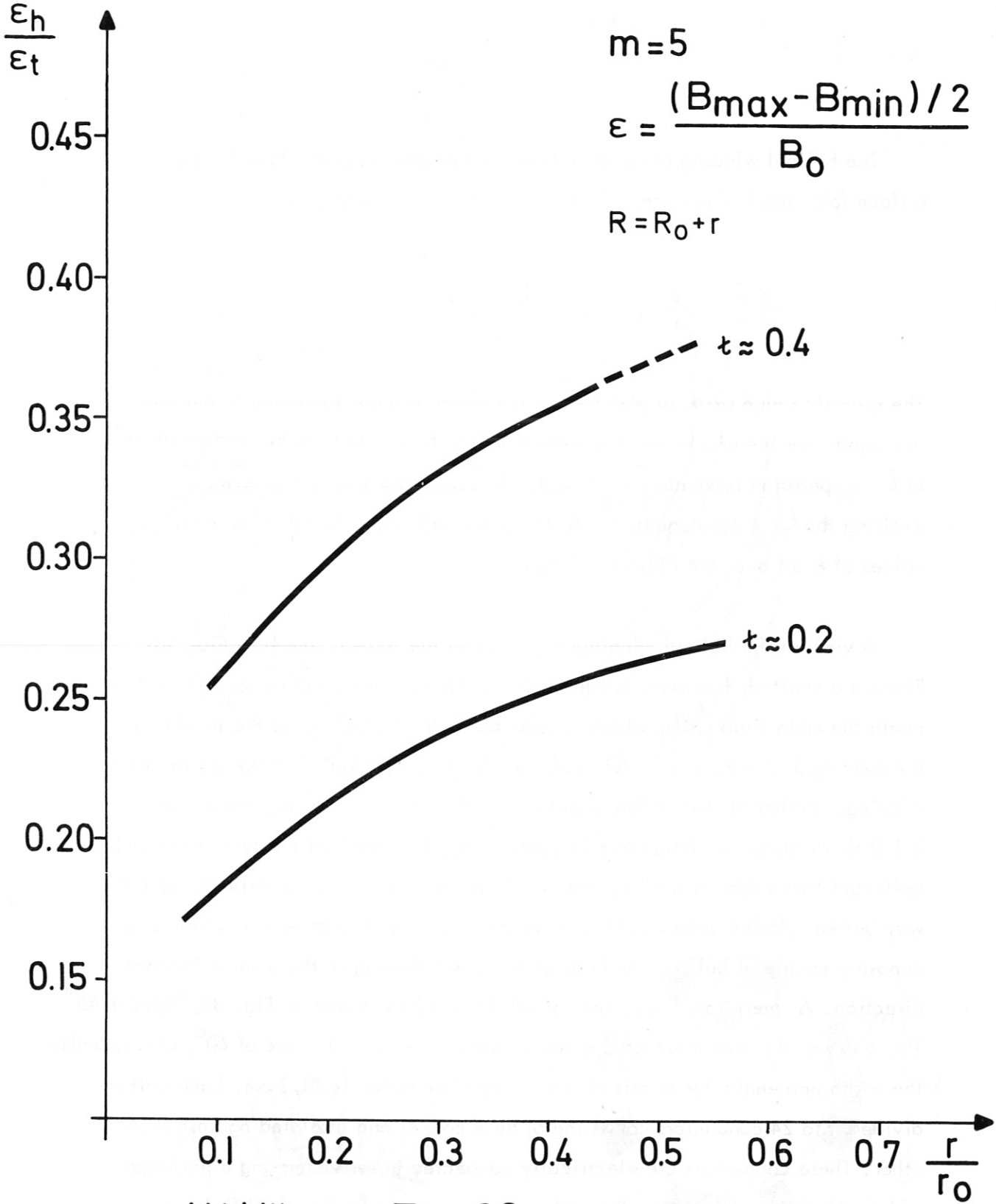

W VII Fig. 29

ε_t: mirror ratio of main field

ε_h: mirror ratio of helical field

r_o: minor radius of helical current lines

The helical winding units are following a geometric path along the torus surface (plus insulating material) at r = 41 cm being described by

$$\frac{d\varphi}{d\vartheta} = \frac{2}{5} \quad (1 - \alpha \cos \vartheta).$$

The specific value of α of about -5 % is chosen in order to minimize the shear averaged over the plasma volume when running the whole helical winding units in $\ell = 2$ operation producing $\iota_o = 0.3$. The reason for this is that without exciting the $\ell = 4$ components the field configuration should allow for irrational values of ι all over the plasma volume.

A view of the helical windings mounted on the torus is shown in Fig. 30. There are omitted, however, all the bolts and bandage-type units located underneath the main field coils, which couple the helical windings to the torus and fix them against each other. According to the m = 5 periodicity, the set of helical windings consists of two independent pairs of "units" enveloping the vessel 2 1/2 times along one long torus circumference, i.e. each of the two individual units runs twice around the long way while it encircles the torus 5-times the short way before closing upon itsself, thus at any meridional cross section forming an opposing couple of helical windings with current flowing in the same azimuthal direction. A meridional cross section of these units is shown in Fig. 30, "Schnitt AB." The width of the unit there at C extends over an meridional angle of 60°; consequently the width perpendicular to this unit's (current) direction is 38,2 cm. Each unit is divided into 24 conductors consisting of hard copper and insolated against each other. These conductors are electrically connected in series forming 3 packages, which all of them taken together either produce a pure $\ell = 2$ helical field or, switched differently, said combination of $\ell = 2$ and $\ell = 4$ (6 conductors per individual $\ell = 4$ package). Part of a detailed meridional cross section through a helical winding unit is shown in "Einzelheit C" of Fig. 30. Note, however, that the cooling channels and the specific shape of the conductors might still undergo

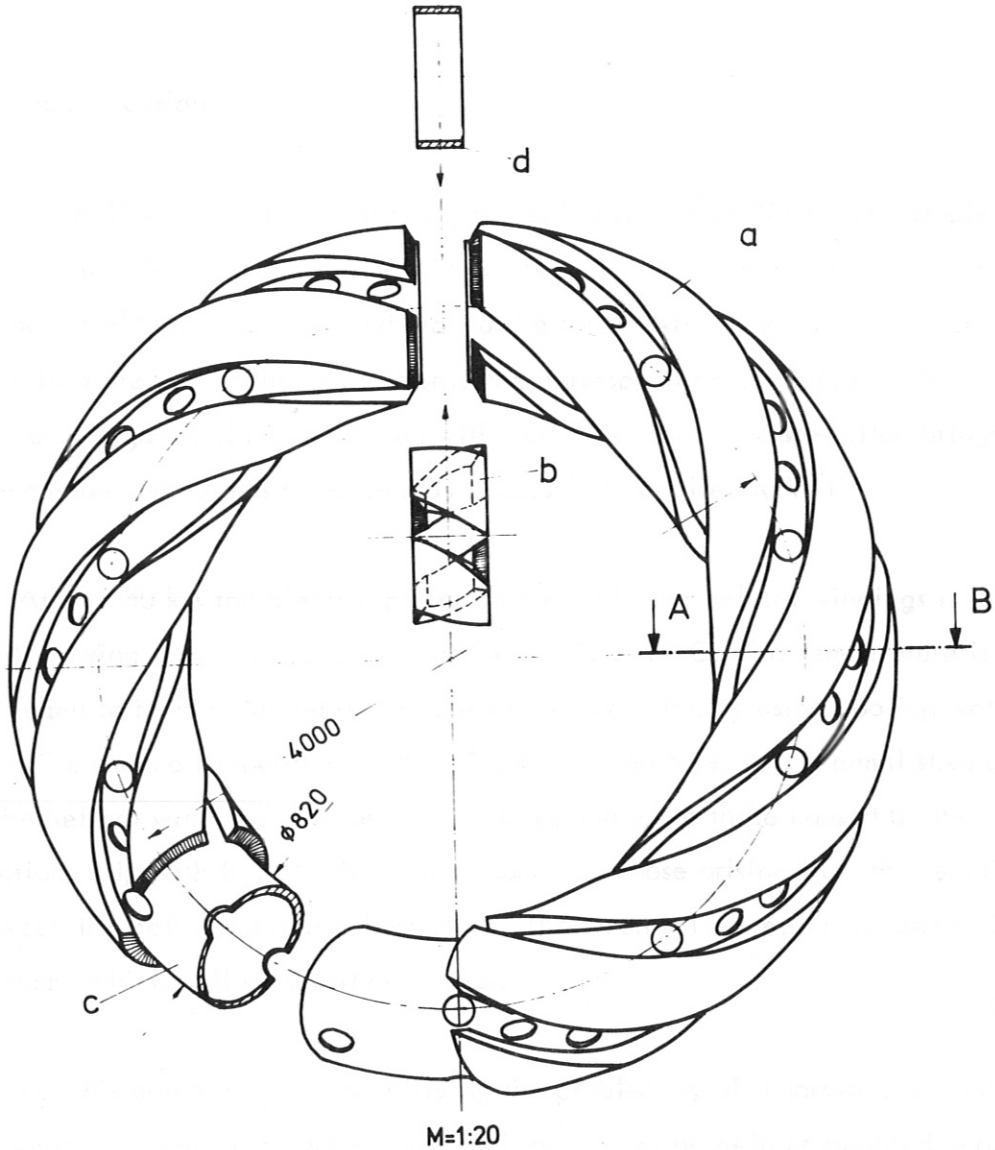

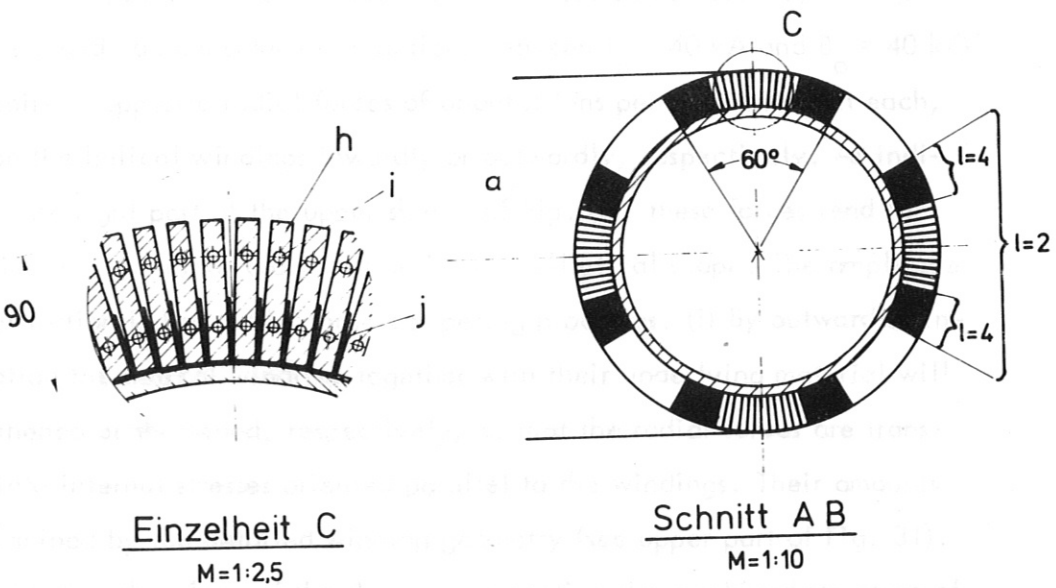

Einzelheit C
M=1:2,5

Schnitt A B
M=1:10

W VII Vakuumrohr mit Helischer Windung

Fig. 30

slight modifications.

The helical windings are interrupted at the so-called "intermediate piece" of the torus, shown in the top drawing of Fig. 30, which has to be removed when the main field coils are mounted around the torus. After inserting the intermediate piece into the gap of the torus vessel, the corresponding conductors ending at both sides of this gap will be connected with particular bars, the so-called bridges, a technique which has been already successfully applied to W II b.

At I_h = 40 kA the electric power consumed in the helical windings is 28 MW owing to a total resistance of 14,5 mΩ at 20 C. This temperature is envisaged to be maintained during the whole operation by using cooling water of 10 C entrance temperature and 30 C exit temperature; thus thermal stresses in the helical windings will be negligible compared to those caused by the reaction of I_h with B_o. The latter also dominate those arising from the reactions between the helical currents themselves. Their control represents a non-trivial problem, which will be shortly discussed.

For this purpose we are simplifying the problem by disregarding, at first, the toroidal shape. Then we are left with the forces on helices mounted upon a cylinder, and can consider the reactions between I_h = 40 kA and B_o = 40 kG as two pairs of opposite radial forces of about 2 tons per cm pathlength each, acting on the helical windings inwardly or outwardly, respectively. As indicated on the right part of the upper sketch of Fig. 31, these forces tend to distort the circular minor cross section into an elliptical shape. The amplitude of this distortion is limited by three competing processes. (i) By outward or inward motion the helical windings together with their underlying material will be lengthened or shortened, respectively, so that the radial forces are transformed into internal stresses oriented parallel to the windings. Their amounts are determined by the detailed winding geometry (see upper part of Fig. 31). (ii) Considering the plane of the shown cross section the combined structure of the vacuum vessel, the helical windings and the bandage type system filling

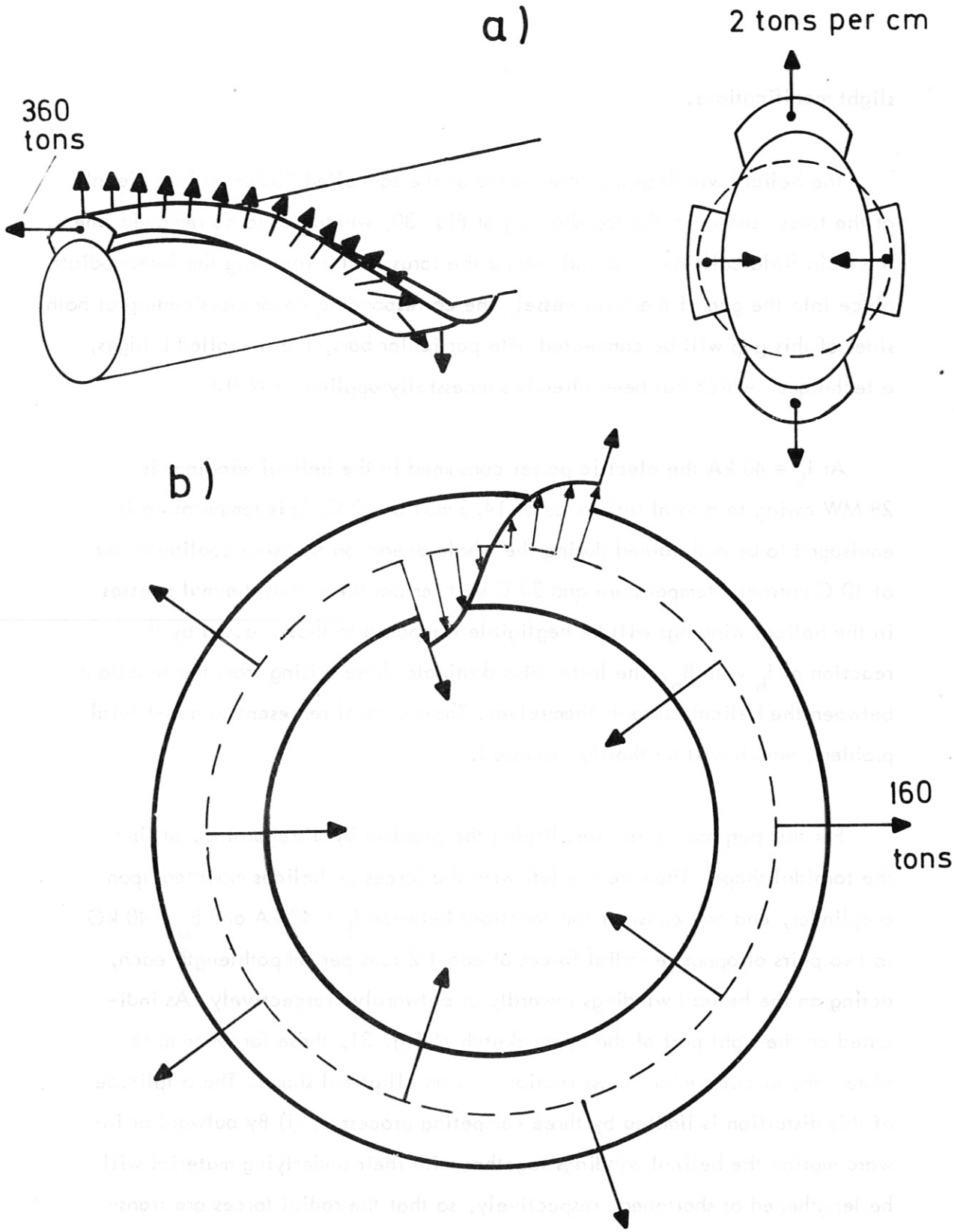

WVII Fig. 31

Schematic diagram of forces on helical windings

a) cylindrical approximation
b) net forces on torus

also the gap between the windings resists the indicated distortion according to its moment of resistance. This has to be evaluated by taking into account a wall thickness of the vessel of 3 cm, 10 cm for the windings or material filling the gap between them and 3 cm for the bandages, yielding a total thickness of about 16 cm. (iii) If the space between the bandages and the surrounding main field coils would be filled by suitable elements hindering the motion of that pair of windings experiencing forces in outward direction the mutual forces between the main field coils and the pair of windings considered would be directly short circuited. With respect to the forces acting on the other pair of windings the problem is then reduced to that of an arc clamped at its ends.

In the following we shall examine the forces arising along the helical windings if considering only case (i). With respect to the radius of curvature of the helical windings the resulting total force along each winding unit (pressure of tension) is then about 360 tons within the framework of the cylindrical model.

One may approximate now the effects arising when this cylinder is bent into a torus, by additionally introducing a net force of about 160 tons per winding period (i.e. integrated over $4\pi R_{o/m}$) on each pair of helical windings, which acts in +R direction on that pair weakening the main field and in -R direction on that increasing the main field. These net forces affect the above figures in two ways. First, as indicated on the lower sketch of Fig. 31, they exert distorting forces on the major torus cross-section which, owing to m = 5, have a five-fold symmetry. With respect of the assumed wall thickness of the torus the corresponding stresses and distortions will be small compared to those given later. The only consequence of this effect is that the intermediate piece has to be placed in an azimuthal region where the bending moments from these forces have a zero point, as is the case at any place where horizontal portholes are located. Secondly, however, this net force leads to an additional net tangential force in the helical windings of about 230 tons (the total force thus amounting to

590 tons), where the bandage structure has to transfer the difference forces cancelling in the averaging process. If this averaging would be neglected, the tangential force per winding would go up to 1000 tons,i.e. about 40 tons per conductor. Although in these figures the strength of the vacuum vessel, which suffers the same distortions, has not been taken into account, their total value would be too high to be supported by these means alone. Therefore, the bandages mentioned under (ii) have to be made strong enough to yield a value of the resistive moment of the compound vessel-helical-windings-bandages sufficient for balancing the arising forces. If this method turns out not to be safe enough additional supports according to (iii) will be applied at a later stage of the construction phase.

In order to use the large pulse generator also as the main power supply for driving the current I_h through the helical windings these will be switched in series with the main magnetic field coils. For varying iota two means are available (see Fig. 32):

1) a digitalized set of 16 shunts, operatet by transistor switches, can be put in parallel to the helical windings thus allowing for an accuracy of $2 \cdot 10^{-5}$ (see Fig. 33) in adjusting the value of I_h;

2) auxiliary generators can be connected to the helical windings and the current increased or decreased about the main field current.

Both methods would seem to have the disadvantage that the thermal time constant of the control circuit differs from that of the main circuit which would result in a variation of iota during the pulse. However, information on the main magnetic field strength, current through the helical windings, plasma current etc. is fed into a small digital computer which calculates iota and controls it by acting on the shunt circuit or the auxiliary generator. The time constant of this feed back circuit is about 1 msec, and it allows to run various programs of iota with time.

4) Vertical fields

Four circular coils (see "g" in Fig. 34) are envisaged for exciting poloidal magnetic fields inside the plasma which by proper choice of the current ratios between the four coils can be directed parallel to any value of the poloidal angle ϑ. A limiting condition is that the total current through the OH-transformer

Helical current control unit

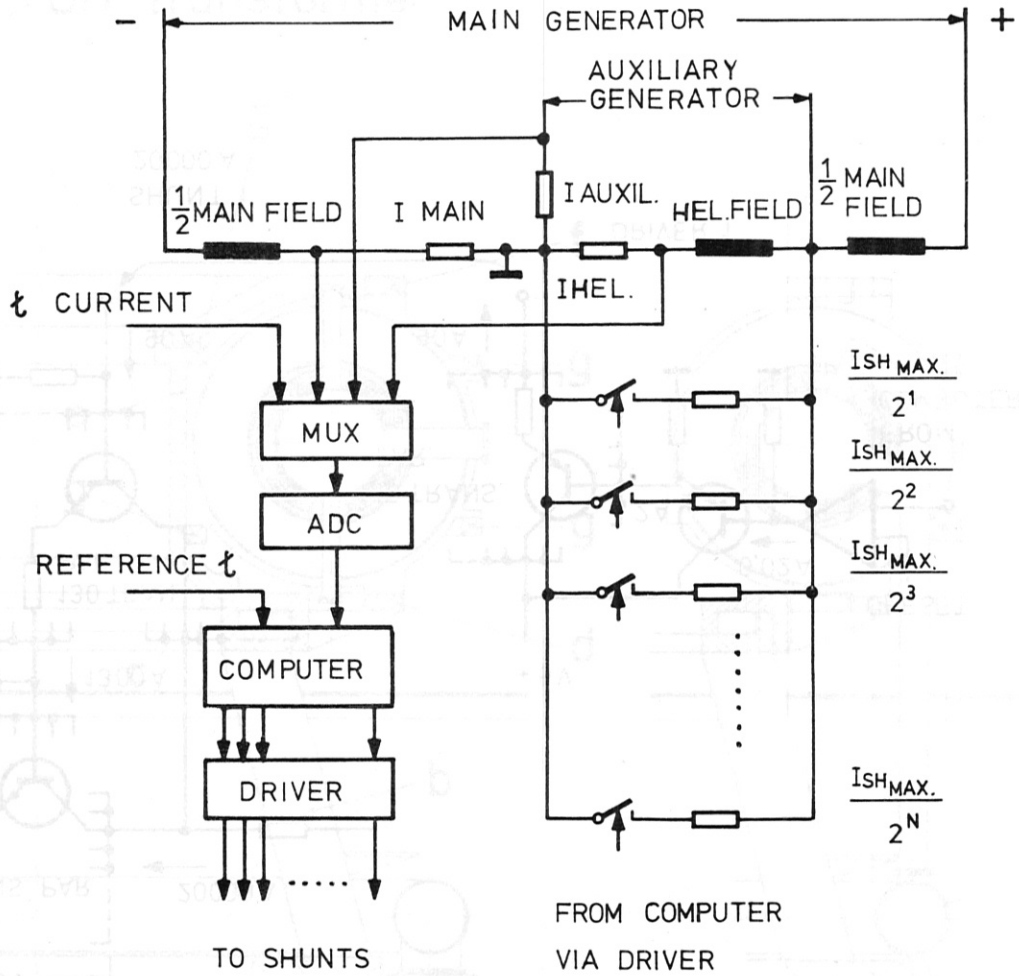

W VII Fig. 32

Transistor operated switch

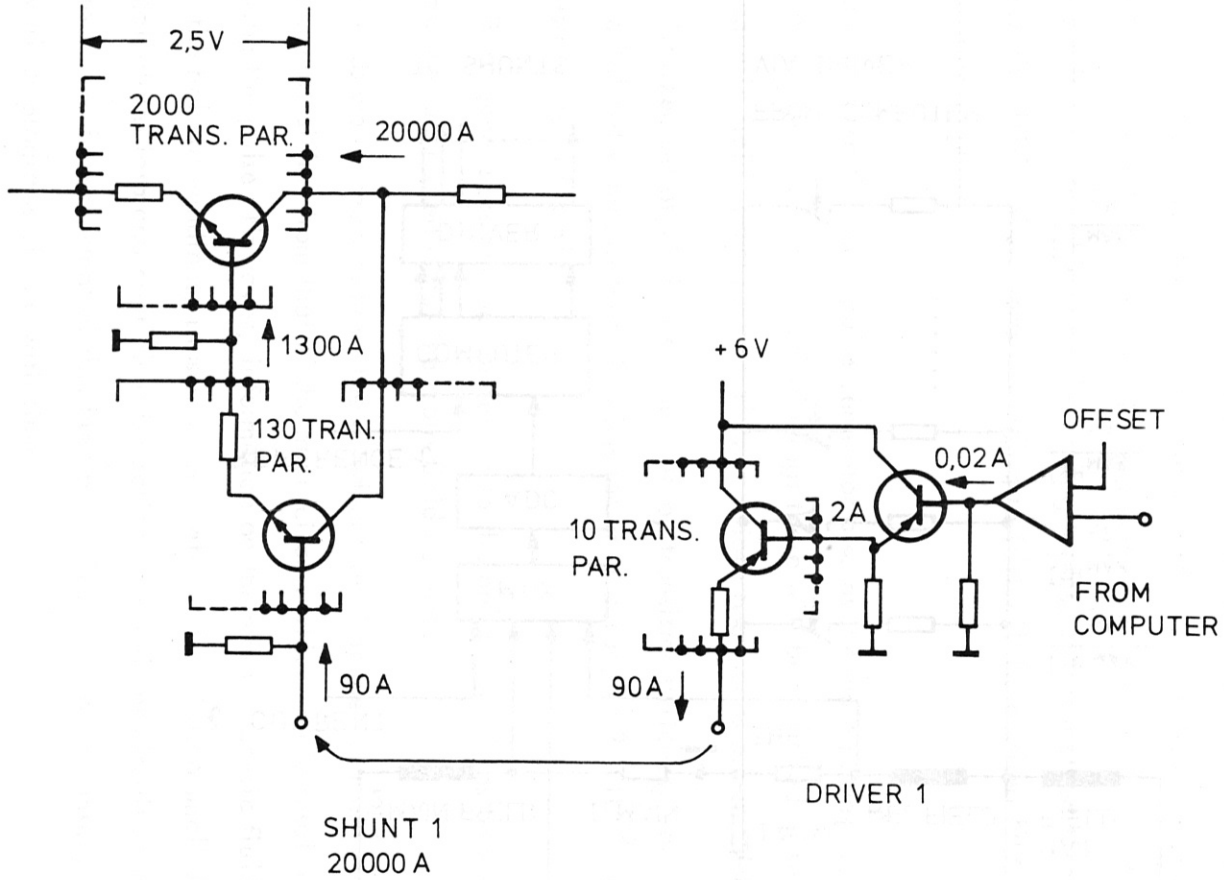

W VII Fig. 33

Side view of W VII

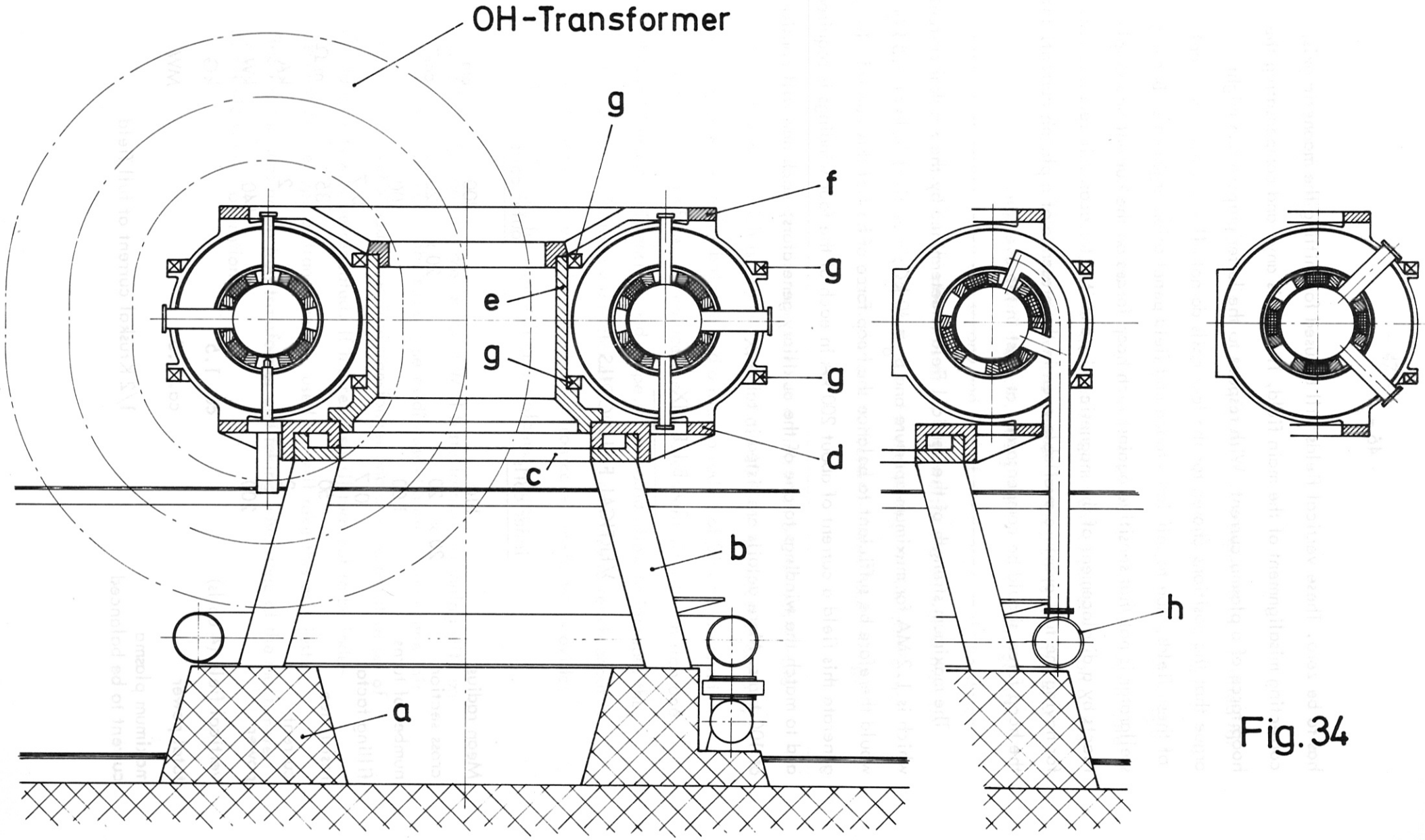

Fig. 34

has to be zero. These vertical fields will be used for shifting the magnetic axis, correcting misalignment of the main field, if there is any, and compensating the hoop force of a plasma current. With respect to the latter purpose one might argue that the positions chosen for the four coils do not allow for fast variations of these fields, due to self-inductance and field penetration arguments. But the stellarator is not that sensitive against such hoop forces on the current and simply reacts by a displacement of the magnetic axis; and it is for economic reasons, i.e. for having the full aperture available even in the presence of a plasma current, that the hoop force should be compensated, at least in the average.

The maximum strength of the vertical field is determined by the Kruskal current which is 1.2 MA for maximum aperture and B_o = 40 kG; a vertical field of 1.5 kG would therefore be sufficient to balance the hoop force of half of this current. To generate this field a current of about 200 kA in each of the four windings is required, and to match the windings to one of the auxiliary generators, each one will consist of 100 turns. More details are listed in table IX.

TABLE IX

VERTICAL FIELD COILS

	inner coils	outer coils	
Mean radius	110	300	cm
cross section	20 x 20	20 x 20	cm^2
number of turns	100	100	
filling factor	0.7	0.7	
resistance	50	135	mΩ
current	2	2	kA
power	200	540	kW
vertical field (4 coils)	ca. 1.5		kG
total power	ca. 1.5		MW
maximum plasma current to be balanced	1/2 Kruskal current at full field		

5) OH-Transformer

At present a toroidal air core transformer is envisaged to be installed for ohmic heating. This solution is favoured since it avoids any stray magnetic fields which otherwise might disturb plasma confinement. The disadvantage coupled to it is the large amount of energy required for operating an air core transformer. Even the fly wheel generator of the central power station of the IPP does not allow for larger fluxes than about 1 Vsec, since the radius of the transformer coils is limited to 60 cm. The generator would charge the transformer within about one second and half of the energy would be stored within the magnetic field after this time. A powerful switch would then be necessary to open the circuit and allow for a discharge of the transformer within 50 msec in order to provide for a sufficiently large loop voltage.

The flux limitation in turn provides a limitation on the achievable plasma current, which is 220 kA, i.e. about 20 % of the Kruskal current, assuming complete flux balance and a plasma radius of 35 cm. It would be desirable, therefore, to replace the air core transformer by an iron one of about the same dimensions and shape. This would allow to increase the available flux variation by a factor of 2.5 or so and thus to reach about half the Kruskal current. In addition, an iron core transformer provides a much easier means for controlling the plasma current.

At the moment the Wendelstein W II b stellarator is running with an air core transformer of the same type as discussed here. In due time this one will be exchanged for an iron transformer and a representative set of measurements will be repeated. If the results will turn out to be independent of the type of transformer used we will take this as a justification for chosing an iron transformer and taking advantage of the much more economic way of operation.

6) Frame

As shown in Figs. 34 and 35 the frame is mounted on a concrete base (a) with concrete pillars (b) which are free of iron. All the pillars are connected by a metallic table (c) which forms the basis for the whole frame. Centered to this table a second table (d) is fixed which is made from an aluminium alloy with high accuracy. It has a strong ring at the positions of the outer lower bolting points of the coils, is provided with bores for the lower vertical portholes and at five positions equipped with hydraulic tools to locate the vacuum tube. Lowering the hydraulic pistons one by one allows to shift the coils around the torus.

Centered to table (d) is mounted a cylindric piece (e) which is designed to take up all the centripetal forces and each coil is bolted to it at a top and bottom ring. For mounting the coils a kind of a gallows can be fixed on the top of that cylinder and a coil mounted to its arm. This way one coil after the other can be moved around in azimuthal direction to its final position. If all coils are in place the gallows will be removed and the top piece (f) be put in place. This piece again has bores for the upper vertical portholes and has also a strong ring for fixing the coils to it.

All the individual parts are slotted in radial direction so that they do not provide a short circuit for the ohmic heating. There are discussions, however, whether the frame will not be better made from glass fibre reinforced epoxy. Such techniques seem to be available now and they would not need an insulation gap. Concerning the large size of these parts, we are not yet certain, however, whether by using these materials the same accuracy can be achieved as with an aluminum alloy.

With respect to the accuracy of the coil arrangement the mounting surfaces and reference bores of each coil will be adjusted according to its individual magnetic axis at first. This will be done by putting a long vacuum tube coaxially into the coil. This tube carries an electron gun on one end and a screen on the other. If the coil is excited it can be positioned such that its magnetic axis is parallel to

Top view of W VII

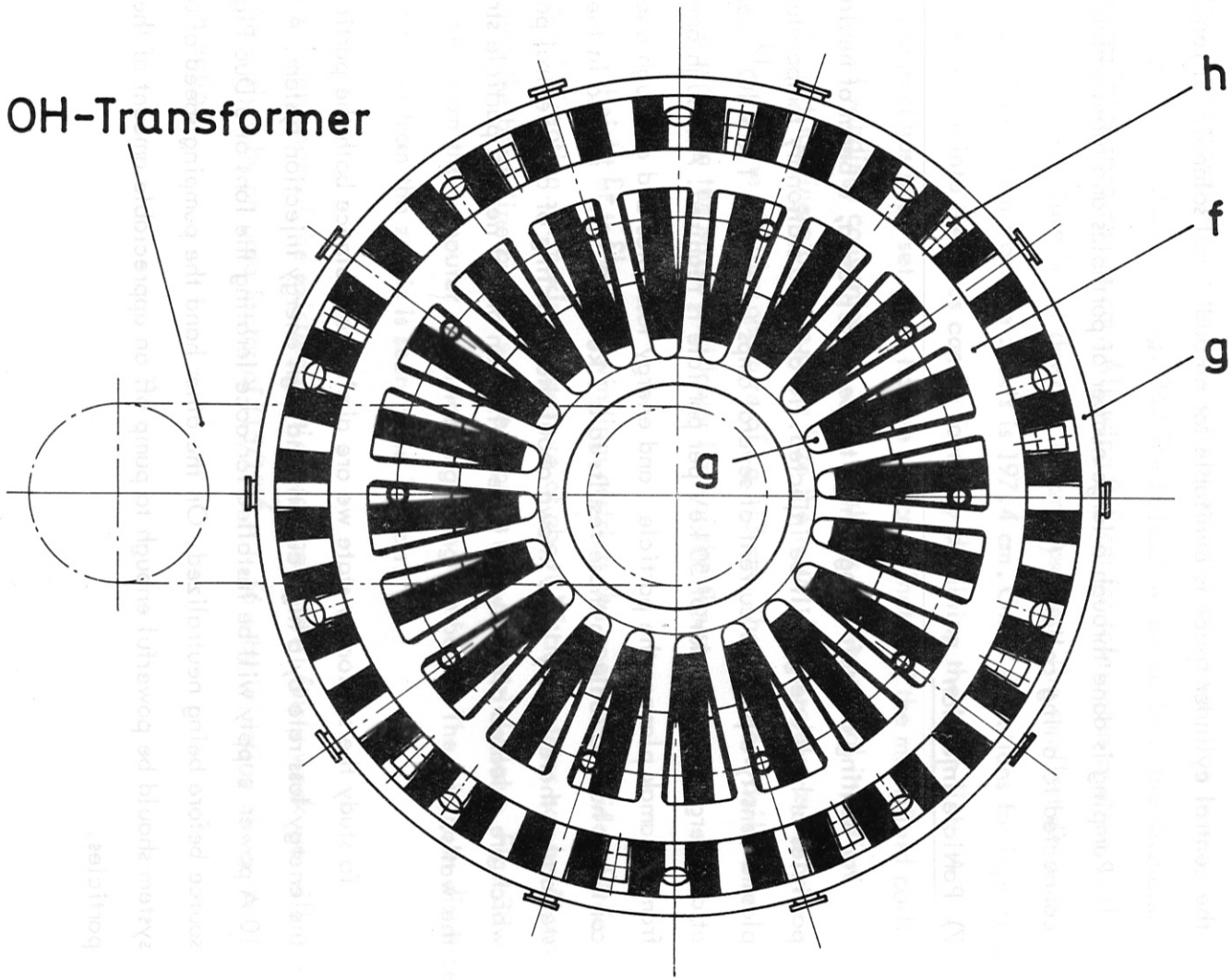

Fig. 35

the axis of the tube which in turn is well adjusted to a coil case fitting to a milling machine. This one then makes the reference bores.

All other parts will be provided with fitting bores and bolts so that adjustment has to be done only once (hopefully). For fine adjustment vertical fields can be used.

The coils for exciting vertical fields are arranged at 4 positions (g). Inside the central cylinder space is available for an additional solenoid, if required.

Pumping is done through a large number of portholes and tubes which are connected to a ring collector (h).

7) Particle Injection

For heating and refuelling a high temperature plasma, a beam of neutral particles at high energy will be injected. To obtain a stationary temperature and plasma density a particle current of several amps (1 amps = 1.6×10^{19} particles/sec) at an energy of the order of 50 keV per particle is required. Although one knows from tokamak plasmas the particle and energy loss rates and although one may be confident how to scale up those results to a 1 keV, 10^{13} cm^{-3} plasma in the W VII stellarator there is very little known about the recycling of cold neutral particles which are released off the walls for each hot ion or fast neutral particle striking the walls.

To study the stationary state we are aiming to balance both the particle and the energy loss rate by a high current and high energy injection system. A 100 kV, 10 A power supply will be installed for acce lerating the ions of a Duo-Pigatron source before being neutralized. On the other hand the pumping speed of our vacuum system should be powerful enough to pump off an appreciable amount of the injected particles.

To avoid "trapped particles" and hence enhanced diffusion or instabilities but to trap the fast ions - after ionizing the fast neutrals - by gyrating in the main field we are going to inject the neutrals tangentially. To balance the angular momentum introduced by this tangential injection we inject a second beam in the opposite direction. For this arrangement and to allow those particles not absorbed by the plasma to leave the torus without hitting the wall we are looking for tangential or nearly tangential parts with a reasonable aperture.

In the plane perpendicular to the z axis - equatorial plane - the access for tangential injection is shown in Fig. 36. The helical windings limit the diameter of the tangential part to ca. 13 cm. Allowing 0.5 cm for tolerances and the wall thickness the beam aperture is cut down to 12 cm diameter. The smallest distance of the center of the beam from the z axis is 197.4 cm. Other directions for injecting almost tangentially into the torus can be found by declining the beam line. A computer program has been set up to handle the coordinates of the main field coils and the helical windings conveniently. Fig. 37 shows the horizontal injection (like Fig. 36) but looking along the beam into the torus. The circle at $z = 0$ and $x = 197.4$ cm shows the circular aperture of ca. 13 cm. The two field coils to be modified are shown in the upper and lower half of the figure.

The 10 cm height of the helical windings restricts the aperture considerably in the horizontal direction. A maximum aperture of about 15 cm diameter can be found if we decline the beam line by 25° with respect to the equatorial plane. Fig. 38 shows the plot from the computer again looking along the beam. The minimum distance of this beam axis from the z axis is seen to be 189 cm.

As the divergence of the existing particle sources is still fairly weak we will gain considerably - by an area factor of $(15/12)^2 = 1.56$ - by injecting along the declined direction.

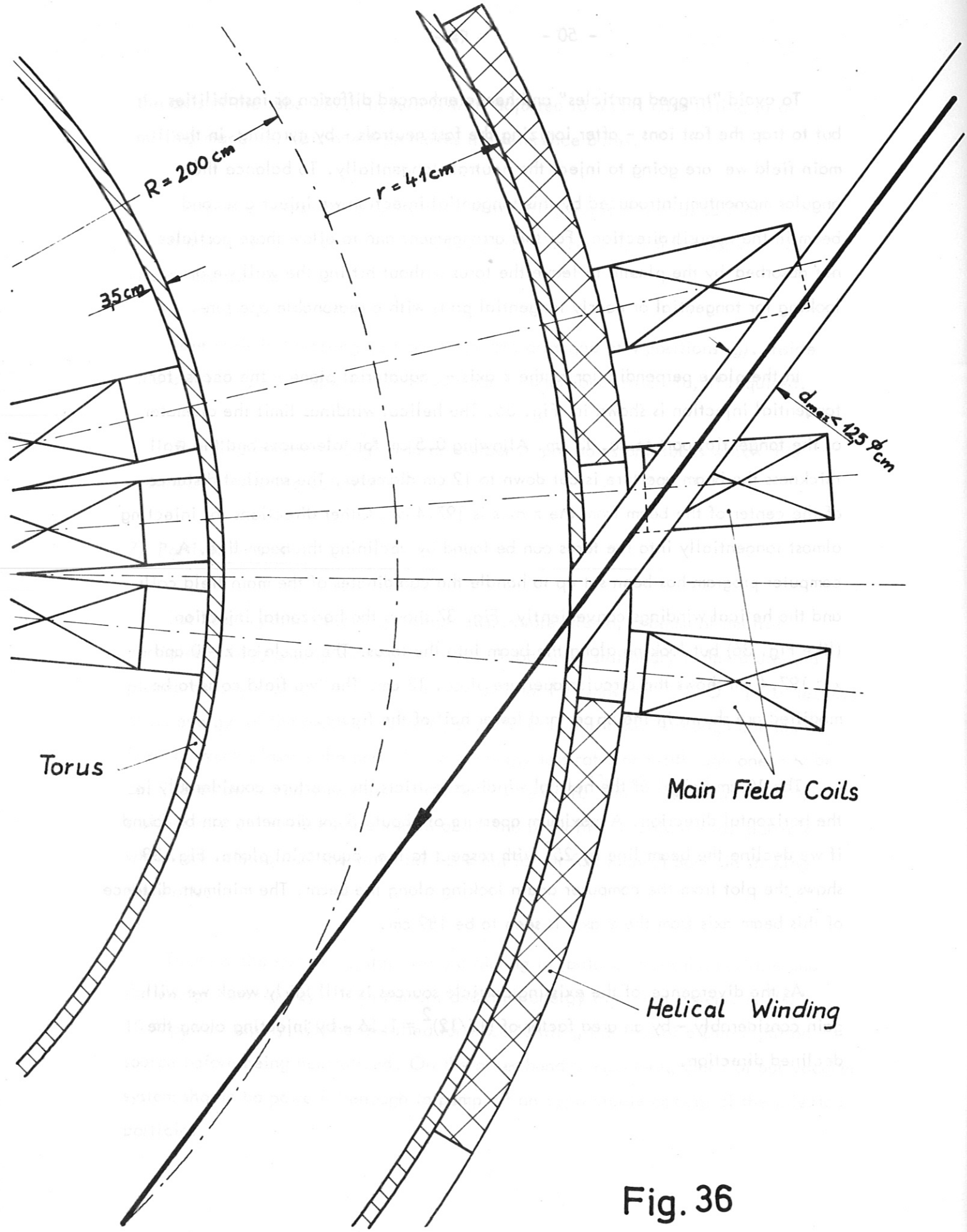

Fig. 36

Tangential Injection in W VII

M 1 : 10

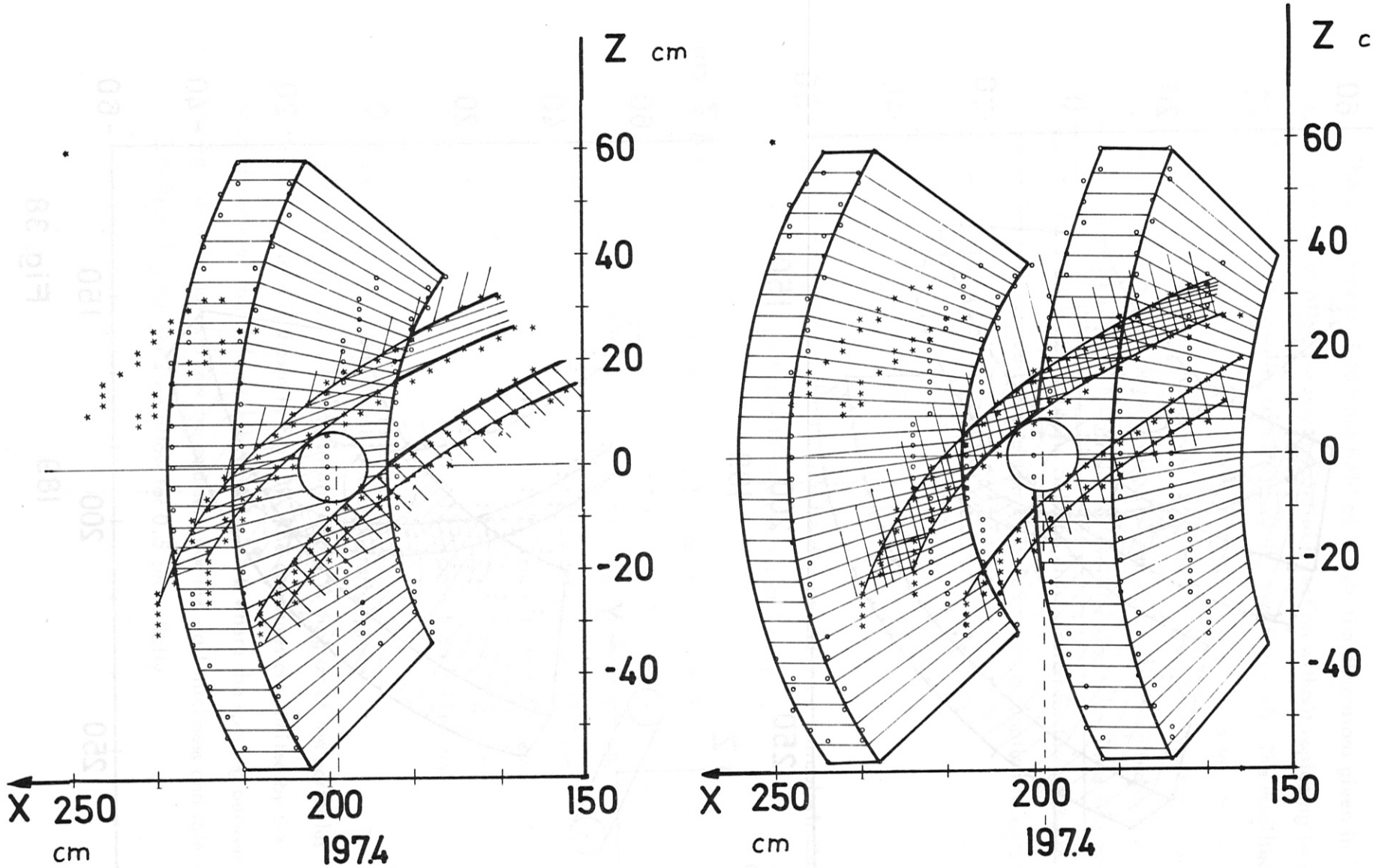
Z cm
60
40
20
0
-20
-40
X 250
cm
200
150
1974
Z cm
60
40
20
0
-20
-40
X 250
cm
200
150
1974

Fig. 37

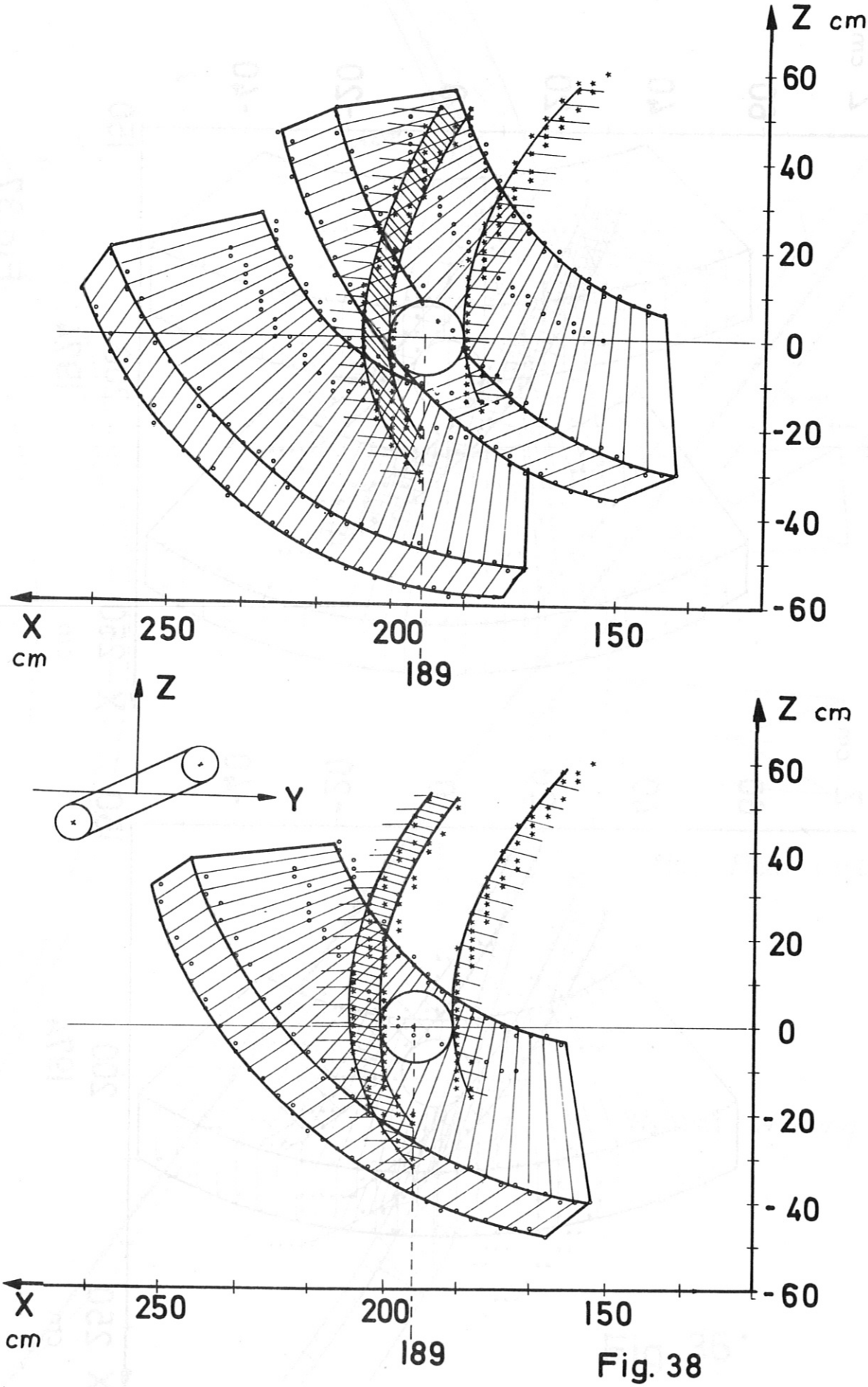
Z cm
60
40
20
0
-20
-40
-60
X
cm
250
200
150
189
Z
Y
Z cm
60
40
20
0
-20
-40
-60
X
cm
250
200
150
189

Fig. 38

The arrangement of 40 main field coils with the dimensions given in table VI does not allow for any tangential injection without replacing two of these for each tangential port by specially modified coils. The modified main field coils will be wound at smaller resp. different cross sections to allow the full beam aperture to pass. By a smaller cross section of the conductor the same number of turns requires less space. Assuming a minimum number of 4 modified main field coils for two injection beam lines directed opposite to each other and assuming half the cross section for the conductor of the modified coils an additional power of 10 % has to be supplied to sustain the original magnetic field strength.

8) Vacuum System and Access

By the periodicity of the 40 main field coils and the 4 helical windings we get the following portholes for diagnostics and pumping:

at ϑ around	number of portholes	with an aperture of
0	10	21 cm - 1 cm = 20 cm
$\pm$ 22.5°	20	20.5 cm - 1 cm = 19.5 cm
$\pm$ 45°	20	19 cm - 1 cm = 18 cm
$\pm$ 67.5°	20	16 cm - 1 cm = 15 cm
$\pm$ 90°	20	12.5 cm - 1 cm = 11.5 cm

$\vartheta = 0$ is the outward direction in the aequatorial plane.
All these portholes go out in radial direction. A diagram of the portholes in the ϑ, φ plane is shown in Fig. 39. The apertures are limited by the spacing between the field coils except for $\vartheta = 0$ where the spacing between the helical windings is a few mm smaller. For the wall thickness and tolerances in manufacturing the ports we allow for 0.5 cm radially.

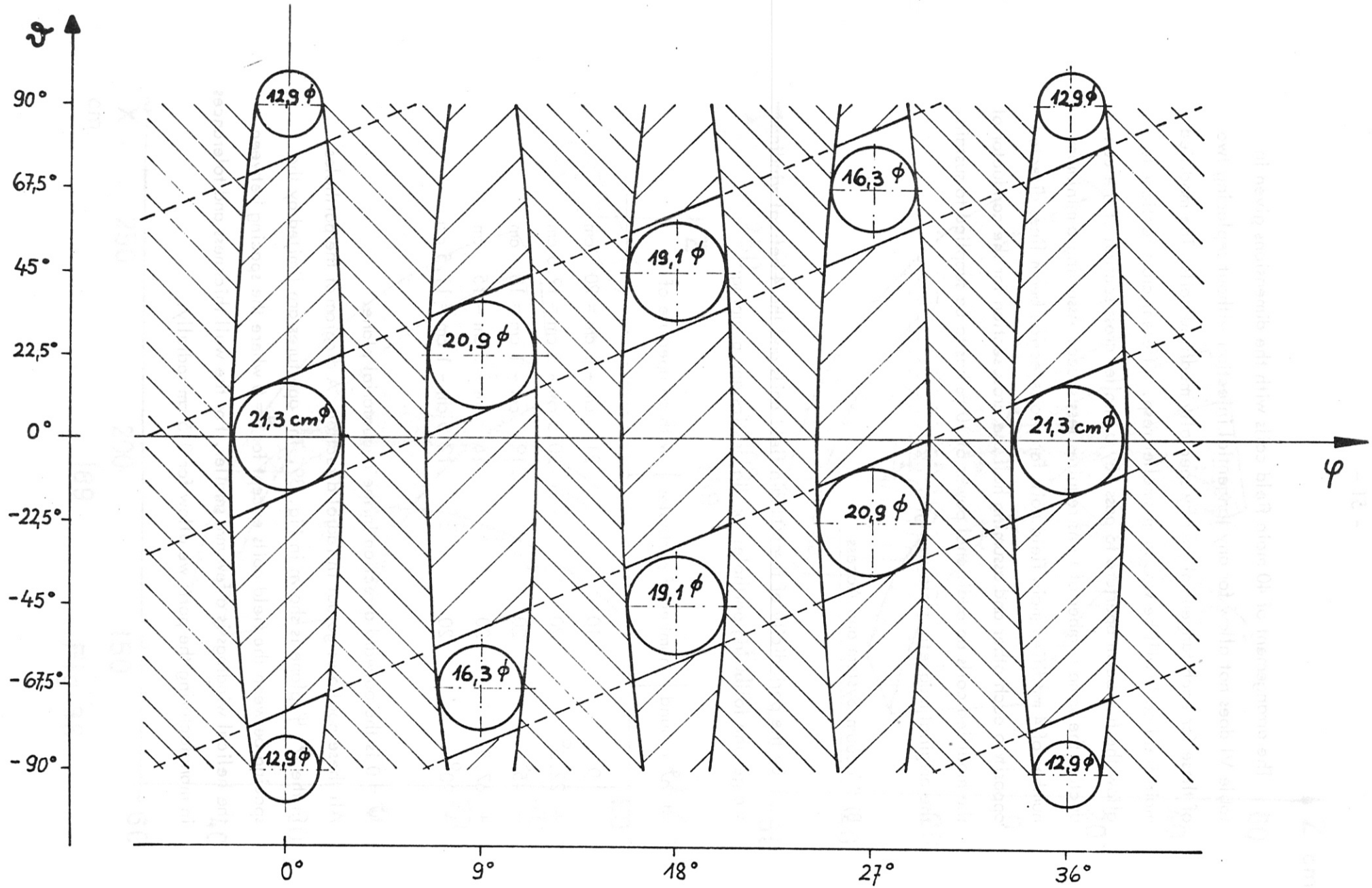
ϑ
90°
67,5°
45°
22,5°
0°
-22,5°
-45°
-67,5°
-90°
φ
0°
9°
18°
27°
36°
12,9 ϕ
21,3 cm ϕ
20,9 ϕ
19,1 ϕ
16,3 ϕ
12,9 ϕ
16,3 ϕ
19,1 ϕ
20,9 ϕ
21,3 cm ϕ
12,9 ϕ

W VII

Fig. 39

Taking all portholes listed above except those at $\vartheta = 0$ we end up at a maximum pumping speed of 6×10^4 ℓ/s. This pumping speed allows for the length of partholes only 15 cm. After having passed the helical windings the cross section can be enlarged so as not to restrict the pumping speed. For the pumping lines and the pumps themselves a reduction by a factor 2 of the maximum possible conductance through the partholes has been taken into account.

For a high energy injected neutral beam of 5 A - a gas load of cold neutrals of the same order is accompanying the beam - a stationary pressure of the order of 10^{-4} torr should be feasible. To reach an even lower stationary pressure a getter pumping system inside the torus is under consideration.

Further access to the torus is possible either through the pumping ports or through the 10 horizontal ports which are not used for pumping purposes. Tangential observation or irradiation by a laser beam is possible without interfering with the helical windings. The maximum aperture is about 12 cm diameter. In the horizontal plane the minimum distance of the tangential observation line and the z-axis is 197.4 cm.

9) Data Aquisition System

1) General Description

The whole system (see Fig. 40) is built around a PDP 11/20 computer. This machine performs two main tasks:

a) Incoming data are routed to mass-storage devices;

b) Simple "Real Time" analysis of raw data followed by a display of the results.

On the input side are several analog as well as digital data channels. To allow recording slow, fast or very fast phenomena we have ADC's (analog/digital converters) of different conversion speeds. To have increased mechanical and

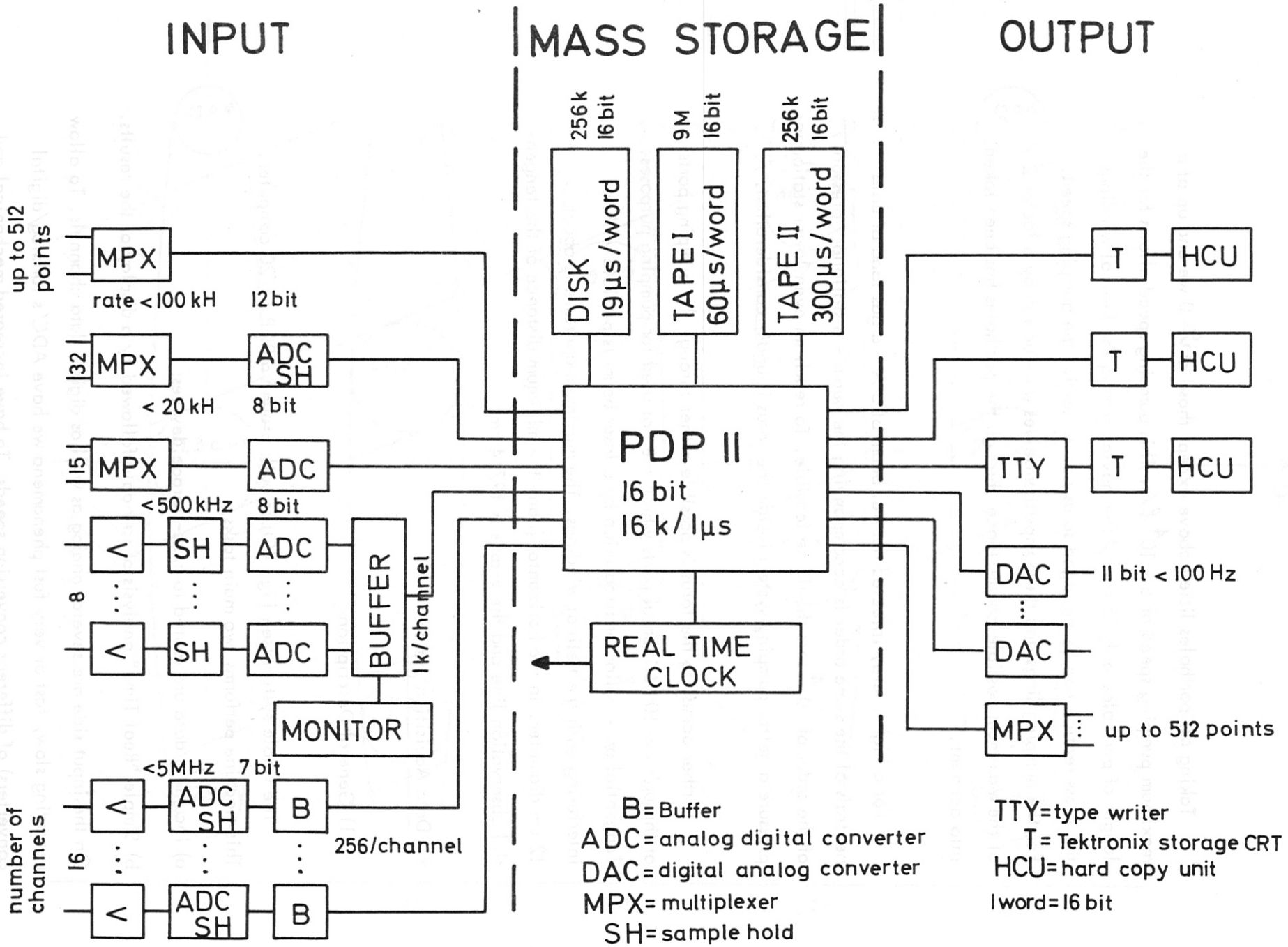

Data acquisition system

Fig. 40

electrical reliability most of the input hardware is designed as a modular system (CAMAC system).

At the present time there are two mass storage devices - a magnetic tape unit and a disk - . A smaller tape unit is used to store the many programs (written in Fortran or Assembler language) for raw data analysis. The big magnetic unit records in IBM compatible format so that a sophisticated analysis of the data can be done at the computer center (IBM 360/91).

While the disk is also used to store data it mainly facilitates to store the subroutines for the operating system. The operating system governs the flow of data from the experiment to the storage places and the simple analysis just after the experiment ("real time" analysis).

The output side consists of a number of analog channels (DAC = digital/analog convecter) and terminals capable of displaying alphanumeric as well as graphic data. These terminals have also a keyboard so they can be used as input devices as well (adjust and set parameters via computer).

10) Experimental hall

For housing the W VII the experimental hall L 7 is available (see Figs. 41 and 42) which is designed particularly for this purpose. The most important parameters are collected in table X. The hall has about 24 x 22 m^2 floorspace and a sufficiently large entrance door of 5 m height and 6 m width which can be increased to nearly 7 m if necessary. Behind the door is a ramp with a capacity of its floor of 12 tons/m^2 so that heavy trucks or movable cranes can directly enter the hall. The built-in crane has a capacity of 25 tons. If this turns out to be too small an additional crane can be put on the same rails.

The main floor is made of an aluminum construction which can be removed in parts. The smallest piece is 20 x 100 cm^2. This design allows to get nearly

Experimental hall L7

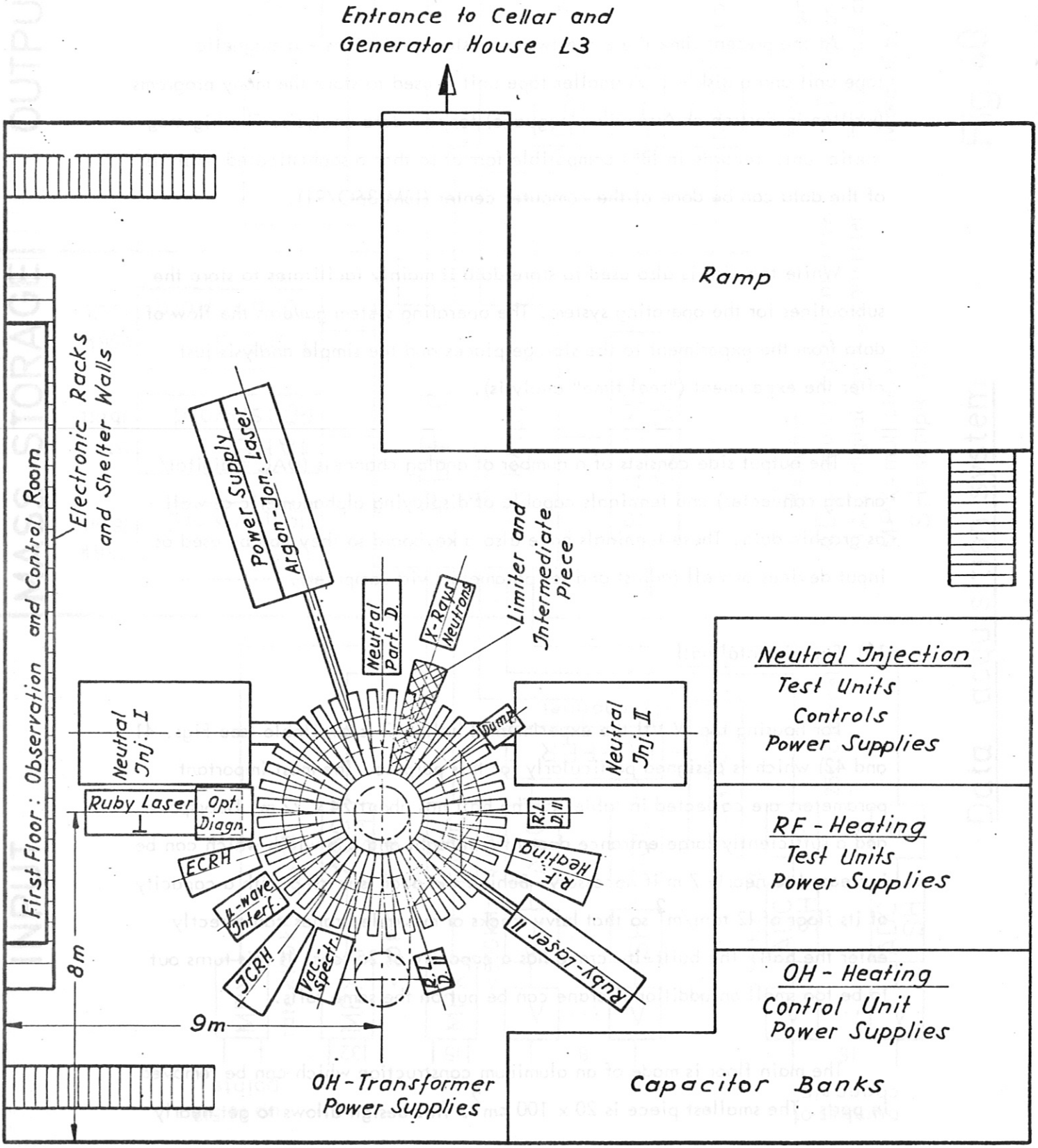

Fig.41

Experimental hall L7

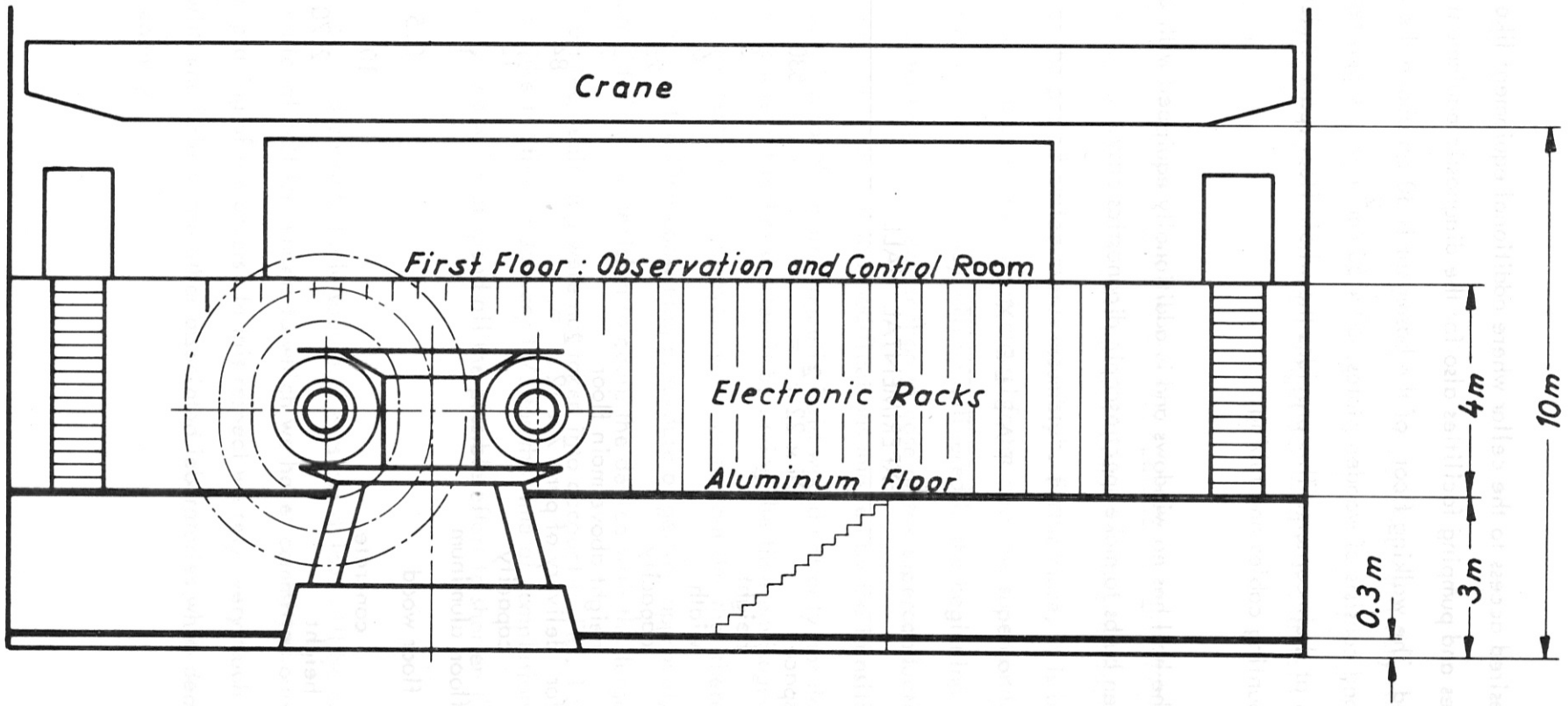

Fig. 42

any desired access to the cellar where additional equipment like power supplies and pumping facilities also for the diagnostic equipment can be located. The walking floor of the basement is 30 cm above the concrete floor and consists of wooden plates, 50 x 50 cm^2 each, supported by small pillars at their corners. This provides the whole floor space underneath for mounting cables and tubing.

The hall has no windows and is additionally equipped with a set of tungsten bulbs to make spectroscopic diagnostics easy.

TABLE X

EXPERIMENTAL HALL

floor space	24 x 22 m^2 =	530	m^2
door	height	5	m
	width	6	m
crane	capacity	25	tons
	height above main floor	7	m
ramp for	delivery of parts 7 x 12 m^2 =	84	m^2
	capacity	12	$tons/m^2$
main floor	aluminum	1	ton/m^2
cellar floor	wood	0.5	ton/m^2
	concrete	10	$tons/m^2$
height		2.70	m

11) Time Schedule

As an extract of a rather detailed computerized schedule a very rough sketch of the time schedule was given in Fig. 15 for the superconducting version. It is now being modified to account for the changes occuring from the transition to the conventional solution.

The earliest time for putting the W VII into operation is April 1974, the time at which the main generator will be available. This time accidentally agrees with the end of the period called "torus assembly". Furthermore, it is believed that the conventional coils could be manufactured faster than the superconducting ones and that there is a chance that they will be delivered in the beginning of 1974. Also their adjustment should be easier than in case of the superconducting coils. These results seem to mean that the modifications implied by the transition to the conventional solution for the main magnetic field would not only not delay the original time schedule but rather shorten it by saving the time envisaged for "main coil adjustment and test runs". However, we have to consider that there is already some time lost due to the time consuming procedure of getting approval, and that the implications provided by the decision to equip the device with the large vacuum tube already from the beginning were not taken into account in Fig. 15. Therefore, we would rather like to stick to January 1975 for the time of completion. But this does not mean that we will not spend all the possible effort to shorten the time of construction.

A very serious and unpredictable source of possible delays will be connected with the international call for tenders to which we have committed ourselves and the following placing of the orders. In this respect we rely very much on the cooperation with and help of the other associated laboratories when dealing with firms of their country.